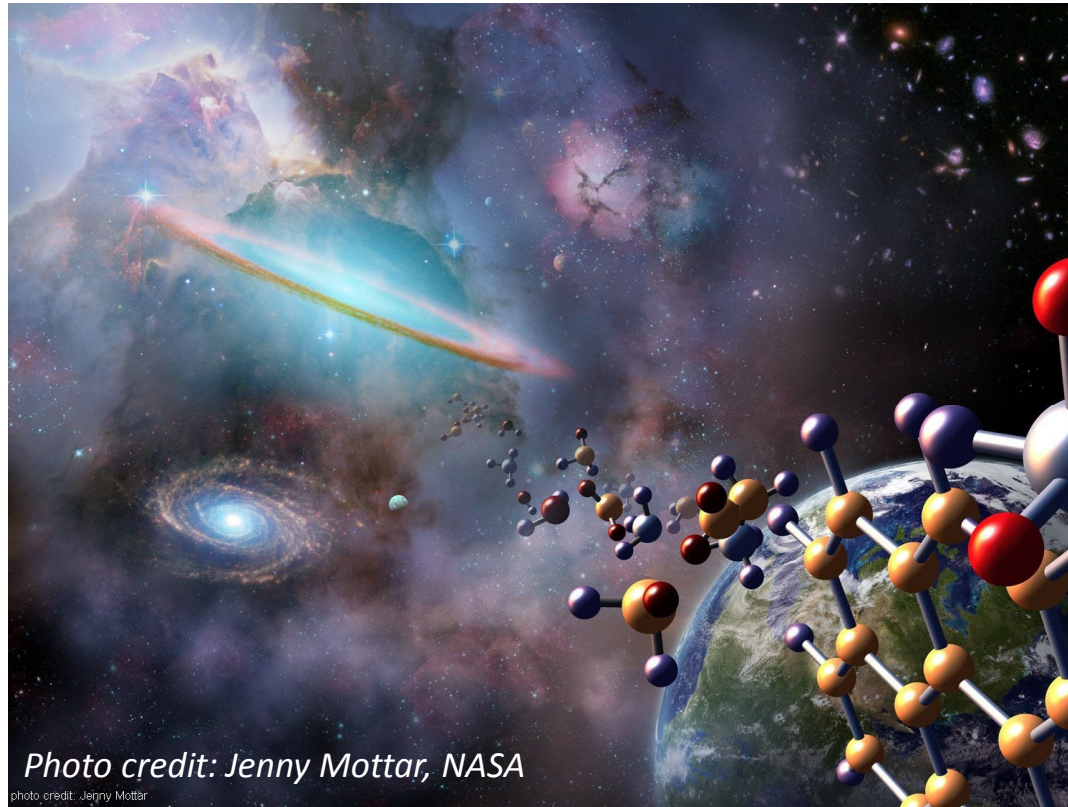


The molecular origins of life



L2 SoSe 2020

Zbigniew Pianowski

Definitions of life

Erwin Schrödinger (1943): Life: heredity and thermodynamics
Order from order (genetics), Order from disorder
ordered arrangements of molecules (cells, tissues) within
themselves on the expense of increasing disorder of the environment

Life is a self-replicating chemical system capable of evolution (NASA, 2009)

Self-replicating: copies itself

Chemical system: based on assembly of molecules

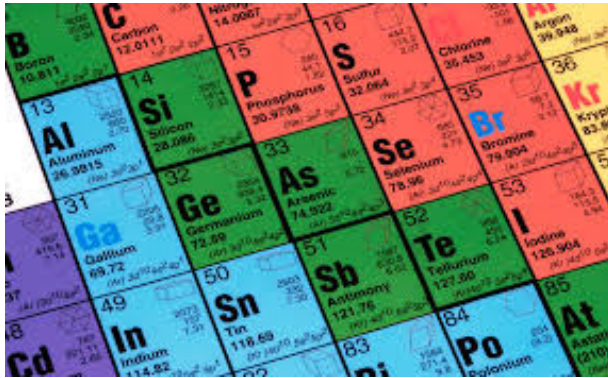
Evolvable: adapt to the surroundings

Life is a self-sustaining kinetically stable dynamic reaction network derived from the
replication reaction

(A. Pross, 2012)

Constraints for the origin of life

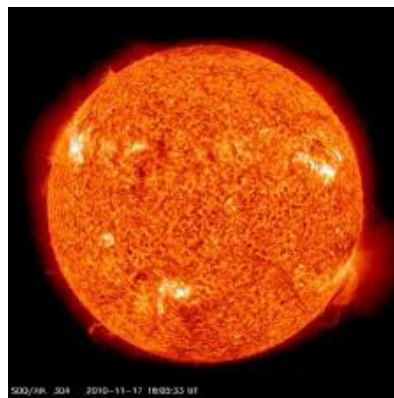
Elements of life



Solvents for life



Energy for life

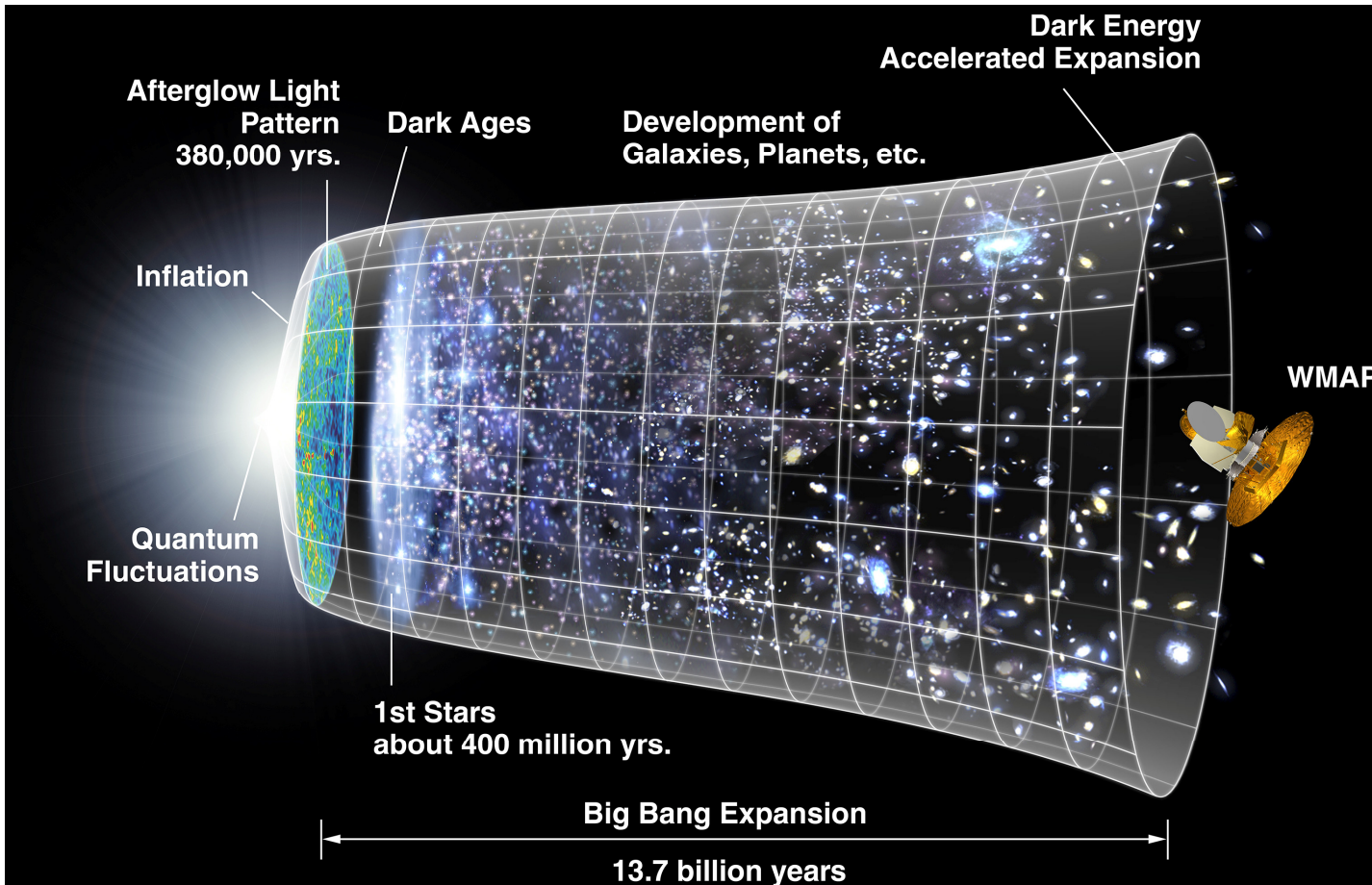


Other limitations

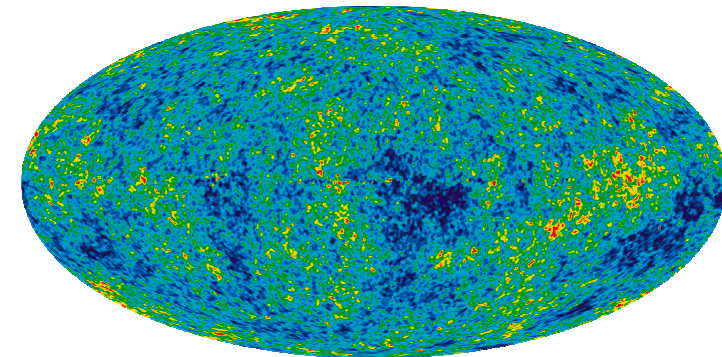


Echoes of the earliest Universe

Red shift of spectral lines in far galaxies (Hubble, 1929)
Theory of the Big Bang – Gamow (1948)

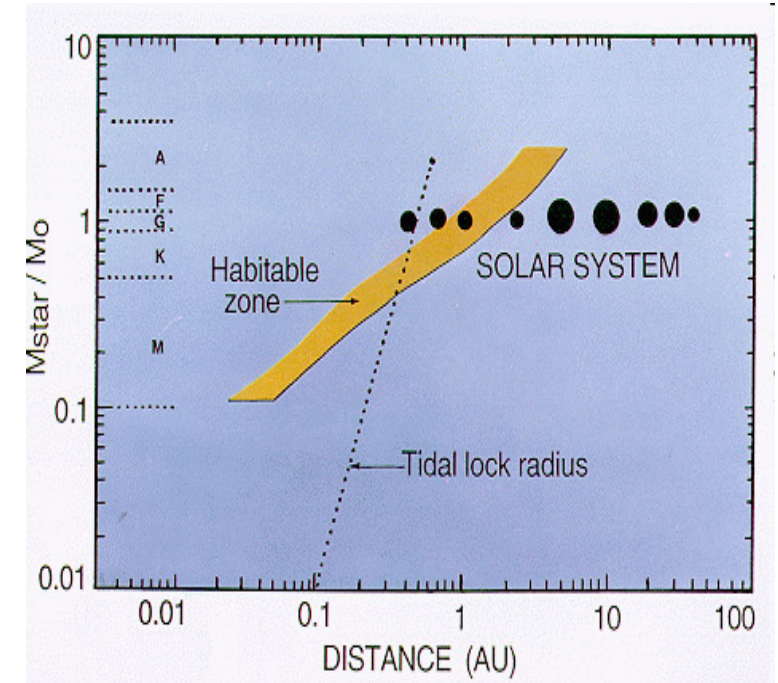


Cosmic microwave background
(Penzias, Wilson, 1965 Bell AT&T)



Heat of the Big Bang dissipated in the
Universe as the 4 K residual radiation

Origins of a habitable planet - conclusions



Earth predominantly composed of refractory metals and silicates – non-biogenic materials
Jupiter provided proto-Earth with water, and allowed cleanup of the Solar System from planetesimals, so no more big, planet-sterilizing impact possible anymore.
Earth is optimally positioned (0.95-1.15 AU) to maintain the acquired water as liquid, and stable surface temperature over billions years.

Overview of the course

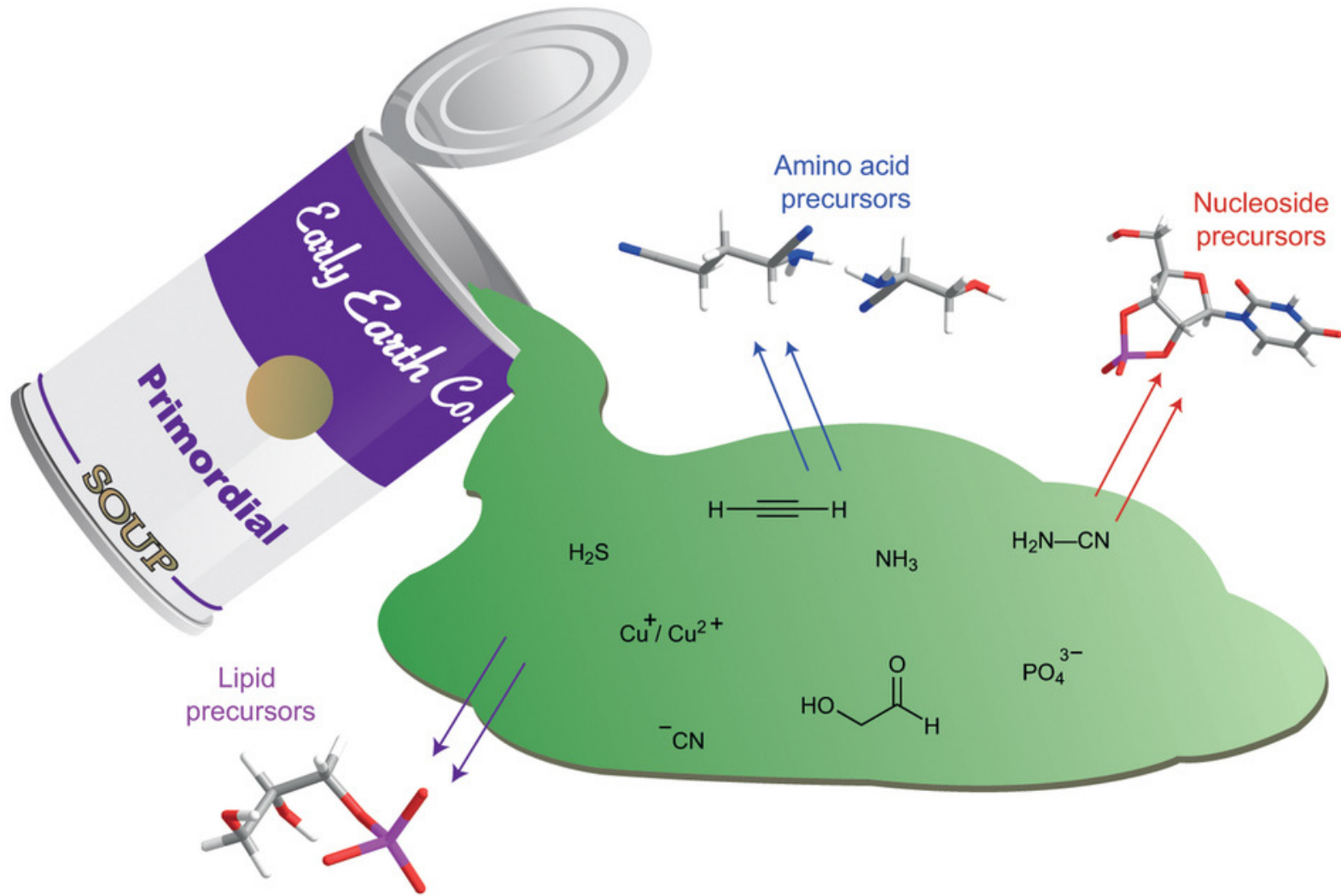
Origin of the Universe – stars, planets, elements

Origin of biorelevant monomers – primordial soup

Complex chemical processes on the way to living systems

Protocells and LUCA

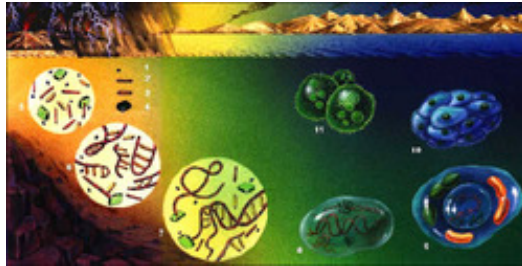
Basic classes of biomolecules



- Aminoacids
- Lipids
- Carbohydrates (sugars)
- Nucleotides
- Nucleosides (sugar+nucleotide)

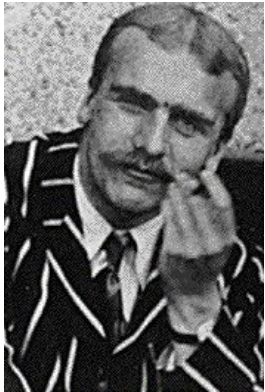
The origin of biorelevant molecules on Earth

Alexander Oparin
(USSR, 1894-1980)



„atmospheric oxygen prevents the synthesis of certain organic compounds that are necessary building blocks for the evolution of life”

John B. S. Haldane
(UK, India, 1892-1964)



- 1. The early Earth had a chemically reducing atmosphere.*
- 2. This atmosphere, exposed to energy in various forms, produced simple organic compounds ("monomers").*
- 3. These compounds accumulated in a "soup" that may have concentrated at various locations (shorelines, oceanic vents etc.).*
- 4. By further transformation, more complex organic polymers - and ultimately life - developed in the soup.*

„Primordial soup”

„Biopoeiesis” – prebiotic oceans as „hot diluted soup” under anoxic conditions: e.g. CO_2 , NH_3 , H_2O

„Life arose through the slow evolution of chemical systems of increasing complexity”

Atmosphere composition for young terrestrial planets

	Reduced	Neutral	Oxic
Carbon (C)	CH ₄	CO, CO ₂	CO ₂
Nitrogen (N)	NH ₃	N ₂	N ₂
Oxygen (O)	H ₂ O	H ₂ O, CO, CO ₂	O ₂
Hydrogen (H)	H ₂ , CH ₄ , NH ₃ , H ₂ O	H ₂ O	H ₂ O

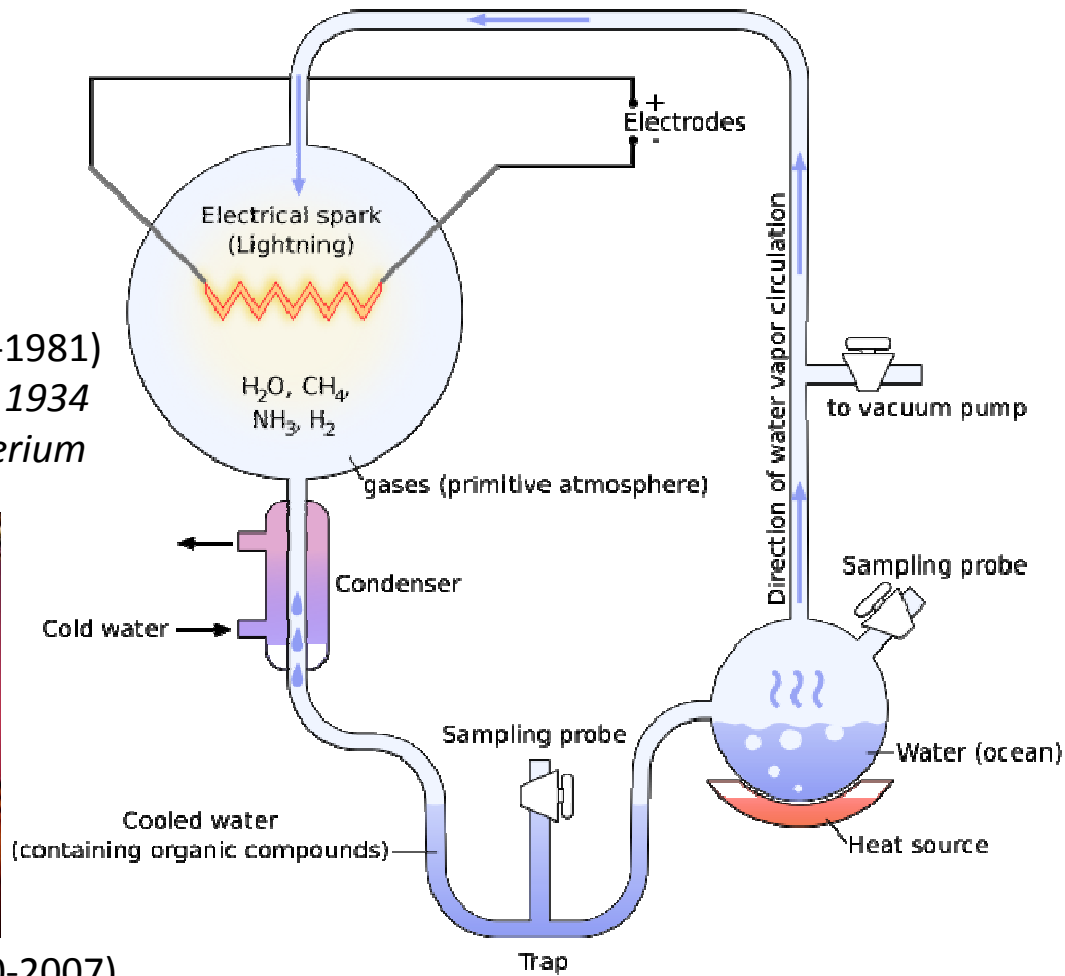
Miller-Urey experiment - 1952



Harold Urey (1893-1981)
UCSD, Nobel prize 1934
Discovery of deuterium



Stanley Miller (1930-2007)
UCSD San Diego, CA, USA



α -Aminoacid production in the Miller-Urey experiment

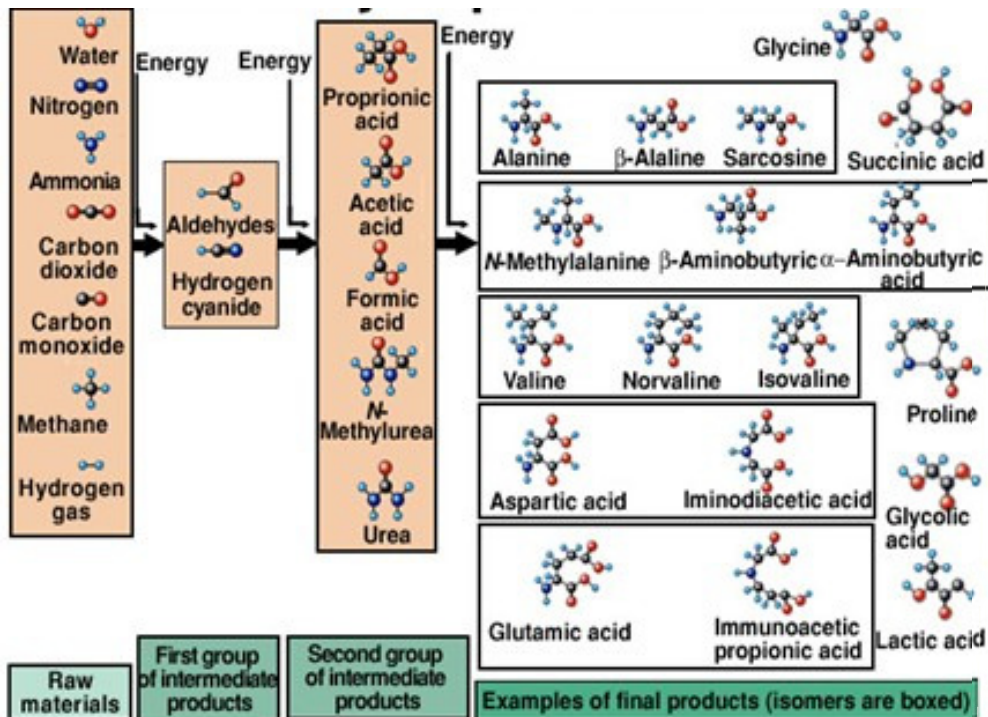


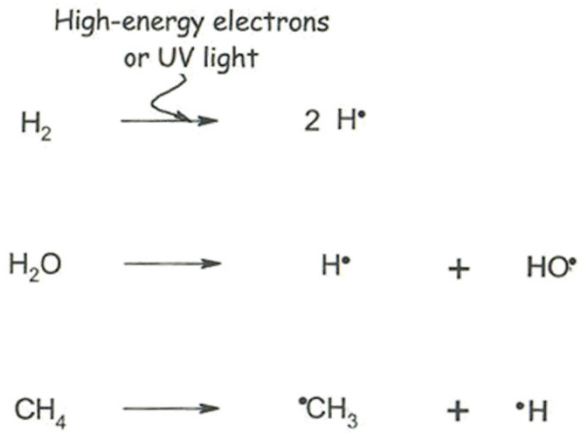
TABLE 4.3

Yields of the α -amino acids in the Miller-Urey experiment

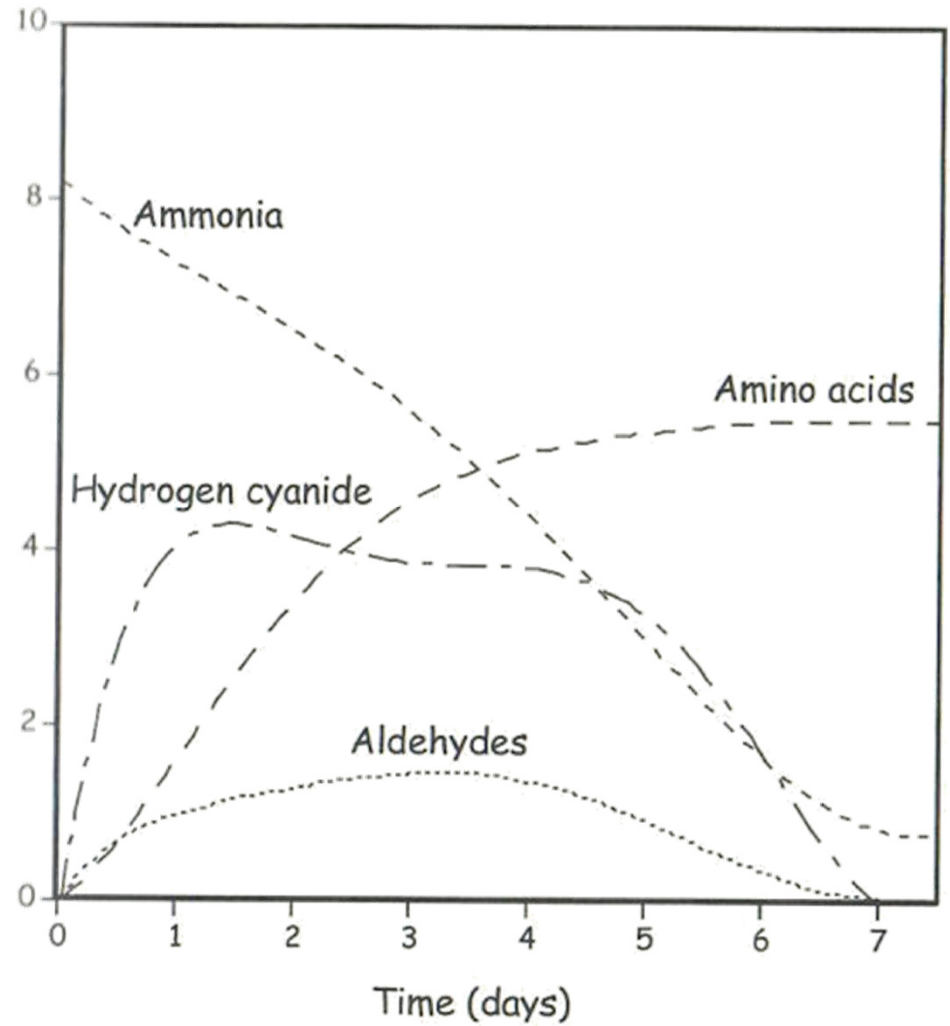
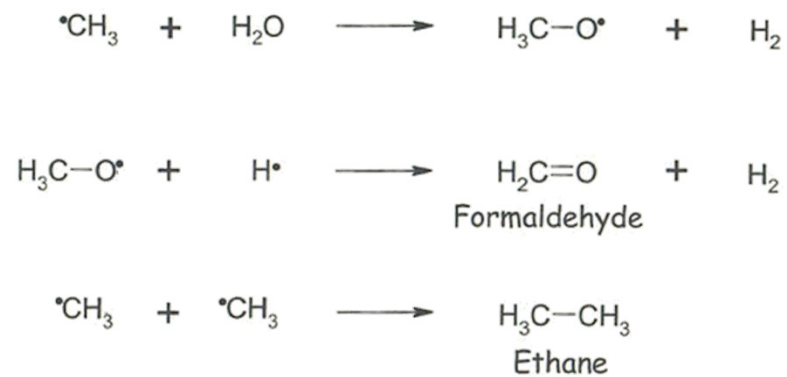
Amino acid	Yield (μ M)	Amino Acid	Yield (μ M)
Glycine	440	Norleucine	6
Alanine	790	Isoleucine	5
α -Aminobutyric acid	270	Serine	5
Norvaline	61	Alloisoleucine	5
Aspartate	34	Isovaline	5
α -Aminoisobutyric acid	30	Proline	2
Valine	20	Threonine	1
Leucine	11	Allothreonine	1
Glutamate	8	<i>Tert</i> -Leucine	0.02

Note: Proteogenic amino acids in bold type.

Generation of radicals



Radical reactions



Aminoacid production under hydrothermal conditions

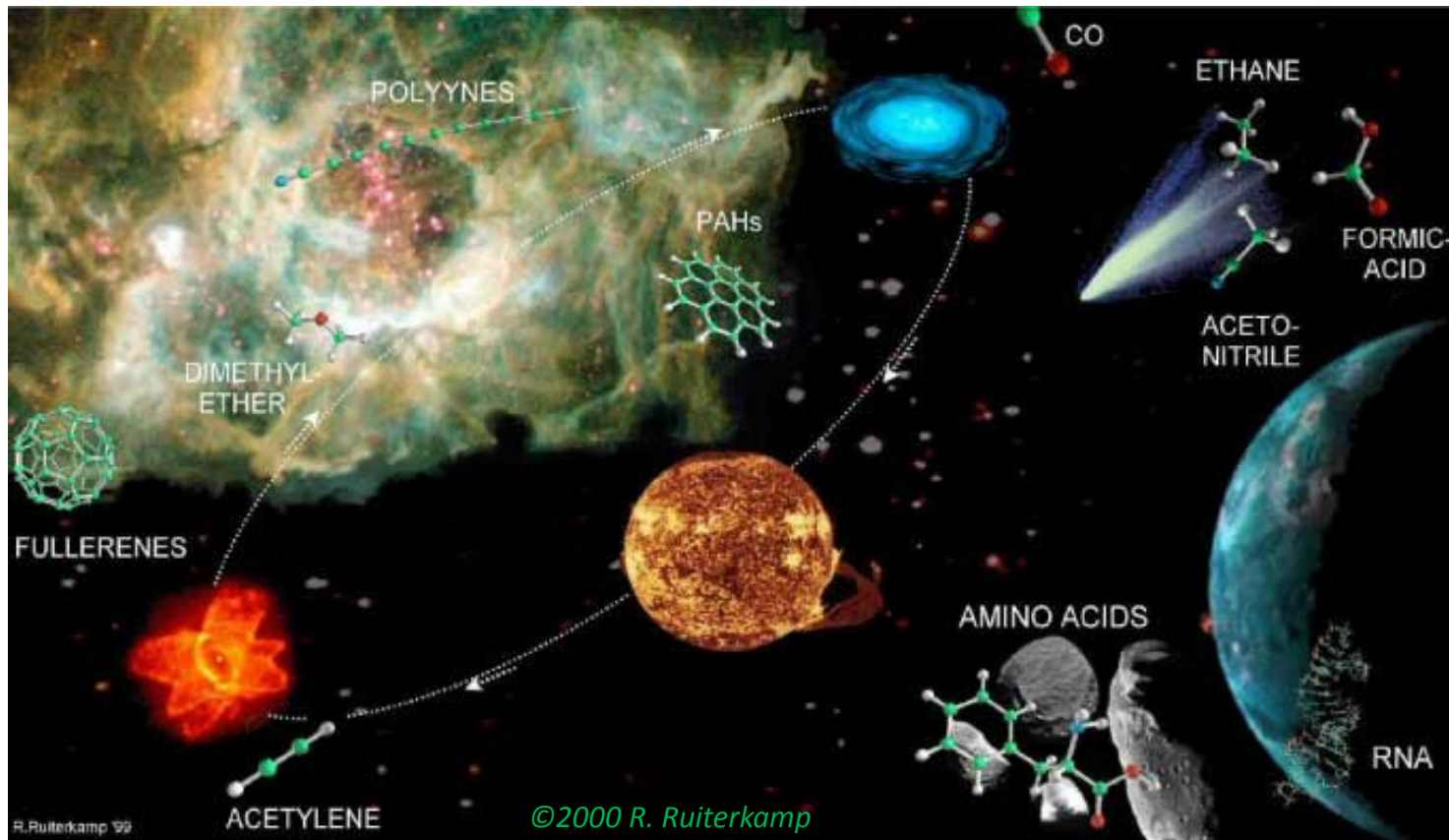
$\text{Ni(OH)}_2/\text{KCN}/\text{CO}$ in alkaline aqueous conditions (80-120°C) → α -amino and α -hydroxyacids

Huber, C.; Wächtershäuser, G. *Science* **2006**, *314*, 630–632

$\text{Ca(OH)}_2/\text{NiSO}_4/\text{KCN}/\text{CO}$ in alkaline (pH 9.1-12.9) aqueous conditions (145-280°C) → α -amino and α -hydroxyacids (higher yields): glycine, alanine, serine, glycolate, lactate, glycerate

Huber, C.; Eisenreich, H.; Wächtershäuser, G. *Tetrahedron Lett.* **2010**, *51*, 1069-1071

Extraterrestrial origin of biomolecules



Extraterrestrial origin of biomolecules



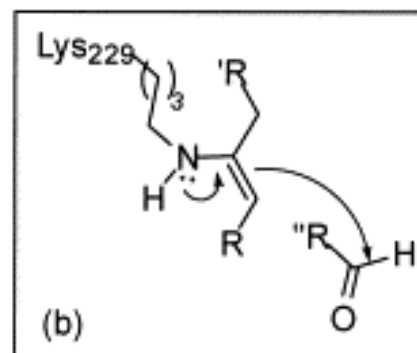
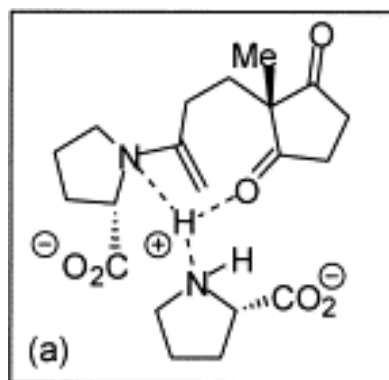
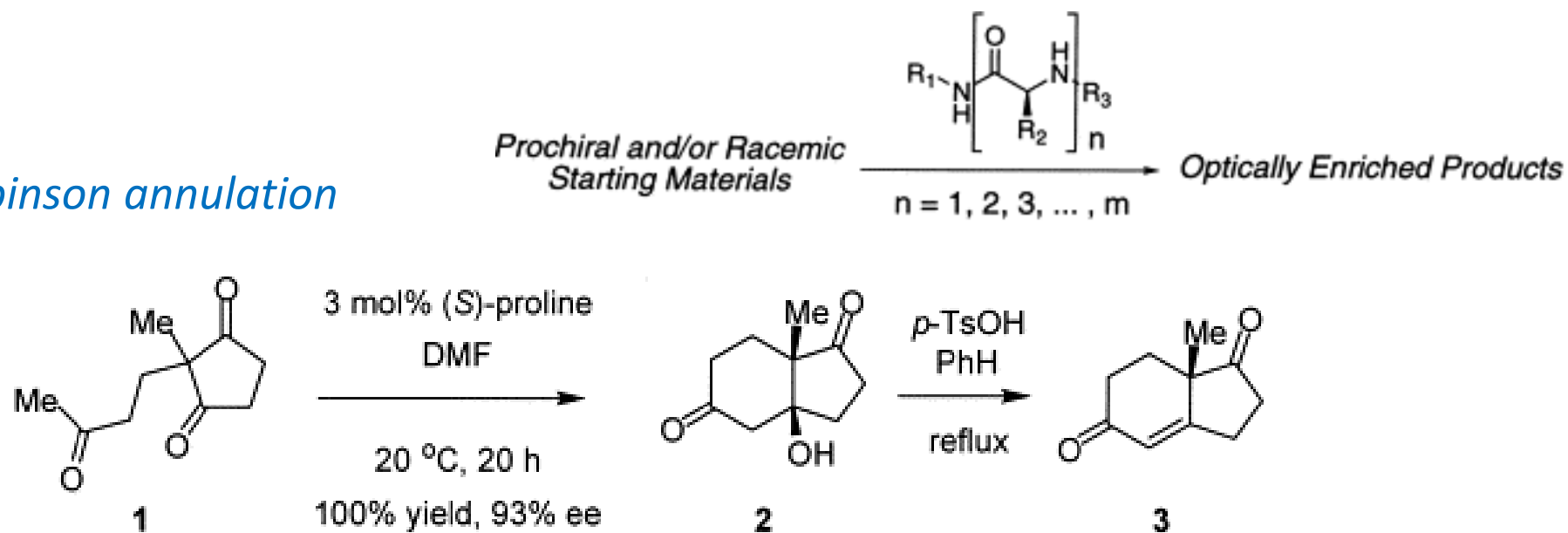
Murchison meteorite
chondrite

Table 1. Soluble Organic Compounds in the Murchison Meteorite^a

class of compounds	parts per million	<i>n</i> ^b
aliphatic hydrocarbons	>35	140
aromatic hydrocarbons	15–28	87
polar hydrocarbons	<120	10 ^d
carboxylic acids	>300	48 ^d
amino acids	60	75 ^d
imino acids	nd ^c	10
hydroxy acids	15	7
dicarboxylic acids	>30	17 ^d
dicarboximides	>50	2
pyridinecarboxylic acids	>7	7
sulfonic acids	67	4
phosphonic acids	2	4
<i>N</i> -heterocycles	7	31
amines	13	20 ^d
amides	nd ^c	27
polyols	30	19

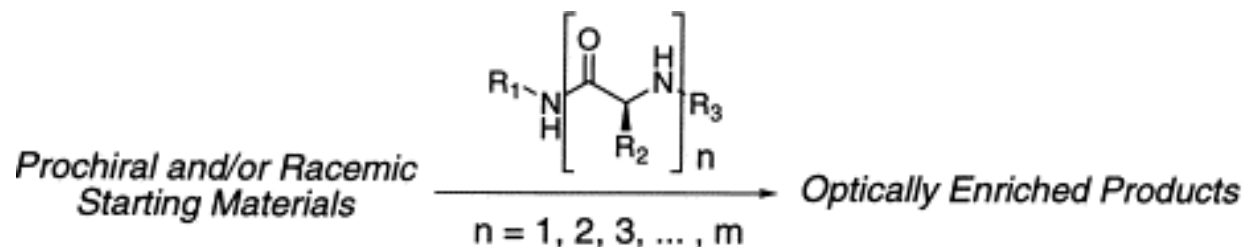
Catalytic properties of aminoacids - organocatalysis

Robinson annulation

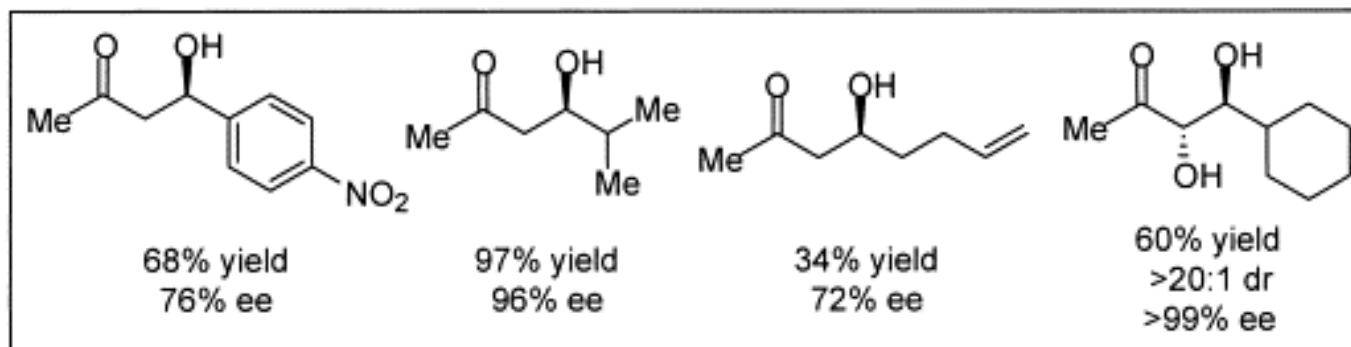
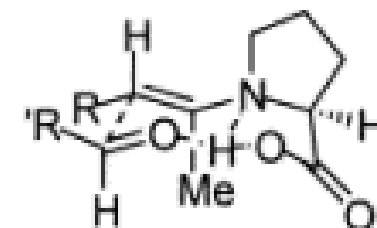
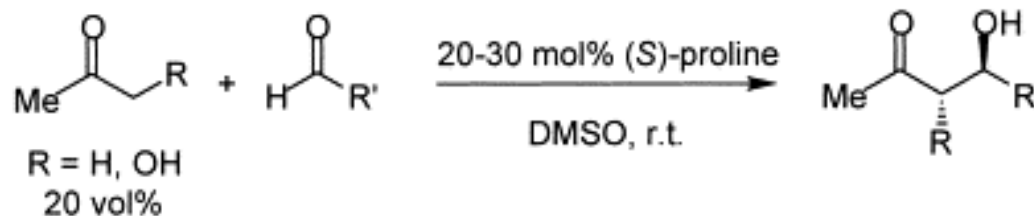


Jarvo, E. R., Miller, S. J. *Tetrahedron* **2002**, 58(13), 2481-2495.

Catalytic properties of aminoacids - organocatalysis

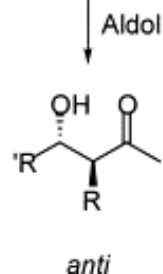
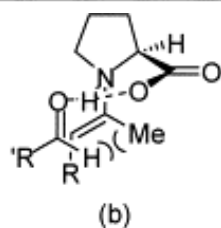
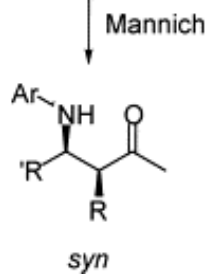
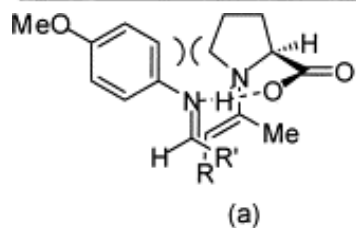
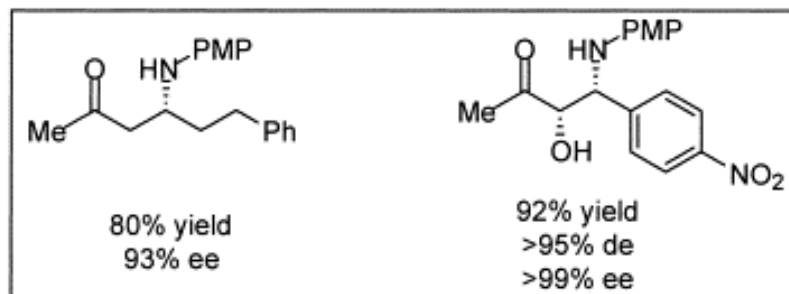
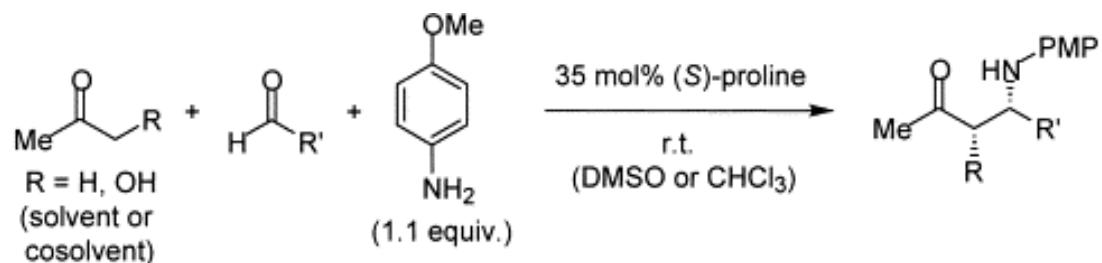


aldol reaction



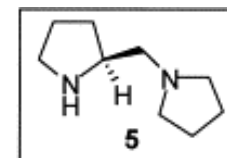
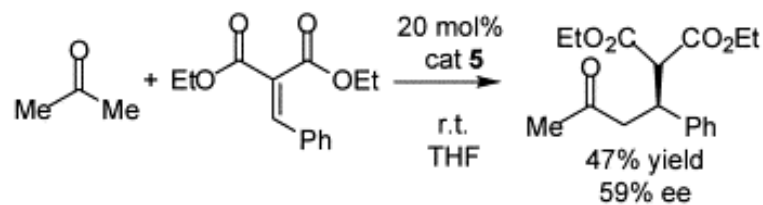
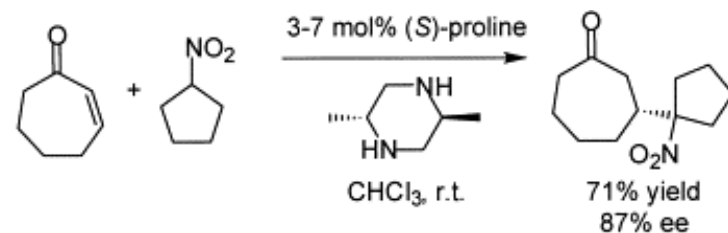
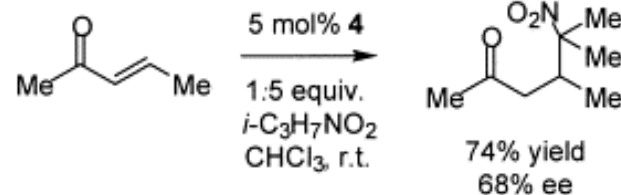
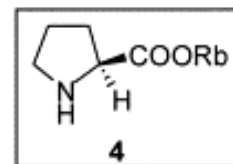
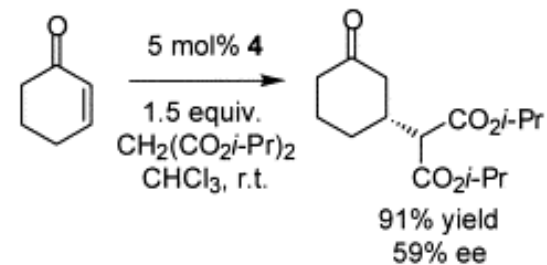
Jarvo, E. R., Miller, S. J. *Tetrahedron* **2002**, 58(13), 2481-2495.

Mannich reaction



organocatalysis

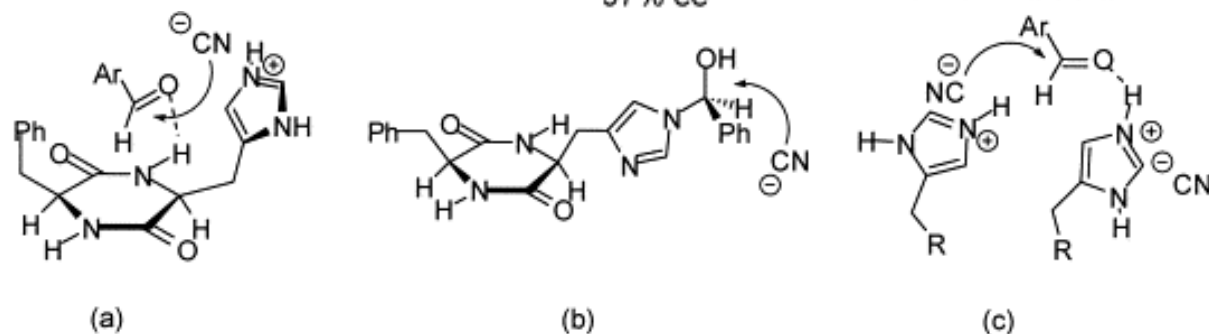
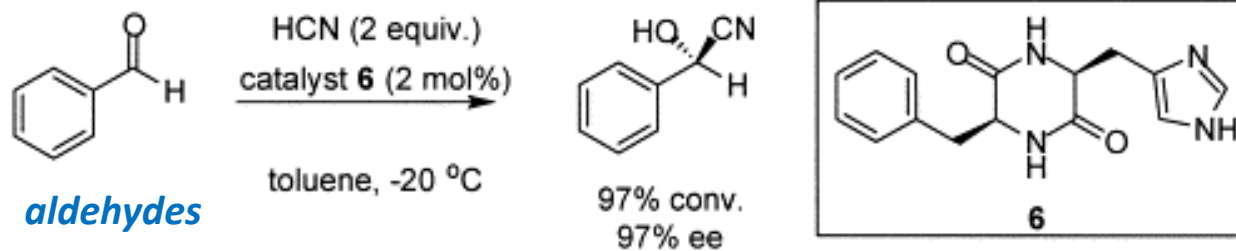
Michael addition



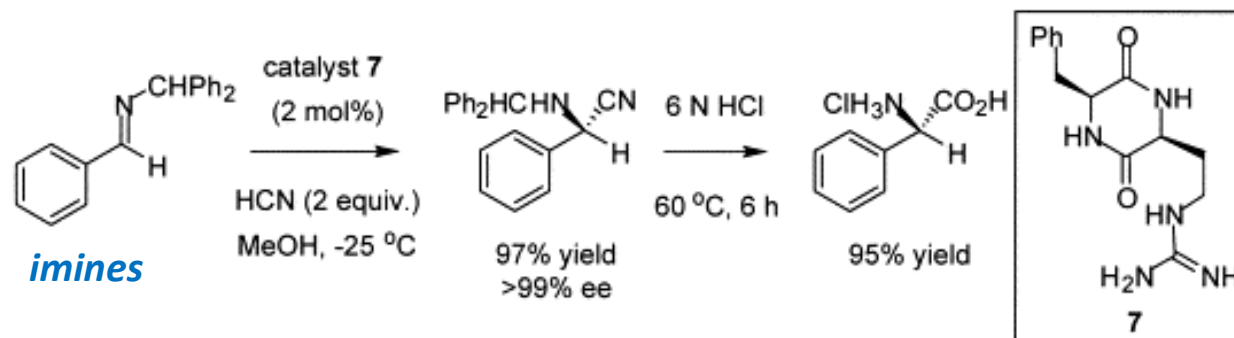
Jarvo, E. R., Miller, S. J. *Tetrahedron* **2002**, *58*(13), 2481-2495.

Catalytic properties of aminoacids - organocatalysis

Hydrocyanation



asymmetric Strecker reaction!!!



Jarvo, E. R., Miller, S. J. *Tetrahedron* **2002**, 58(13), 2481-2495.

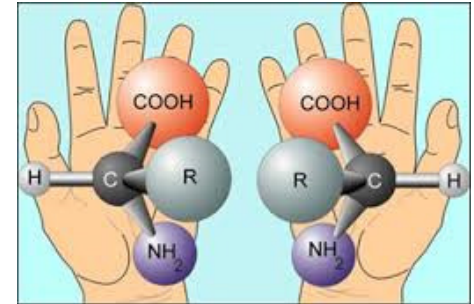
The origins of homochirality

Currently known biopolymers are homochiral

Structural propensity and catalytic activity strongly depends on the enantopurity

→ Homochirality must have been involved early in the process of life formation

→ Chiral monomers could be only partially enantioenriched



General cause of homochirality:

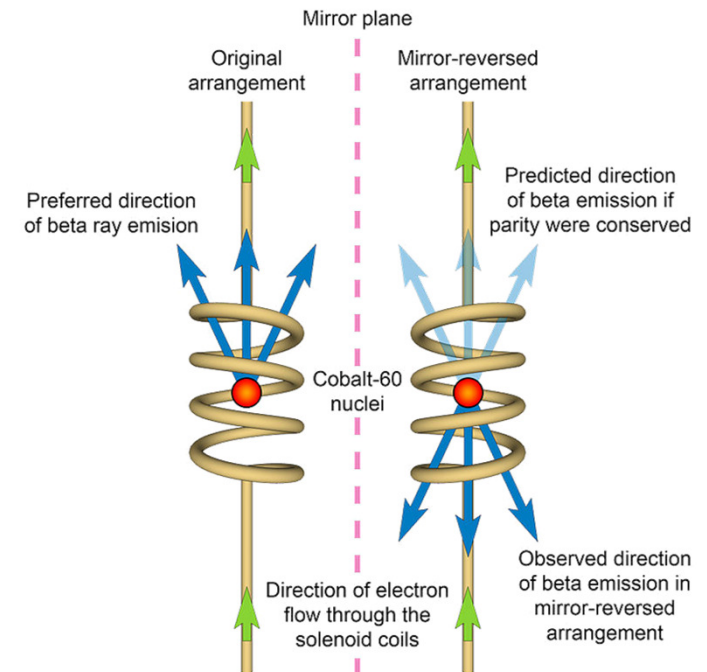
the initial symmetry breaking + subsequent asymmetry amplification:

- *The parity violation*
- *Stochastic symmetry disturbances*

Electroweak interactions and the parity violation principle cause *L*-aminoacids and *D*-sugars to be SLIGHTLY MORE STABLE than their enantiomers

Differentiation in left and right handedness is inherent property of weak interactions

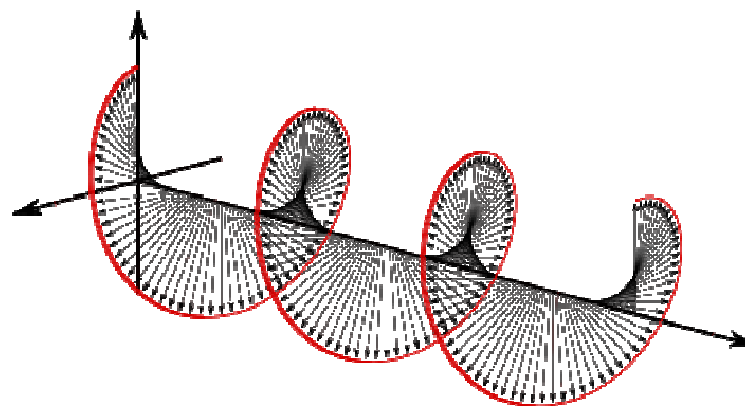
Chien-Shiung Wu (1956) – experiment on ^{60}Co decay



The origins of homochirality

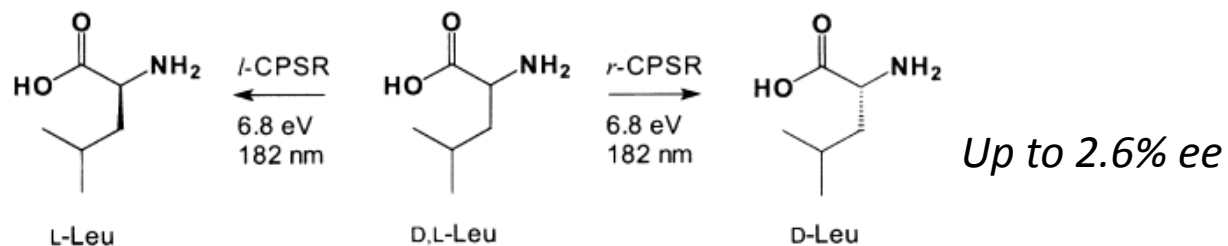


Circularly polarized light (CPL) from gamma ray bursts



K. Wiersema et al., *Nature* **509** 201, 2014

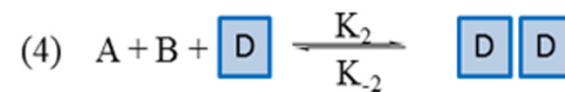
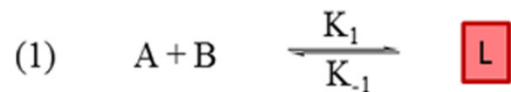
Small enantiomeric excess can be obtained by enantioselective degradation of aminoacids with CPL



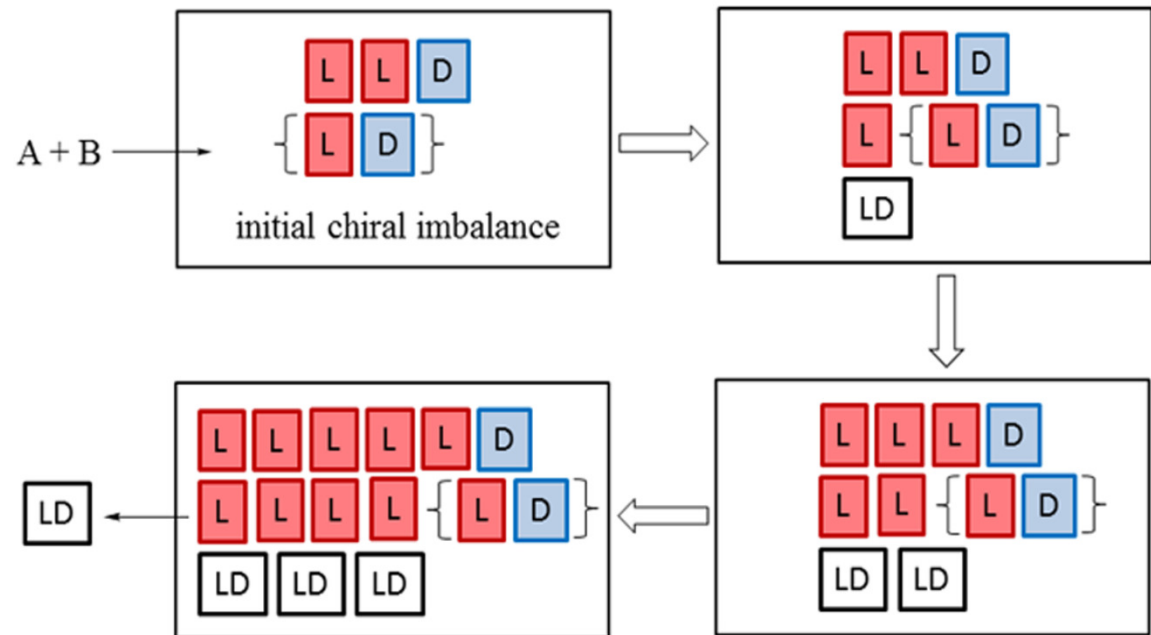
Meierhenrich, U. J.; Nahon, L.; Alcaraz, C.; Bredehoff, J. H.; Hoffmann, S. V.; Barbier, B.; Brack, A. *Angew. Chem., Int. Ed.* 2005, 44, 5630

Stochastic induction of asymmetry – Frank model

Reactions (3) and (4) are autocatalytic

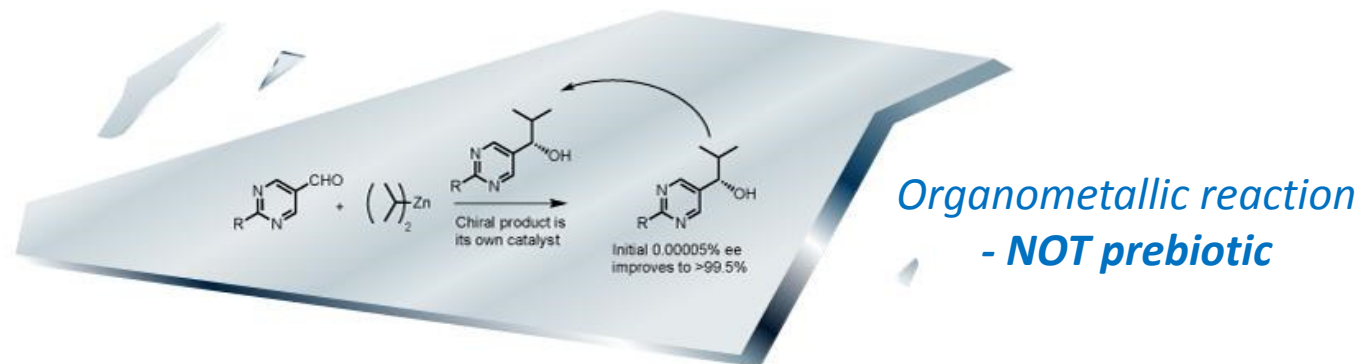


Open flux reactor in non-equilibrium stationary state

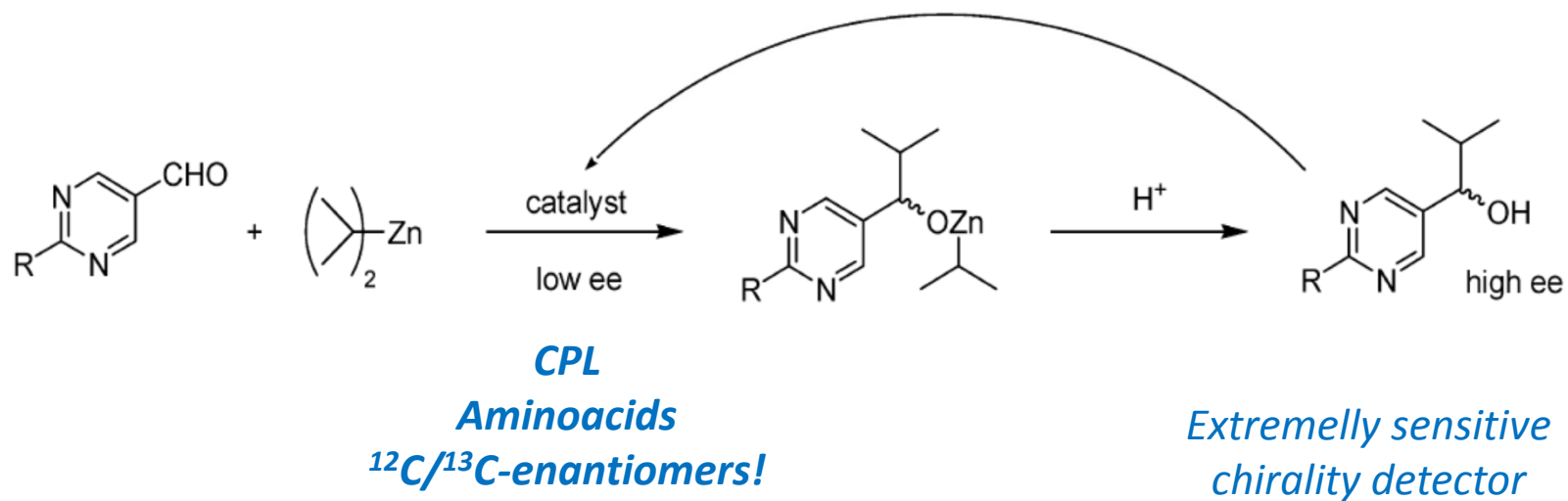


If a chiral dissipative structure catalyzes its own formation and inhibits formation of the opposite enantiomer, any stochastic symmetry breaking in the system will be amplified

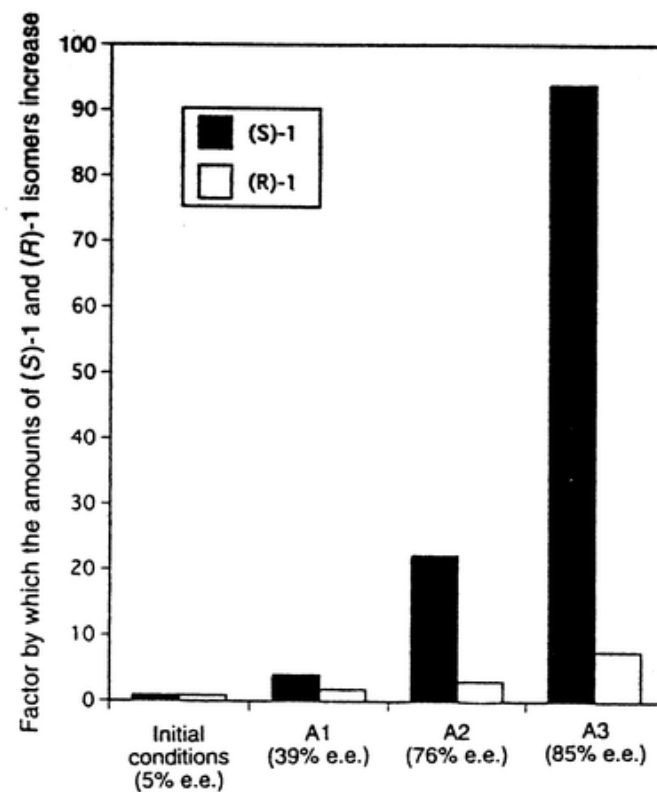
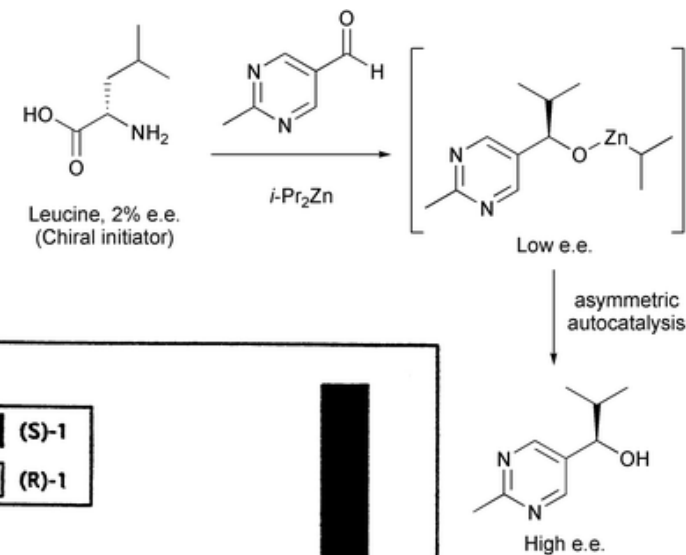
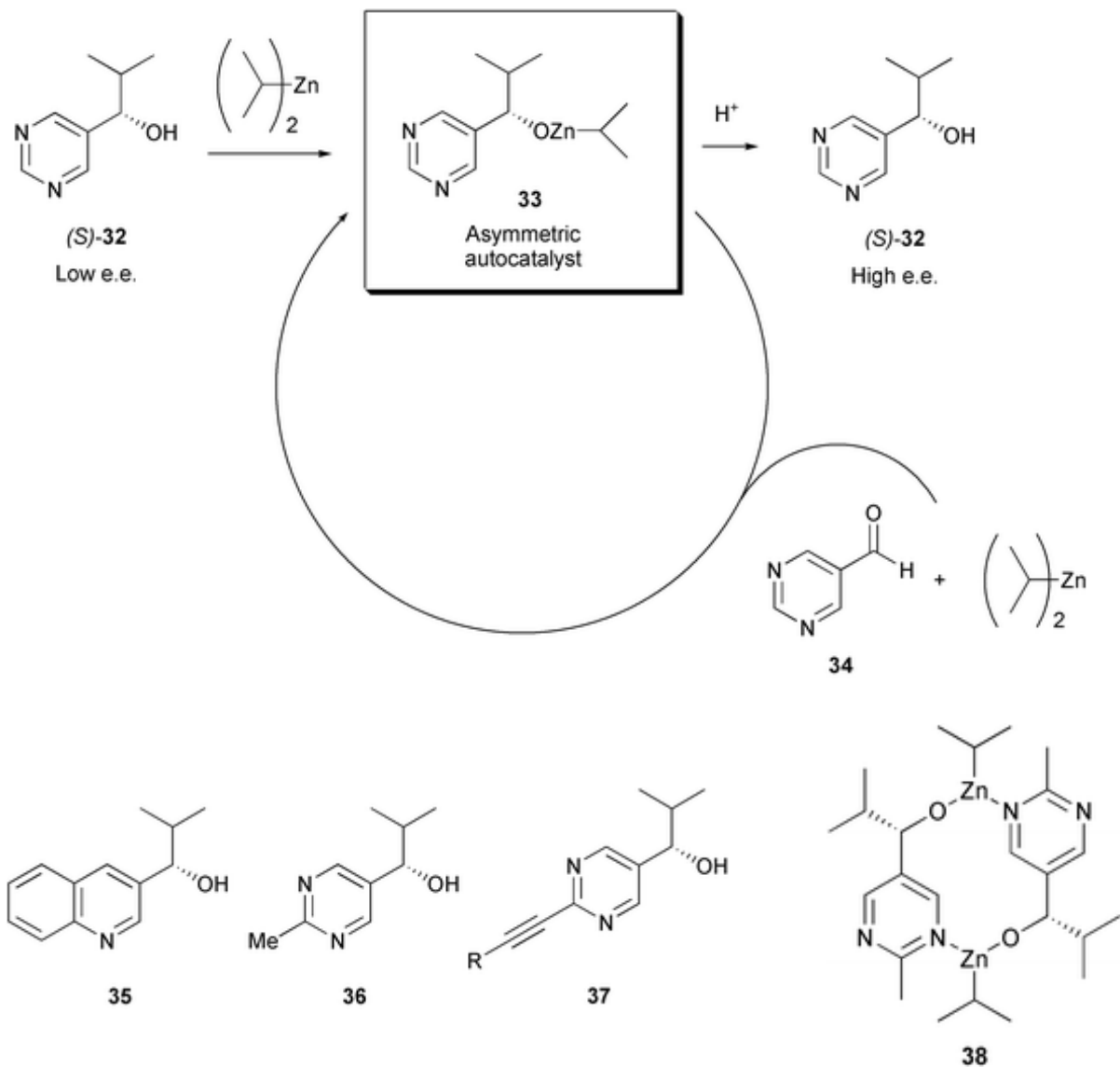
autocatalytic Soai reaction – extreme chirality amplification



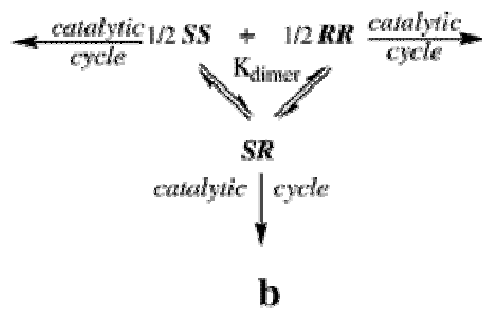
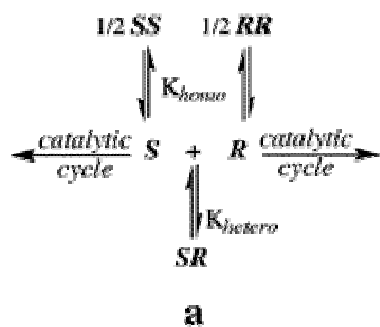
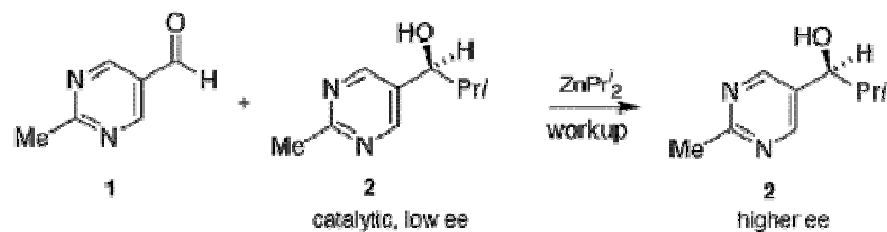
Scheme 9. Soai Autocatalytic Reaction



autocatalytic Soai reaction – extreme chirality amplification

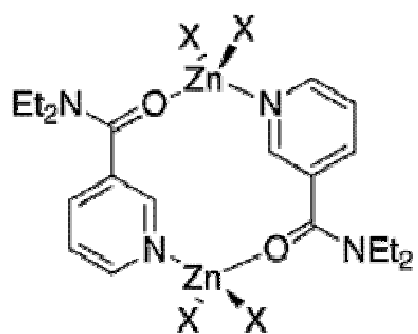


autocatalytic Soai reaction – extreme chirality amplification

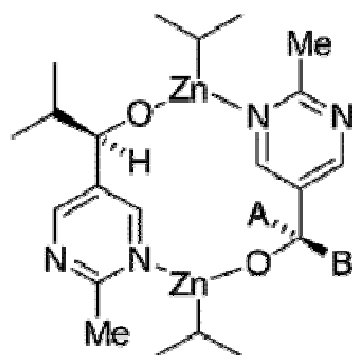


$$g = \frac{\text{activity of } [SR]}{\text{activity of } [RR]} \quad \beta = \frac{[SR]}{[RR] + [SS]} \quad K = \frac{([SR])^2}{([RR])([SS])}$$

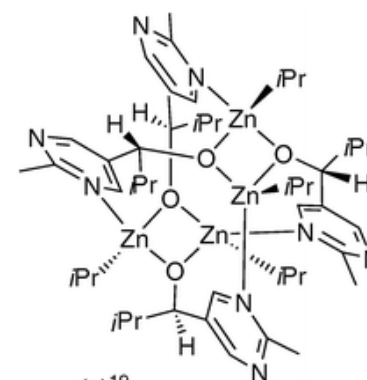
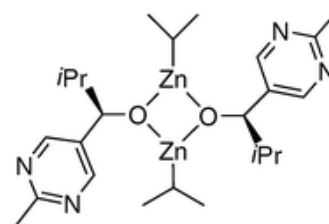
$$ee_{dx} = \frac{[RR] - [SS]}{[RR] + [SS] + g[SR]} \quad ee_{x+dx} = \frac{ee_x[2] + ee_{dx}\frac{dx}{2}[1]_0}{[2] + \frac{dx}{2}[1]_0} \quad (2)$$



7a, X = Cl,
7b, X = SCN

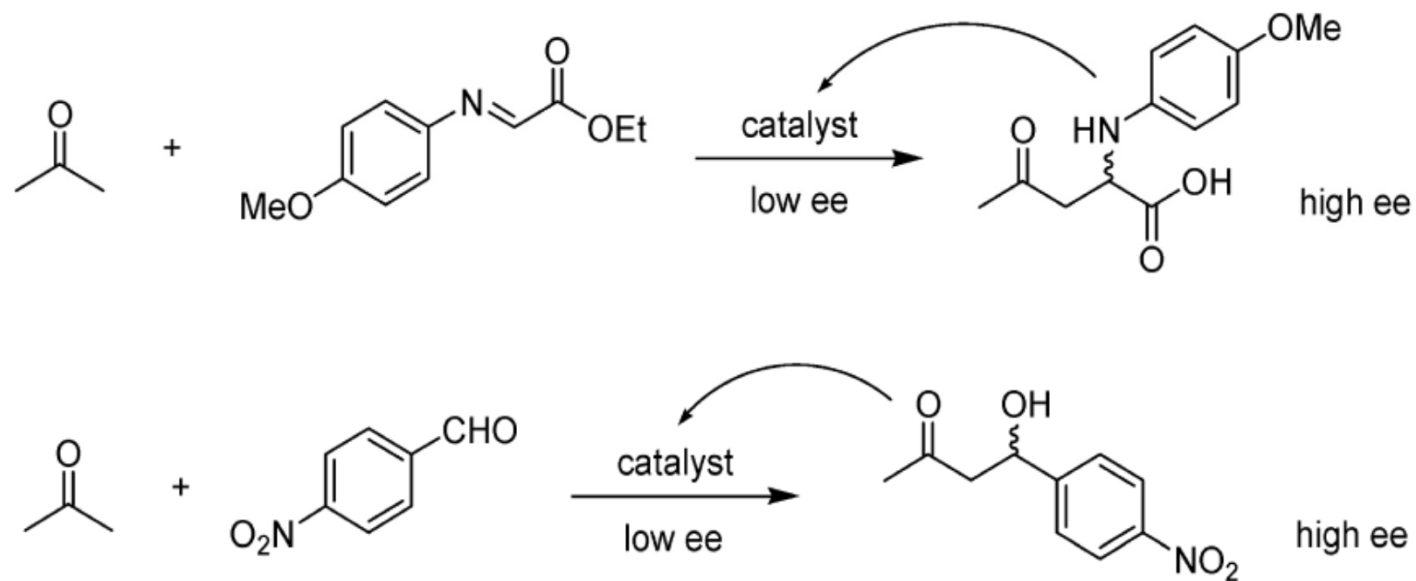


(S,S)-8 A = H, B = Pr'
 (R,S)-8 A = Pr', B = H



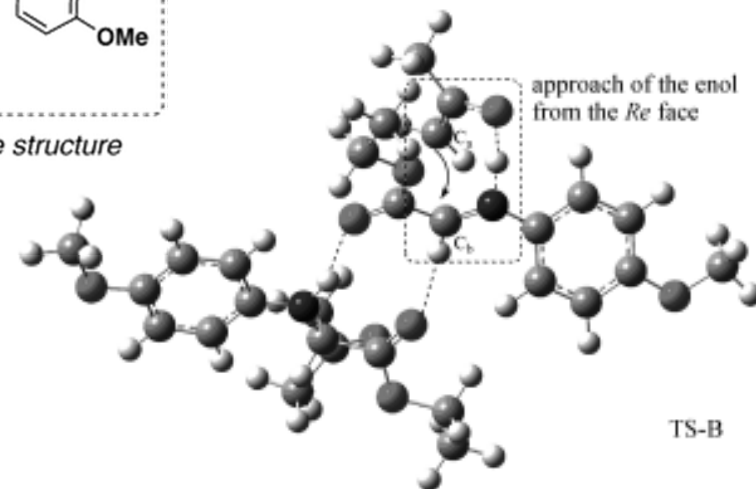
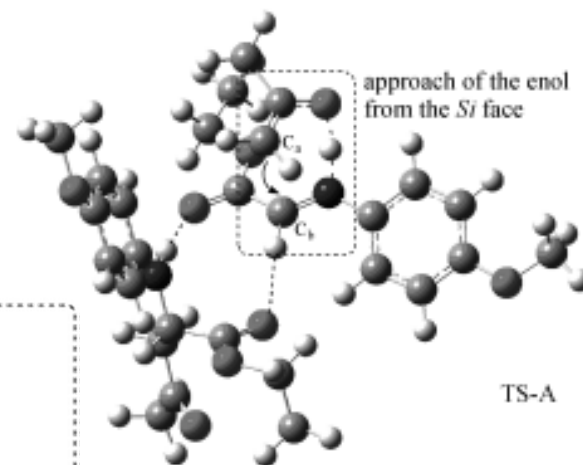
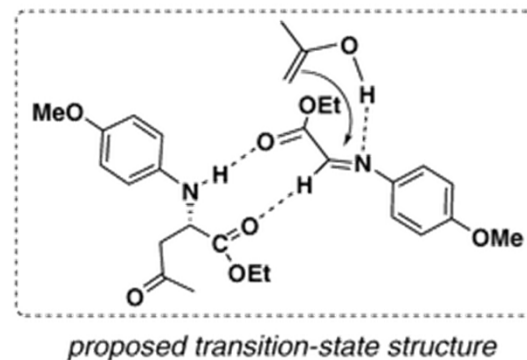
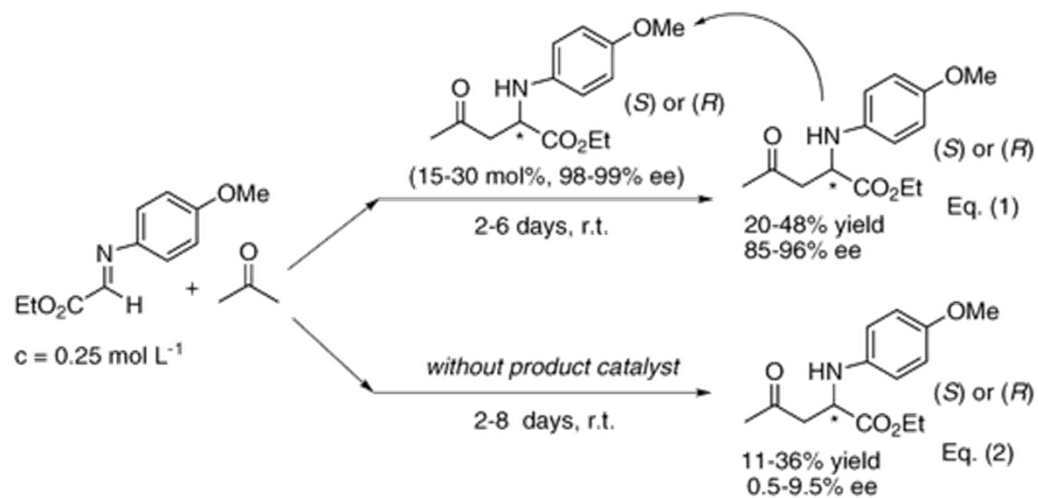
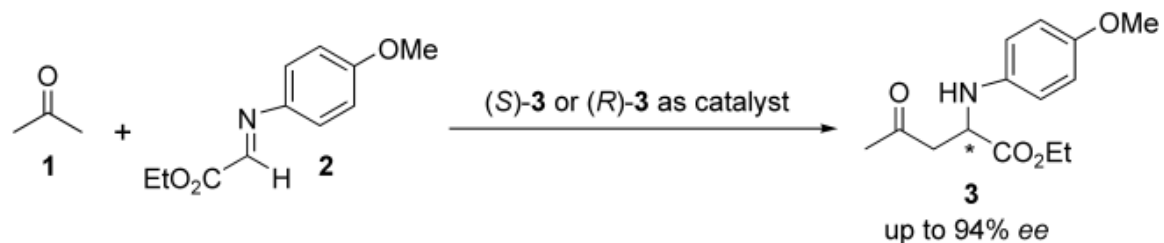
autocatalytic organic reactions

Scheme 10. Mannich and Aldol Autocatalytic Reactions^a



Meaningful transformations for the prebiotic syntheses of aminoacids and sugars

autocatalytic organic reactions



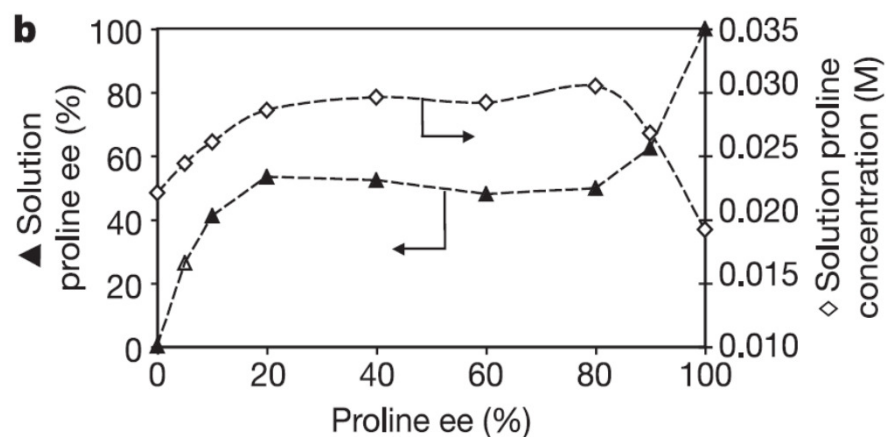
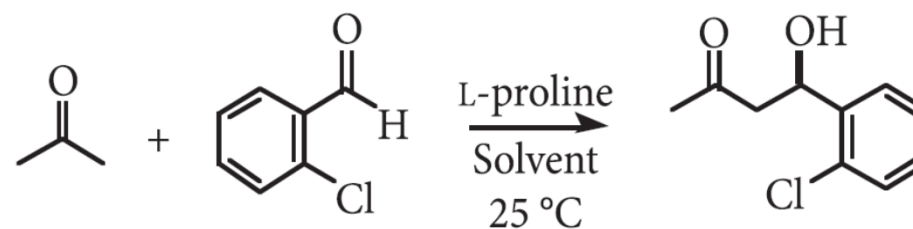
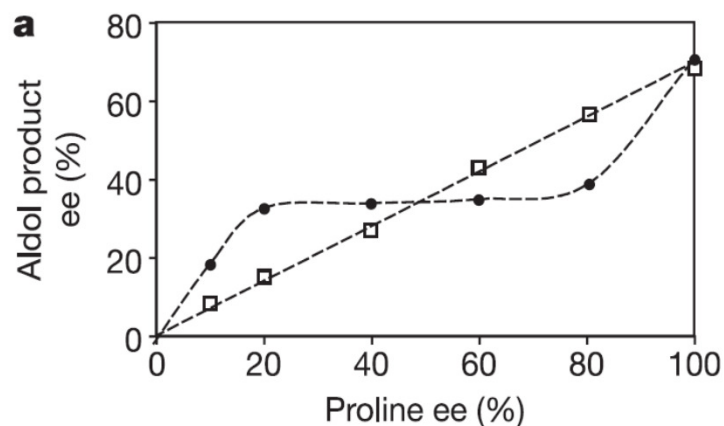
Organocatalysis – the origin of homochirality

Table 1. Enantiomeric concentration amplification of phenylalanine after two crystallizations from water

Component	Initial ee, %	Final ee, %
D	10	90.0 ± 3.7
	5	91.7 ± 1.5
	1	87.2 ± 2.0
L	10	88.3 ± 1.1
	5	88.6 ± 0.9
	1	90.9 ± 0.3

Solutions with as little as 1% enantiomeric excess (ee) of D- or L-phenylalanine are amplified to 90% ee (a 95/5 ratio) by two successive evaporations to precipitate the racemate. Such a process on the prebiotic earth could lead to a mechanism by which meteoritic chiral α -alkyl amino acids could form solutions with high ee values that were needed for the beginning of biology.

Chirality amplification in biphasic systems



Reaction and solution behaviour as a function of the overall proline enantiomeric excess.

a, Product enantiomeric excess versus proline enantiomeric excess for the aldol reaction of equation

b, Solution proline enantiomeric excess (left axis, triangles) and solution proline concentration (right axis, diamonds) as a function of the overall enantiomeric excess for proline at 0.1 M

Chirality amplification in biphasic systems

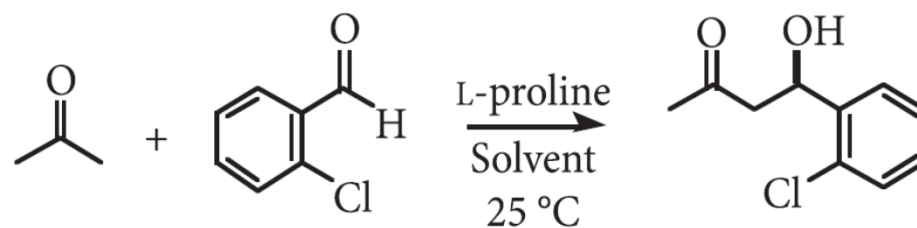
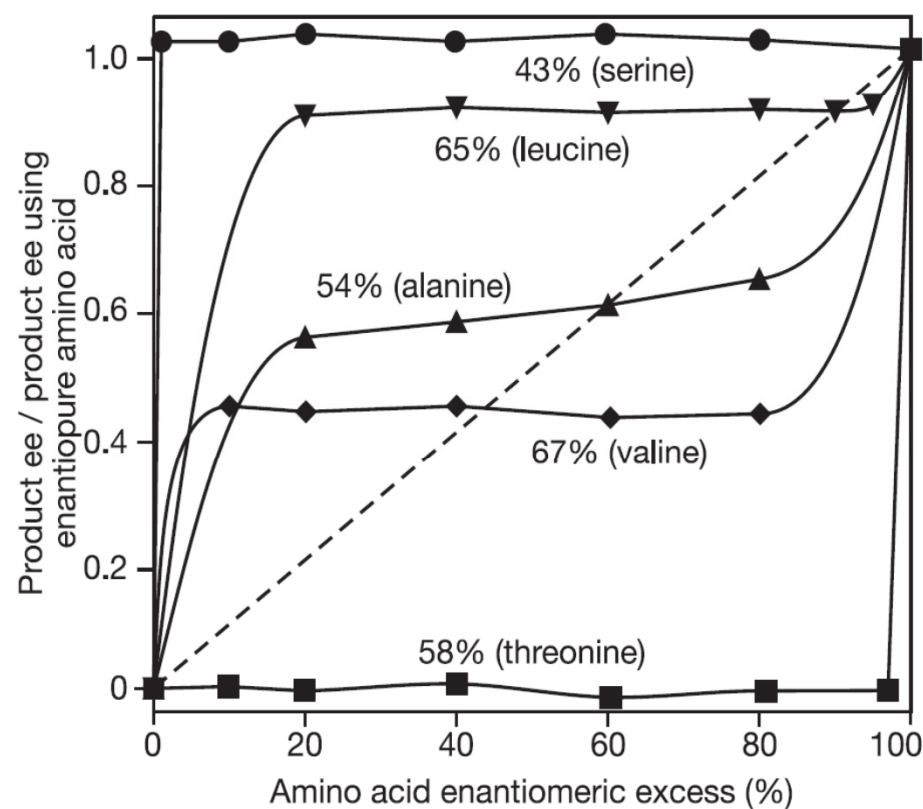


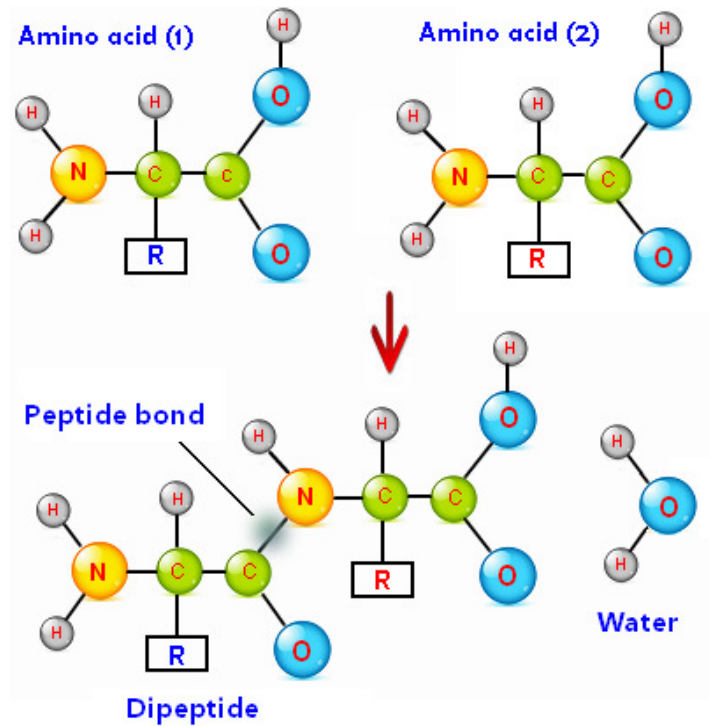
Table 1 | Solution enantiomeric excess at the eutectic point in water at 25 °C for selected amino acids

Amino acid	ee of solution at eutectic (%)	Amino acid	ee of solution at eutectic (%)
Threonine	0	Methionine	85
Valine	46	Leucine	87
Alanine	60	Histidine	93
Phenylalanine	83	Serine	>99

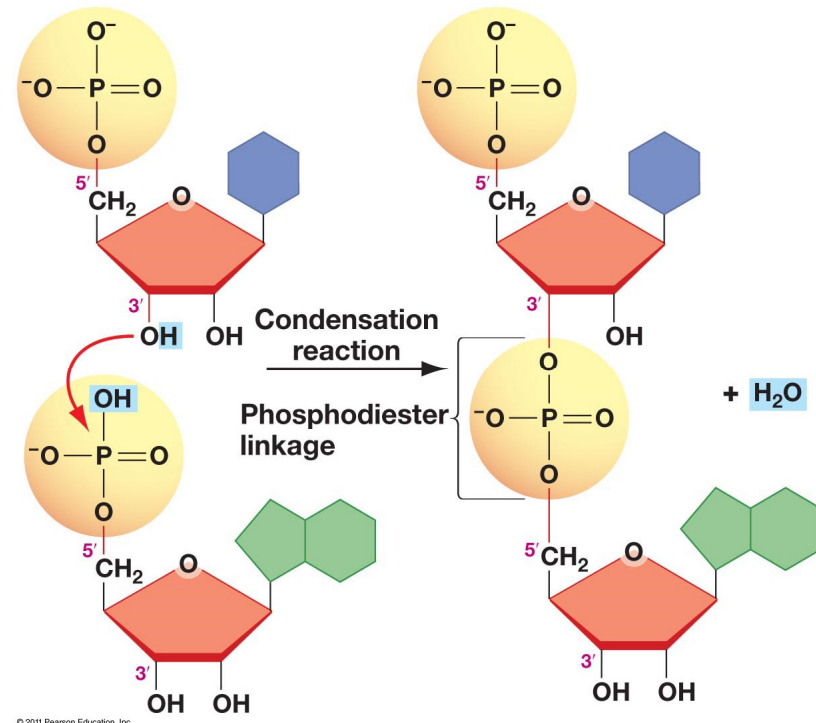


Vital chemical reactions

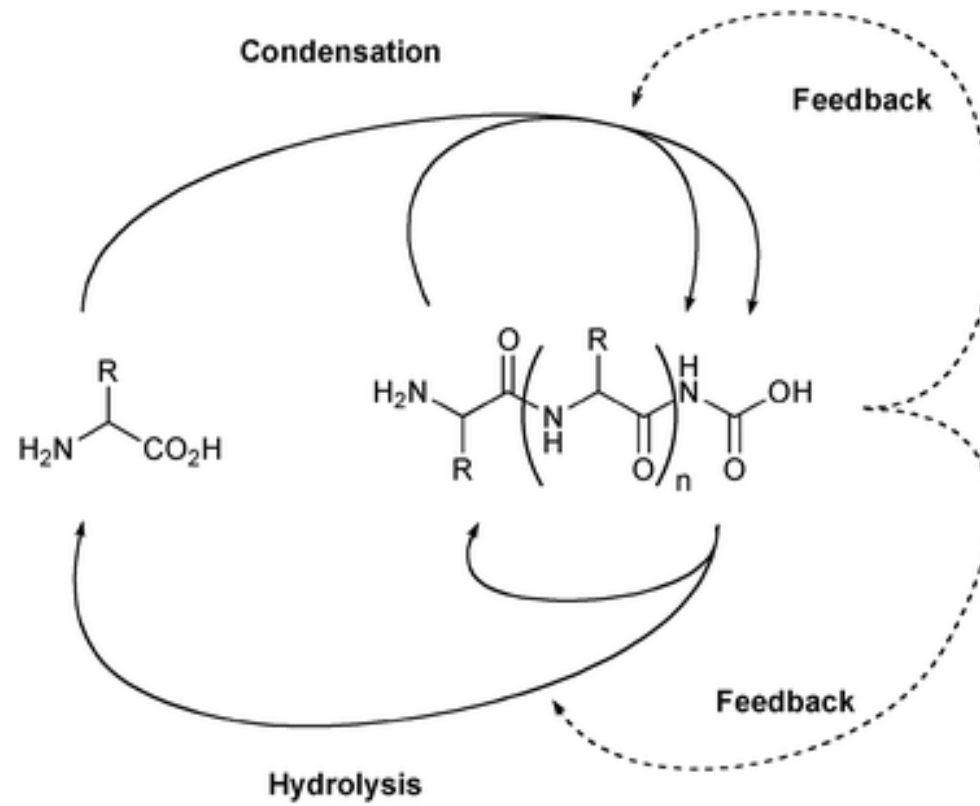
Amino acid polymerization



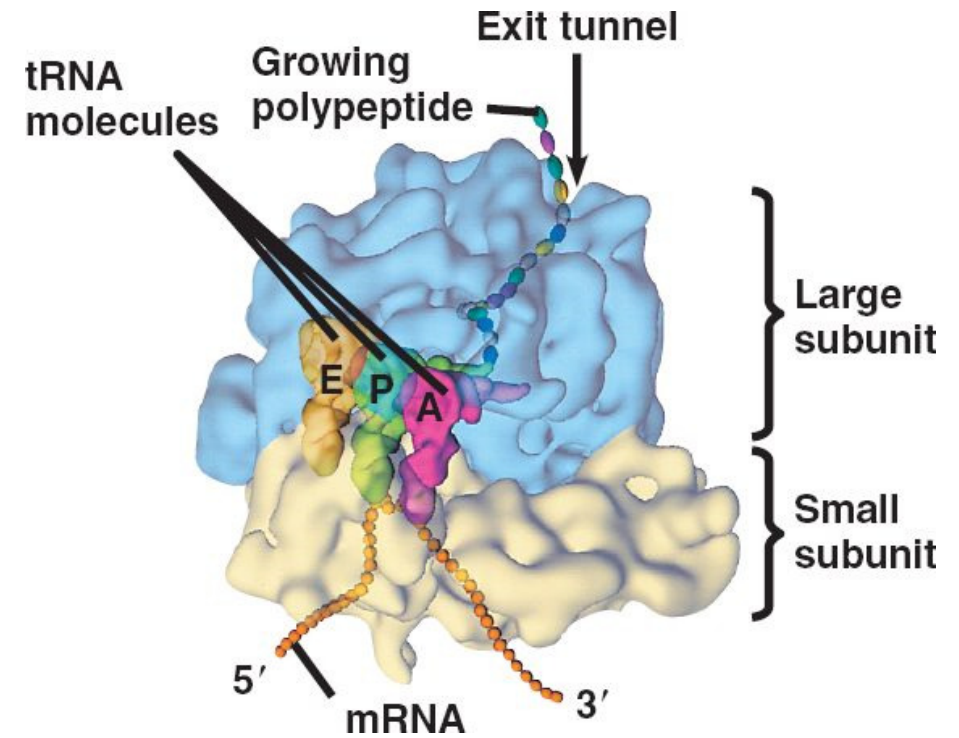
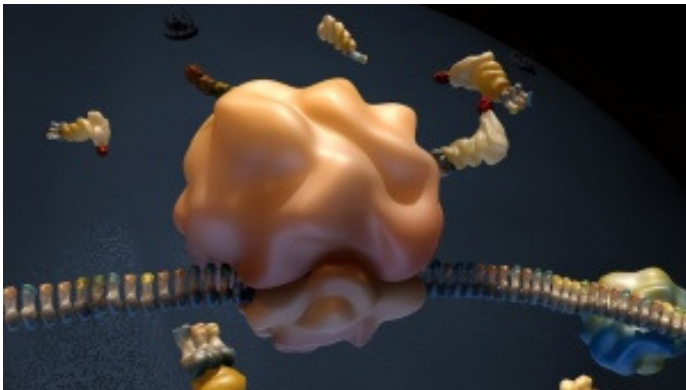
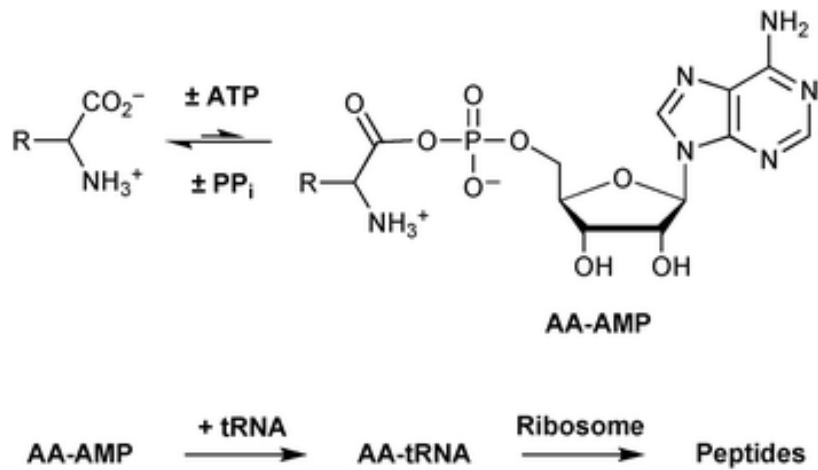
Nucleotide polymerization



Condensation of aminoacids into peptides

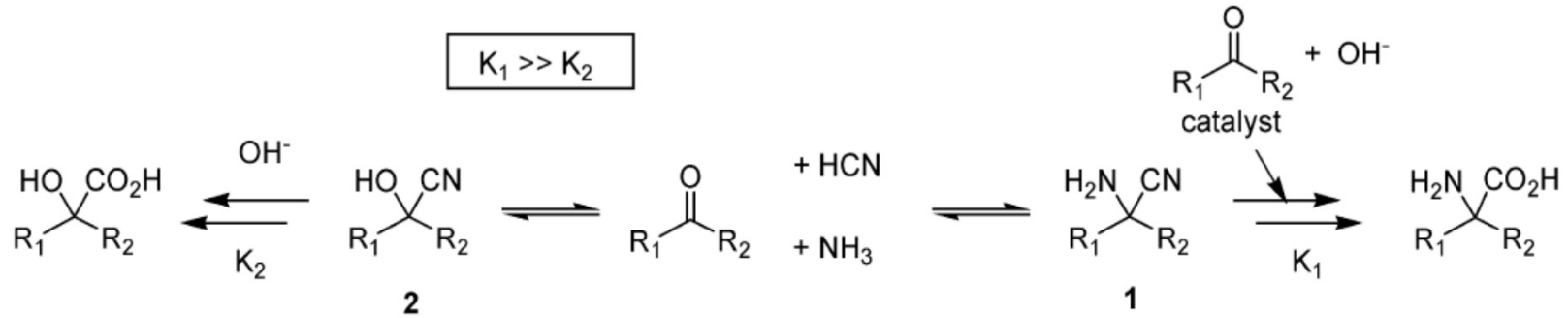


Biochemical condensation of amino acids into peptides

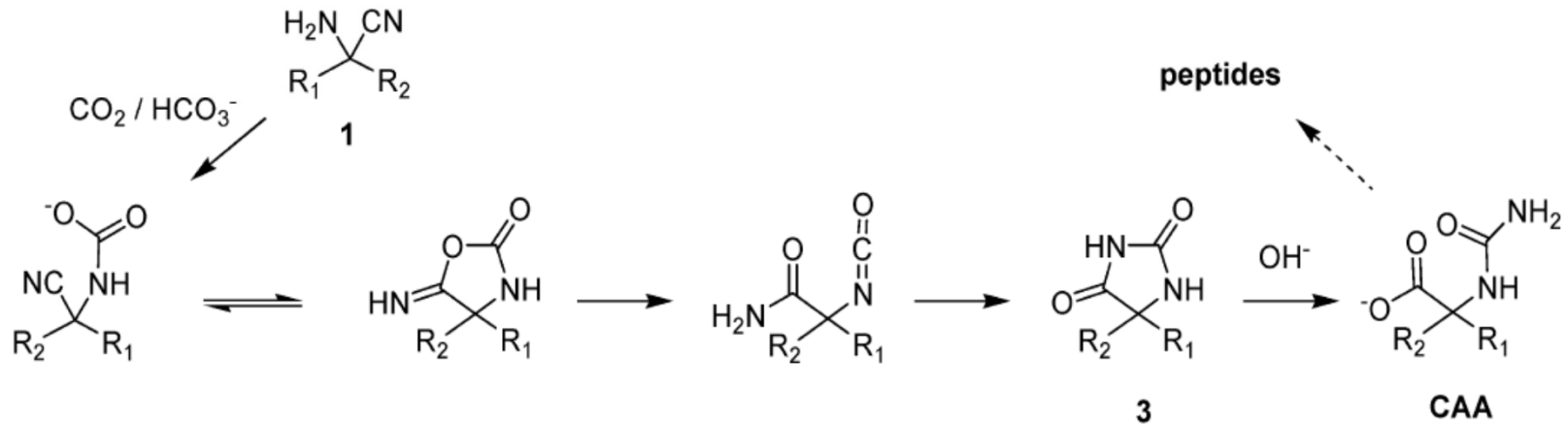


Condensation of aminoacids into peptides

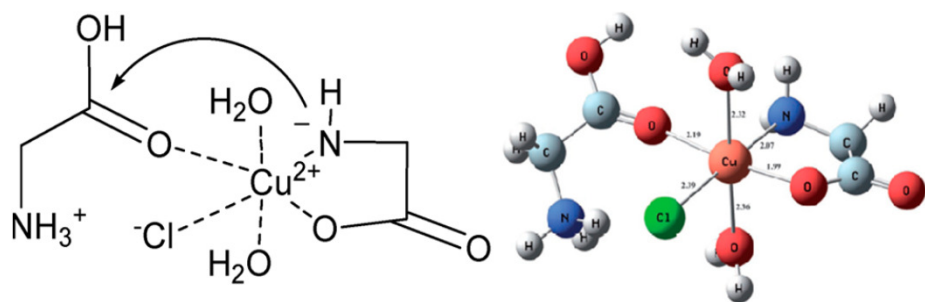
Scheme 1. Synthesis of α -Amino Acids through the Strecker Reaction



Scheme 2. Bücherer–Bergs Hydrolysis of α -Aminonitriles



Prebiotically relevant peptide condensation agents



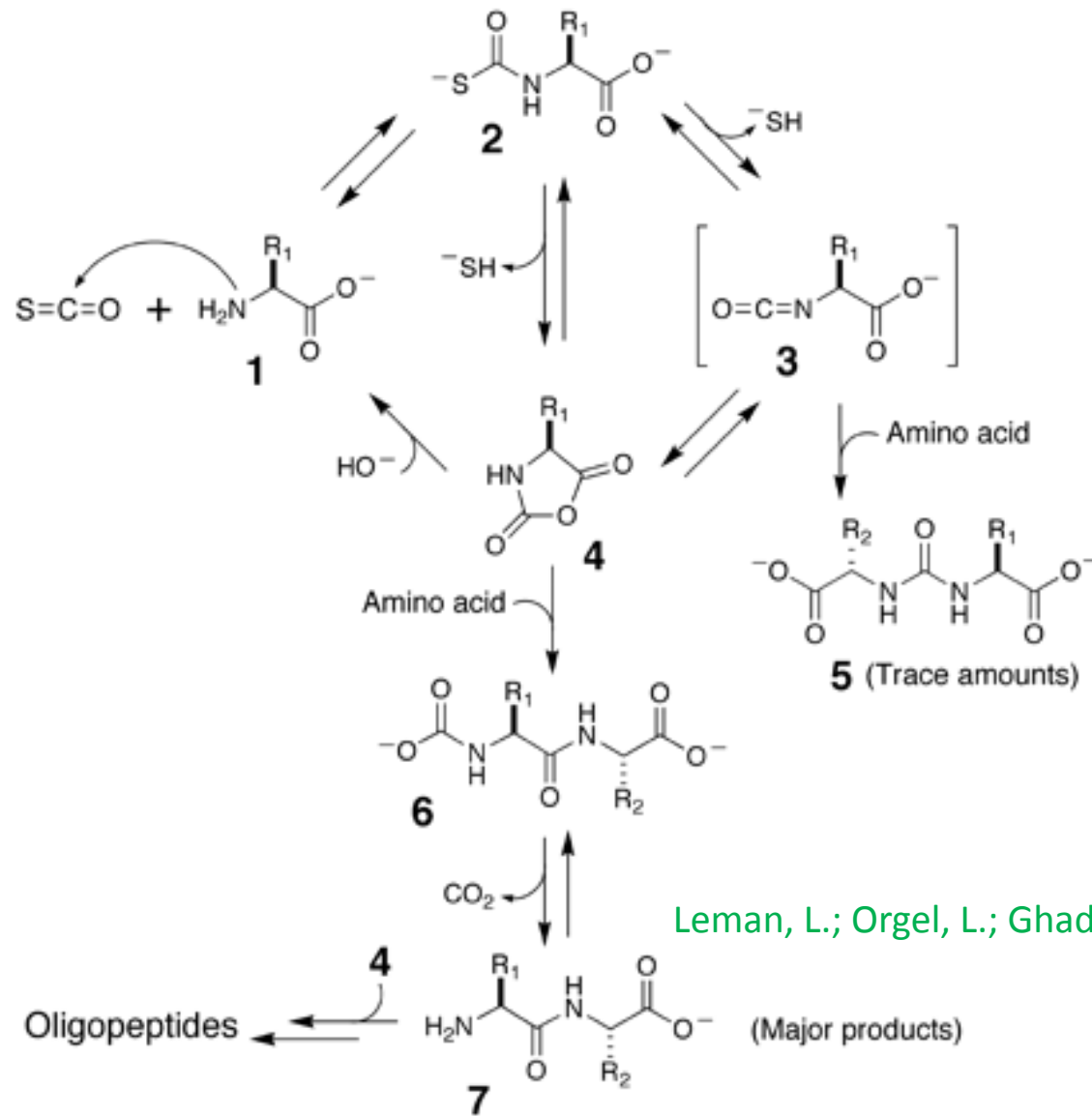
SIPF copper complex geometry with two glycine ligands, optimized by ab initio Hartree–Fock calculations.

Rode, B. M.; Fitz, D.; Jakschitz, T. *Chem. Biodiversity* **2007**, 4,2674.

Entry	Activating agent	Hydrolysis/ hydration product	$\Delta G^{0'}/$ kJ mol ⁻¹
1	NH ₂ CONH ₂	CO ₂ + NH ₃	-16 ^a
2	COS (g)	CO ₂ + H ₂ S	-17 ^a
3	Pyrophosphate	Phosphate	-19 ^b
4	CO (g)	HCO ₂ H	-16 ^a
5	HNCO	CO ₂ + NH ₃	-54 ^a
6	HCN	HCO ₂ H + NH ₃	-75 ^a
7	RCN	RCO ₂ H + NH ₃	-80 ^c
8	NH ₂ CN	Isourea	-83 ^d
9	HNCNH	Isourea	-97 ^d
10	HCCH (g)	CH ₃ CHO	-112 ^a

Danger, G.; Plasson, R.; Pascal, R. *Chem. Soc. Rev.* **2012**, 41, 5416.

Carbonyl sulfide – condensing agent



Leman, L.; Orgel, L.; Ghadiri, M. R. *Science* **2004**, *306*, 283-286.

Carbonyl sulfide – condensing agent

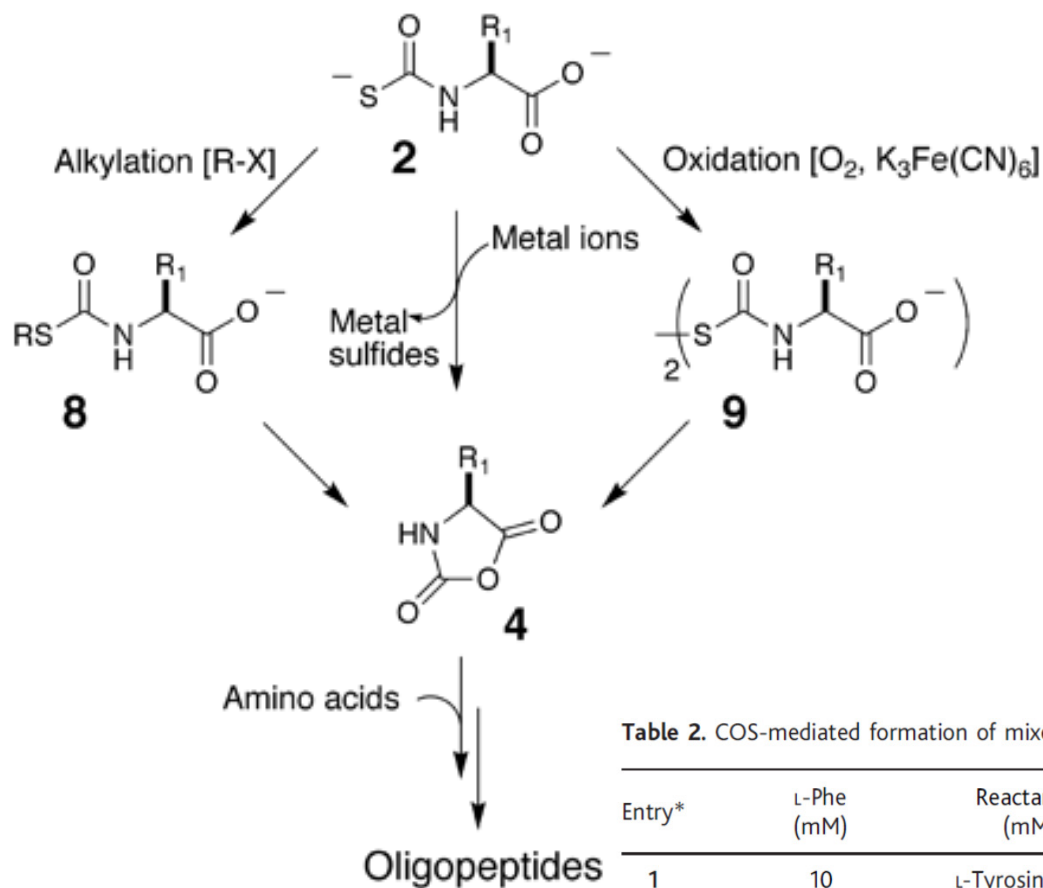


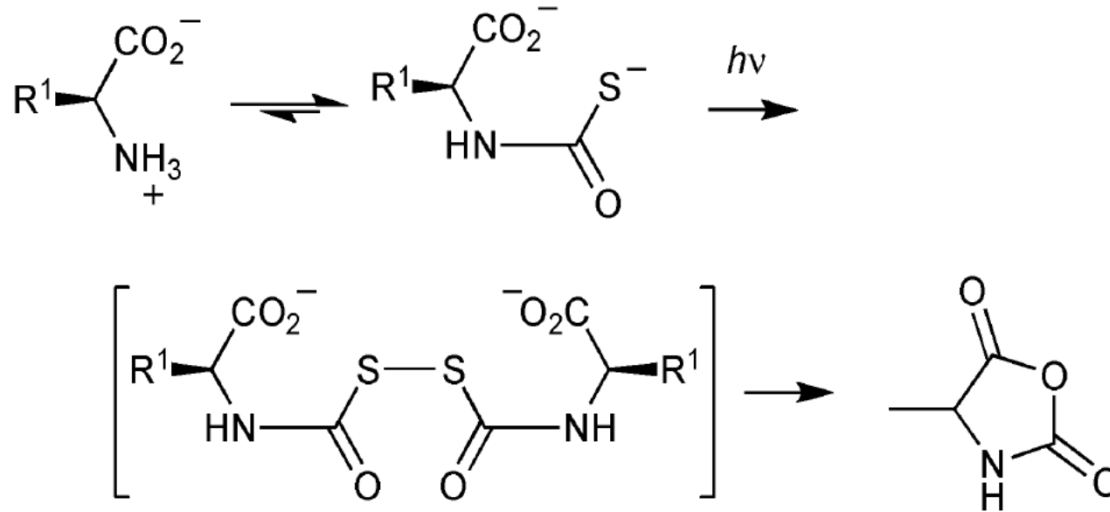
Table 2. COS-mediated formation of mixed peptides. Abbreviations for the amino acid residues: A, Ala; F, Phe; L, Leu; S, Ser; Y, Tyr.

Entry*	L-Phe (mM)	Reactant 2 (mM)	PbCl ₂ (mM)	Final pH	Time (hours)	Observed dipeptides†	Observed tripeptides†
1	10	L-Tyrosine (10)	20	7.2	3	FF, YY, (YF), (FY)	YYY, (YYF), (YFF), FFF
2	25	L-Leucine (25)	50	7.1	3	FF, LL, (FL)	(LLF), (LFF), FFF
3	25	L-Alanine (25)	50	5.9	3	FF, (AF)	(AAF), (AFF), FFF
4	25	L-Serine (25)	50	6.3	3	SS, FF, SF, FS	SSS, (SFF), FFF

*Each experiment was initiated by admitting ~20 ml of COS gas to an argon-purged reaction vessel containing 2 ml of the reaction mixture indicated dissolved in 500 mM Me₃N buffer, at an initial pH of 9.1. Peptide products were identified by LCMS after quenching the reaction at 3 hours. †Peptides for which product masses were observed but primary amino acid sequences which were not determined are indicated in parentheses.

Leman, L.; Orgel, L.; Ghadiri, M. R. *Science* **2004**, *306*, 283-286.

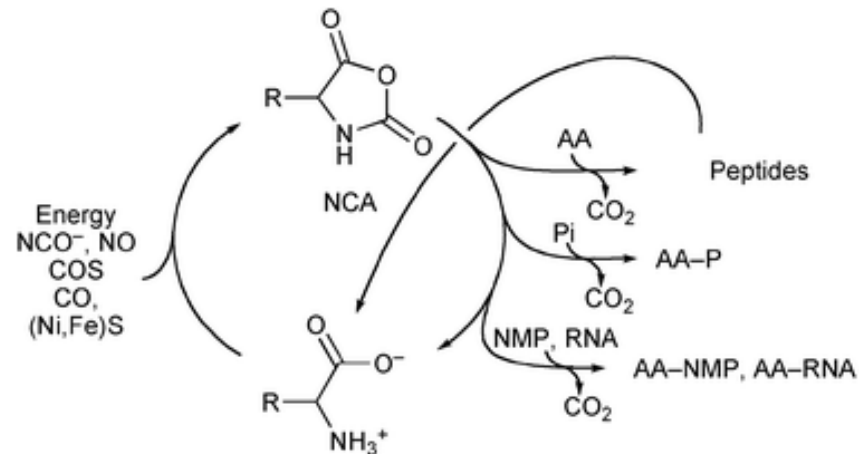
Carbonyl sulfide – photochemical activation



A slow formation of NCAs from free amino acids and COS in the absence of oxidizing or alkylating agents has been reported and studied through theoretical chemistry investigations. However, it seems unlikely that COS ($\Delta G_0 = 16.9$ kJ/mol) could be able to generate NCA ($\Delta G_0 = 60$ kJ/mol) in spite of its cyclic structure.

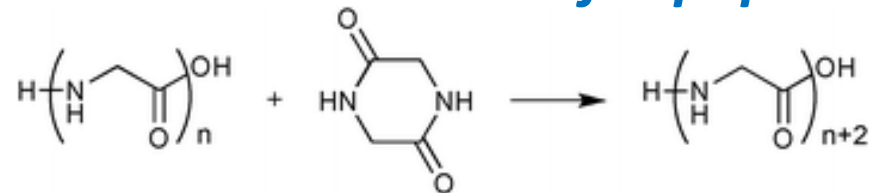
A photochemical activation of thiocarbamate that could take place in a way similar to that of thioacetate in aqueous solution may provide an explanation to this observation. This potential photochemical reaction may also constitute an efficient pathway for the prebiotic formation of NCAs.

Carbonyl sulfide – photochemical activation

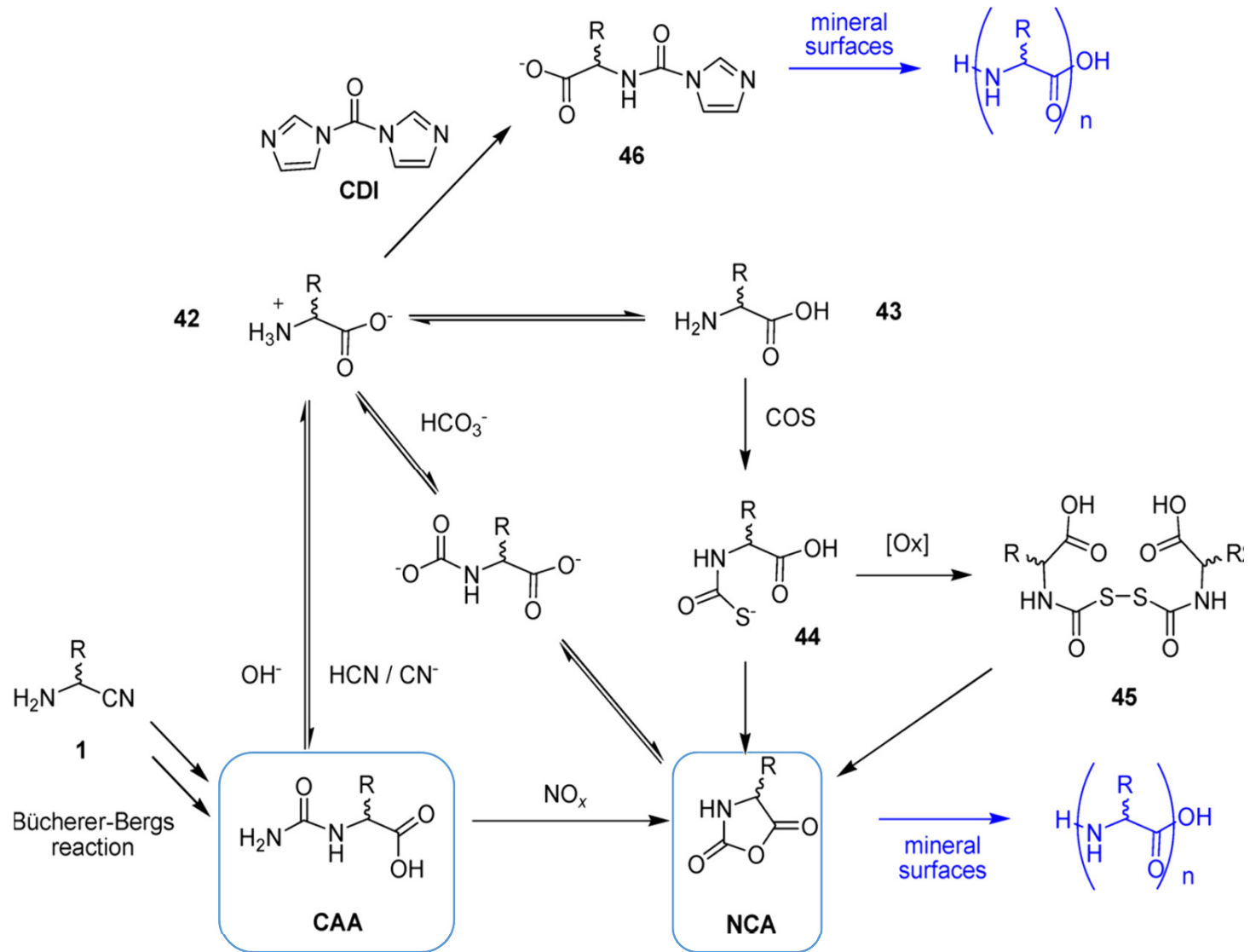


Pathways for the formation of NCAs and further reactions including polymerization and interactions with inorganic phosphate (Pi), nucleotides (NMP), and RNA.

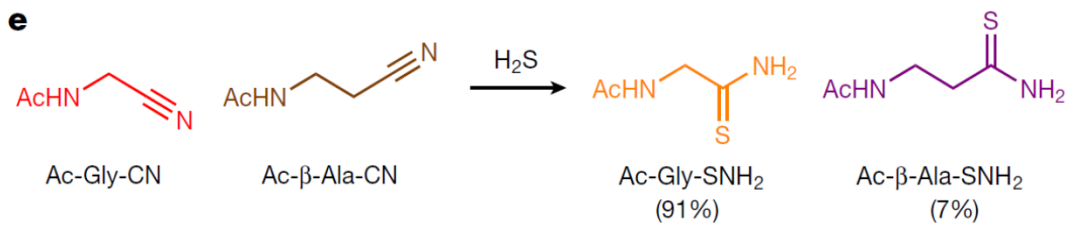
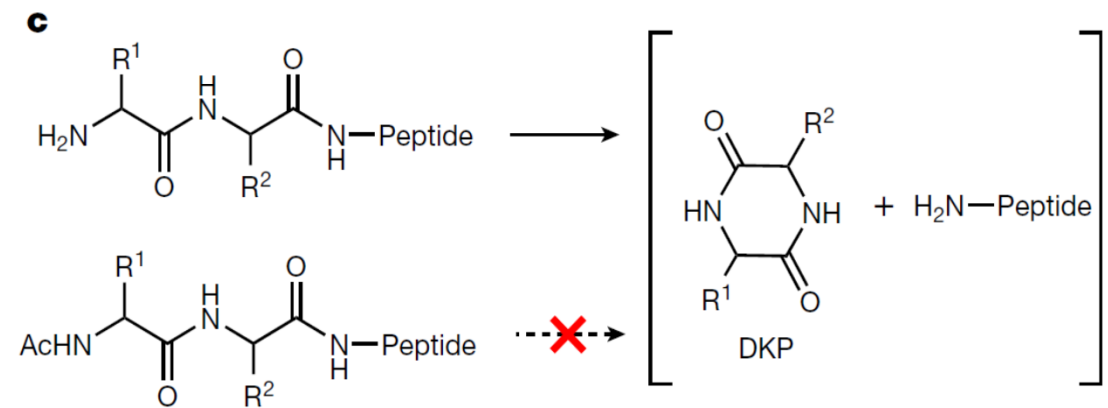
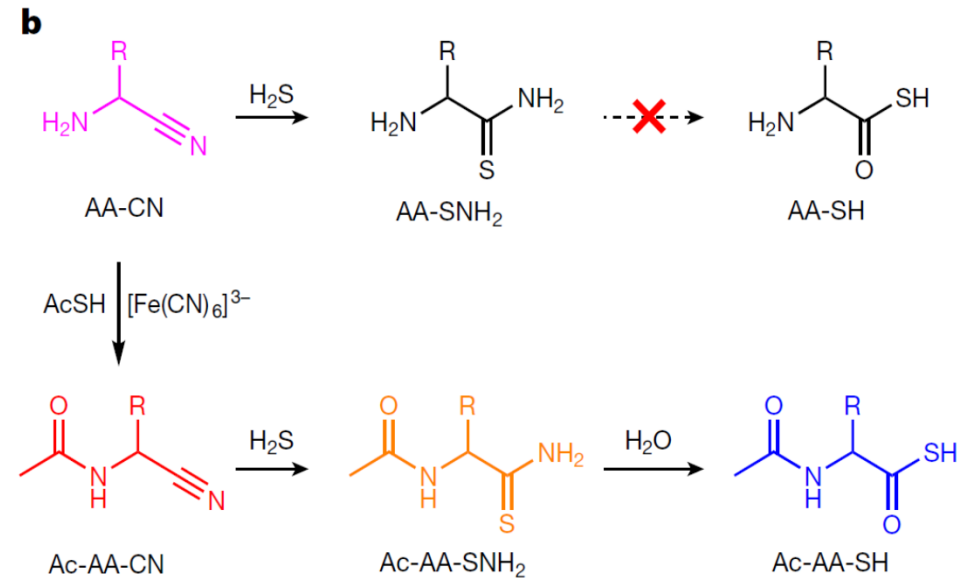
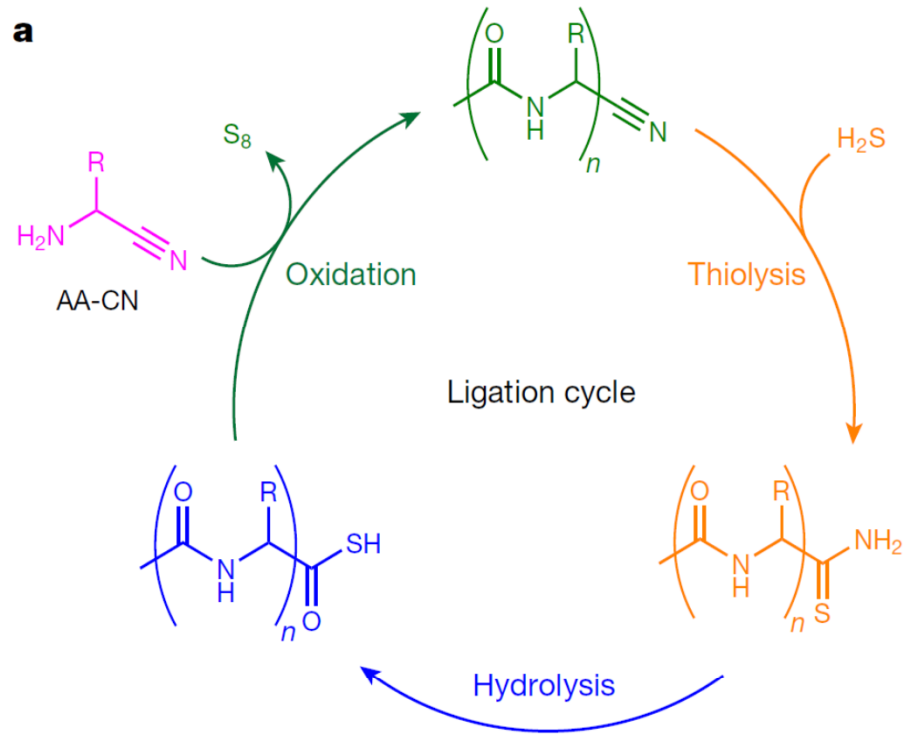
Diketopiperazines as intermediates for peptide condensation



Condensation of aminoacids into peptides

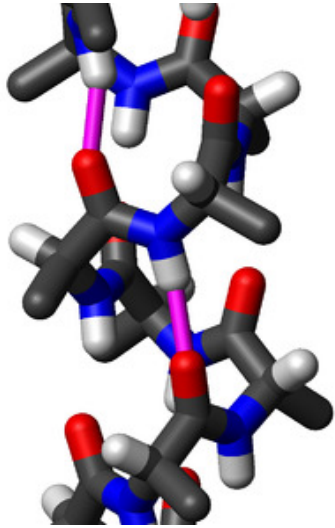


Prebiotic peptide condensation in water

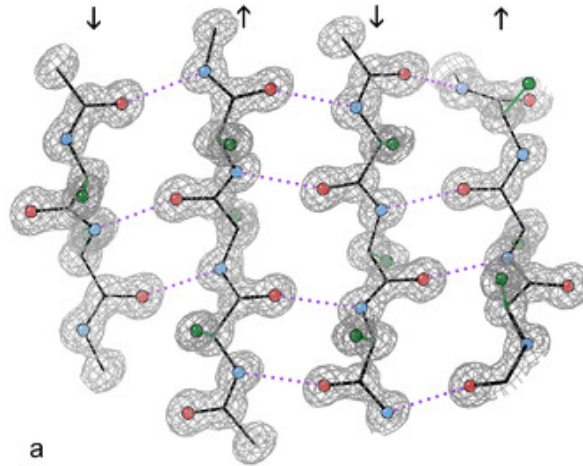


P. Canavelli, S. Islam & M. W. Powner *Nature* **2019**, 571, 546-549.

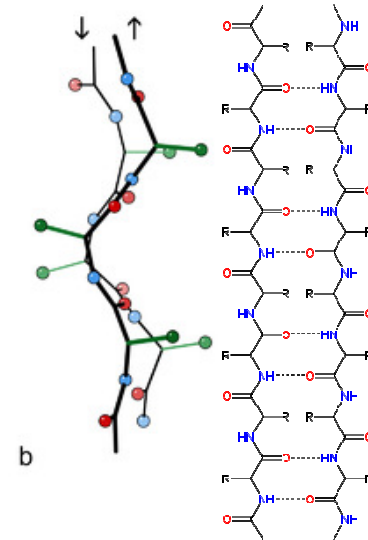
GADV-protein world



*α -helix
(Ala)*



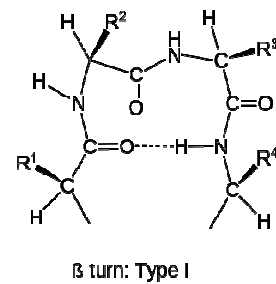
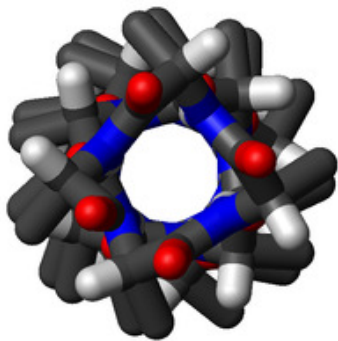
*β -sheet
(Val)*



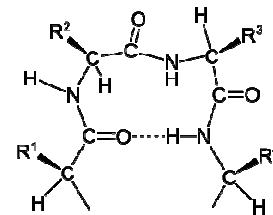
*hydrophilic
and
hydrophobic
structures*

*globular
structures*

*catalytic
activity
(Asp)*

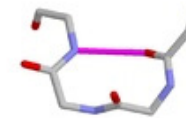


β turn: Type I



β turn: Type II

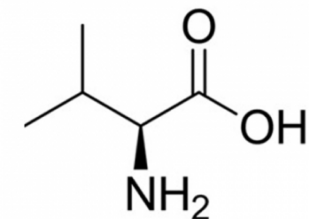
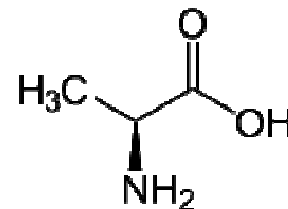
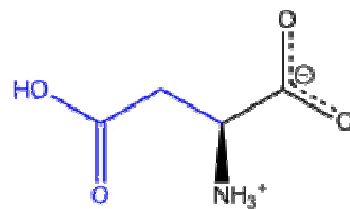
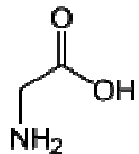
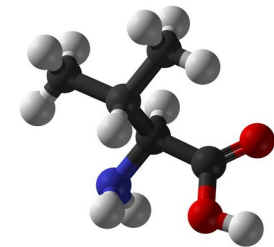
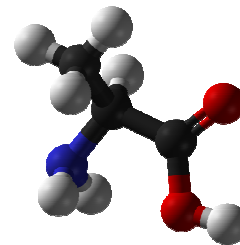
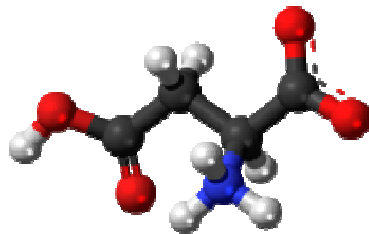
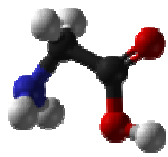
*β -turn (coil)
(Gly)*



Basic aminoacids for primitive genetic code?

Primordial genetic code might have involved only 4 „GNC” codons:

- *GGC for glycine*
- *GCC for alanine*
- *GAC for aspartic acid*
- *GUC for valine*

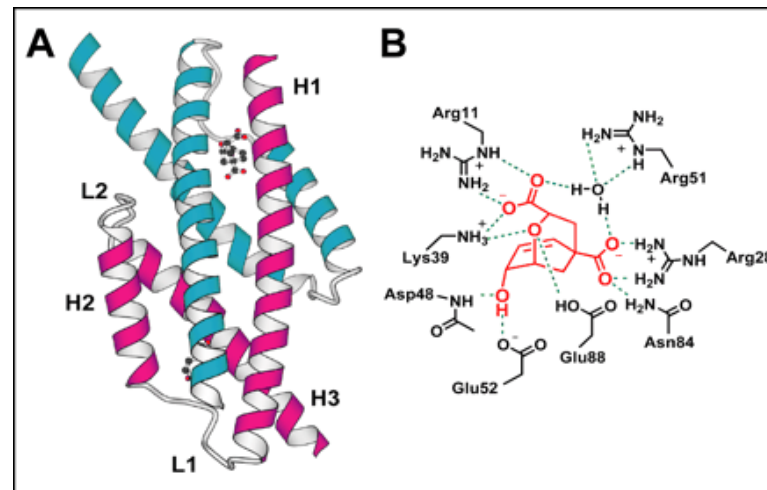


Later, the ‚GNC’ code probably evolved into ‚SNS’ code (S = G/C, N = A, U, G, C) – 16 codons encoding 10 basic aminoacids (Gly, Ala, Asp, Val, Glu, Leu, Pro, His, Glu, Arg)

Reduced aminoacid alphabet

9-aminoacid alphabet is sufficient to construct functional enzymes

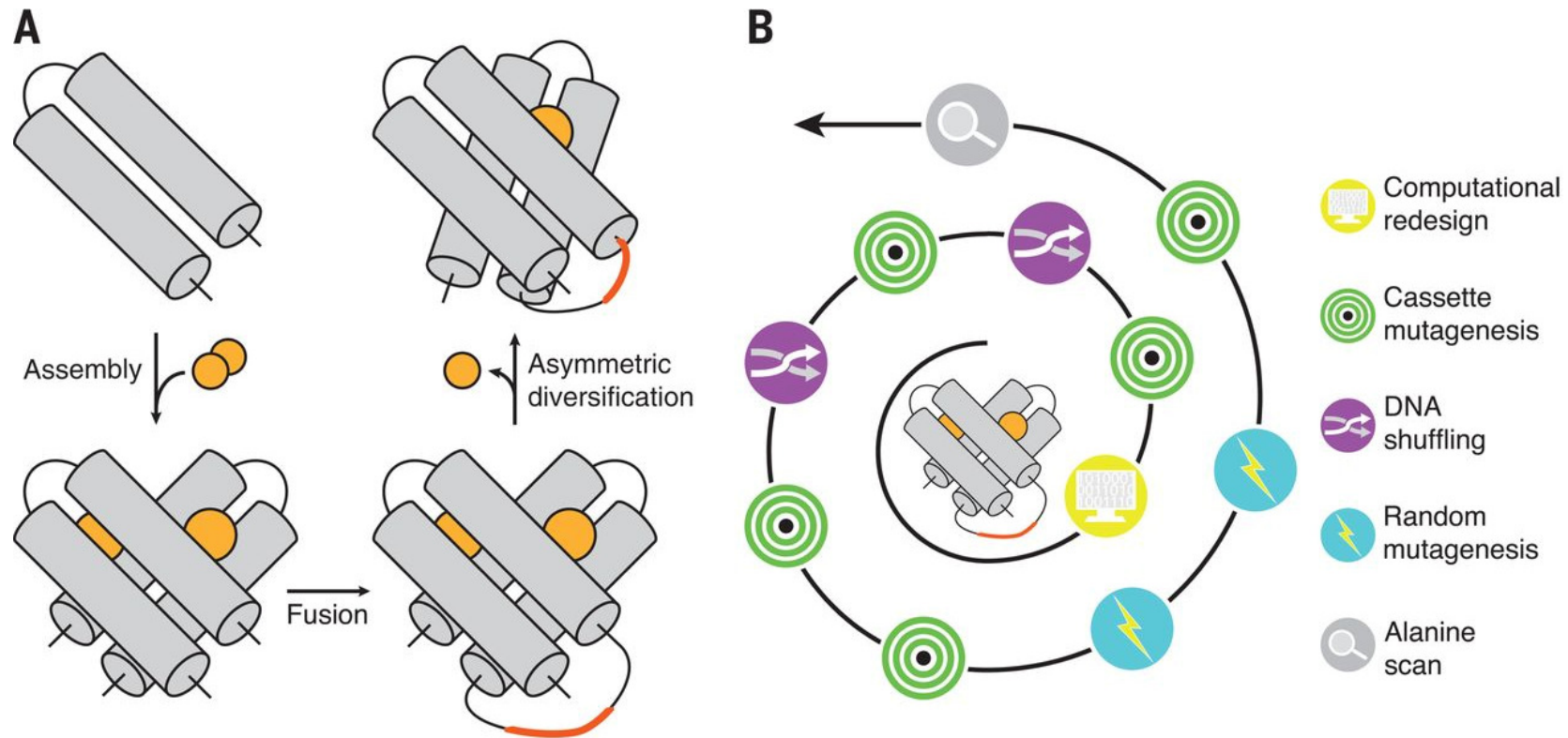
Aminoacids: Asp, Glu, Asn, Lys, Phe, Ile, Leu, Met, Arg



AroQ structure and active site. *A*, the homodimeric EcCM is shown with a transition state analog inhibitor bound at its active sites; the two identical polypeptide chains are colored *blue* and *pink* for clarity. *B*, proposed interactions between residues in the evolved active site of the simplified enzyme and the transition state analog inhibitor, compound **1** (*red*), based on the x-ray structure of EcCM. Residues Gln⁸⁸ and Ser⁸⁴ in EcCM are substituted with Glu⁸⁸ and Asn⁸⁴ in the 9-amino acid enzyme. Residue numbers are referenced to EcCM.

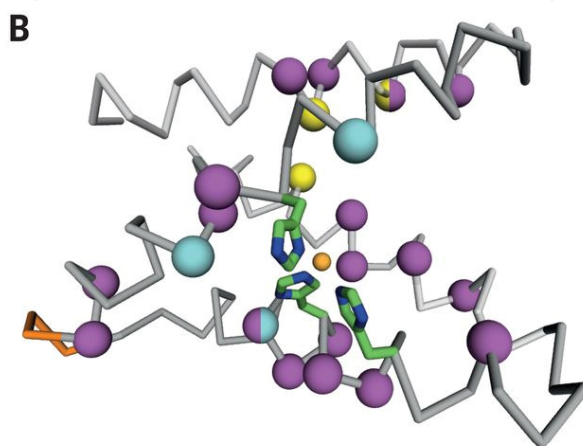
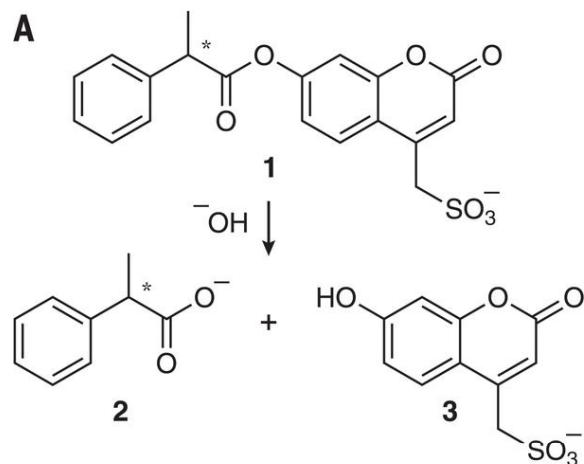
Walter, K. U., Vamvaca, K., Hilvert, D. J. *Biol. Chem.* **2005**, 280,37742-37749.

Evolution of a metalloenzyme from short peptides



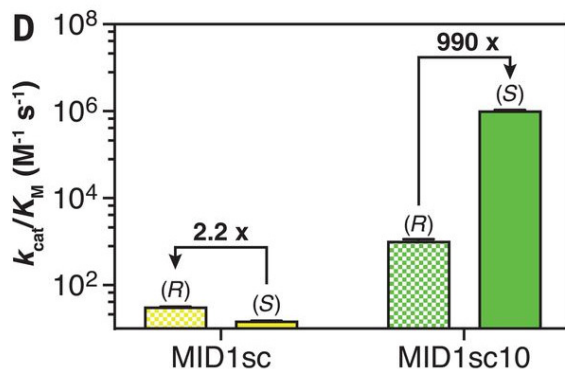
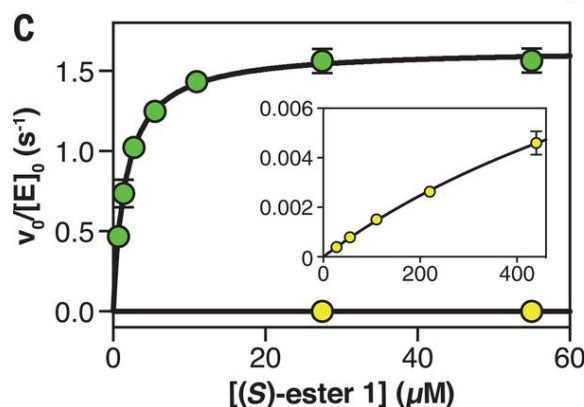
Zinc-mediated assembly of helix-turn-helix fragments, followed by fusion and asymmetric diversification, afforded MID1sc10, an efficient metalloesterase.

Evolution of a metalloenzyme from short peptides



Crystal structure of MID1sc10

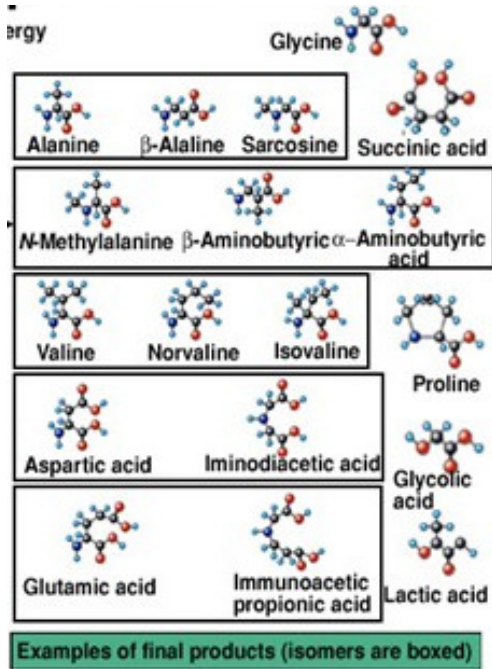
zinc ion - orange sphere,
coordinating histidines - green sticks
linkage of two polypeptides - orange sticks
beneficial mutations - magenta spheres,
residues replaced to prevent competitive zinc
binding modes - cyan spheres).



Michaelis-Menten plots for **MID1sc** (yellow and inset) and **MID1sc10** (green) show a 70,000-fold improvement in hydrolysis efficiency for (S)-configured **1** after optimization.

The evolved variant MID1sc10 is highly enantioselective as a consequence of a 2200-fold specificity switch from the modestly (R)-selective starting catalyst MID1sc

Aminoacids - Summary



Prebiotic generation plausible – variants of the Miller-Urey experiment
Strecker-type of chemistry likely

Aminoacids are good catalysts, can perform various chemical transformations

The origin of homochirality in the Universe caused by the parity violation
and stochastic fluctuations

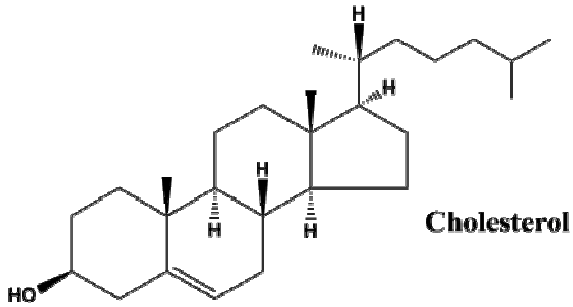
Chirality amplification possible in numerous chemical reactions

Aminoacids can catalyse their own formation with chirality amplification and undergo physical
enantioenrichment processes

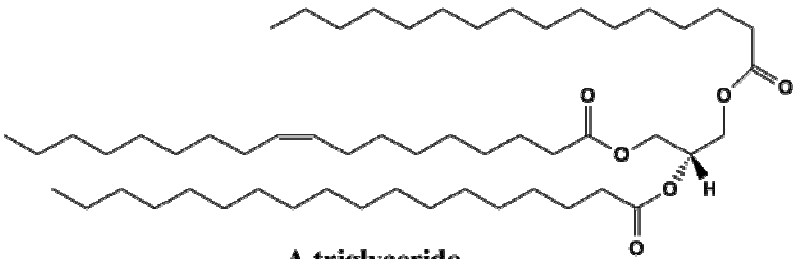
Condensation of aminoacids into peptides plausible under prebiotic conditions using condensing agents

Simple peptides can exhibit broad structural variety,
catalytically active enzymes can be constructed with reduced aminoacid alphabet

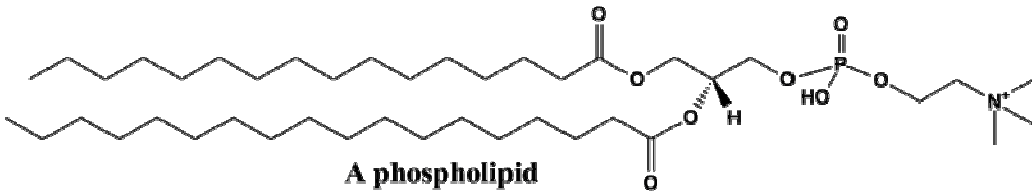
Lipids



A free fatty acid

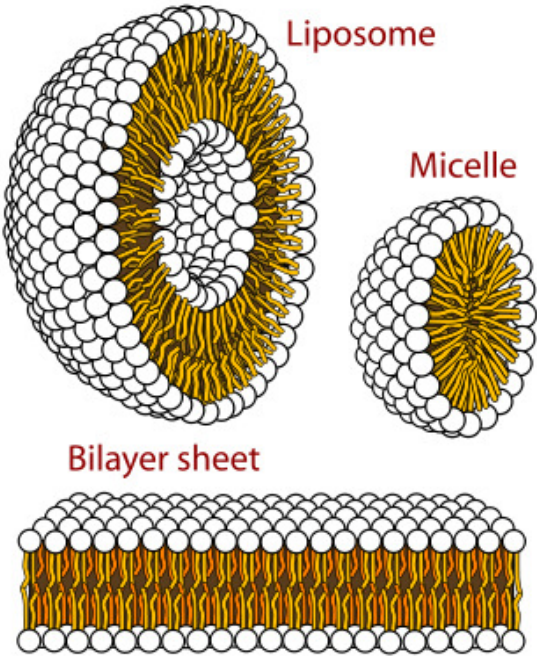


A triglyceride



A phospholipid

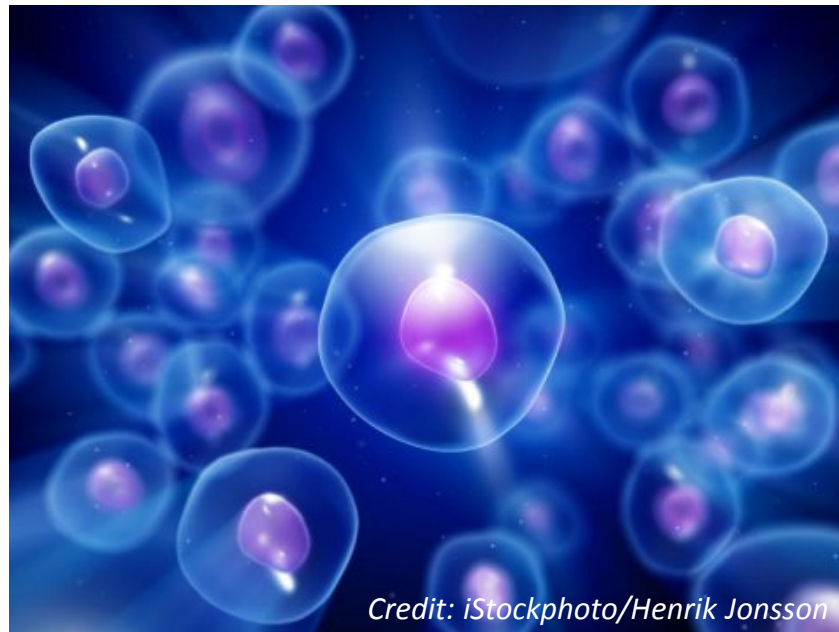
By Lmaps



By Mariana Ruiz Villarreal

Encapsulation – essential for life

Evolving chemical systems require compartments for Darwinian evolution – to compete, to store information and to concentrate reactants/metabolites



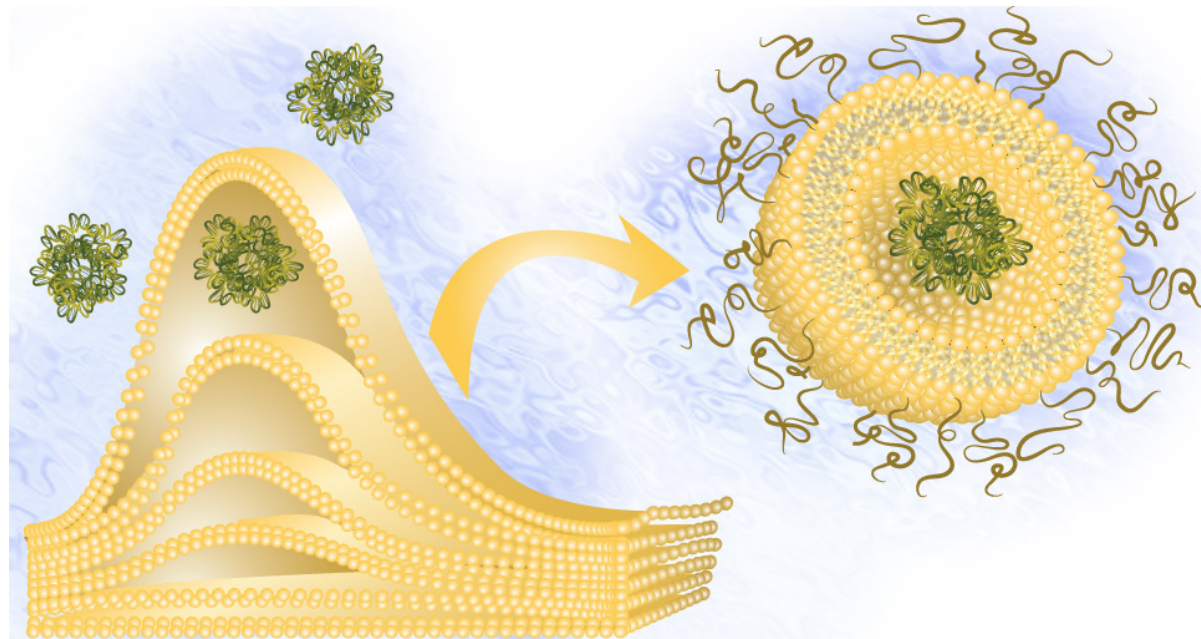
Credit: iStockphoto/Henrik Jonsson

Encapsulation into membranes is considered an early stage in prebiotic chemical evolution and essential requirement for the emergence of life

Encapsulation – essential for life

Formation of membranes is most easy to explain among major cellular components of the prebiotic Earth.

Many amphiphilic organic compounds spontaneously form vesicles in water at sufficiently high concentrations

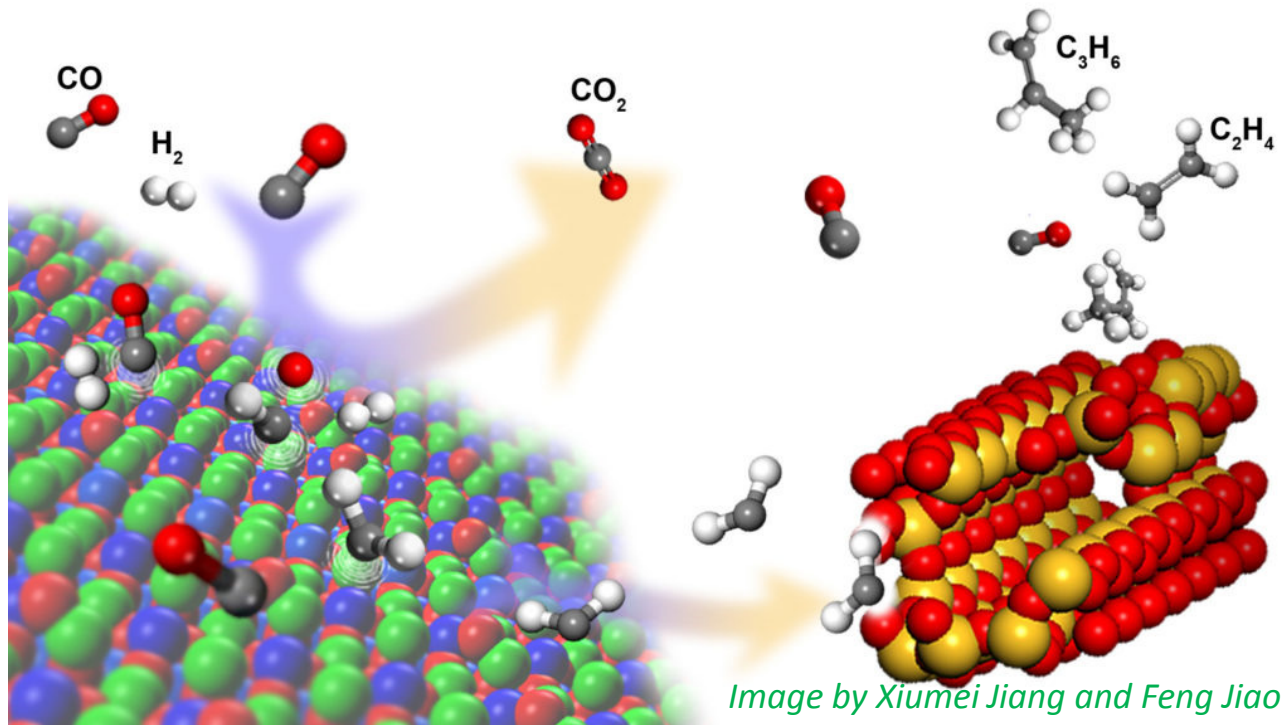


Levine, R.M., Pearce, T.R., Adil, M., Kokkoli, E. Langmuir, 2013, 29 (29): 9208–9215.

The vesicle will encapsulate an aqueous solution inside a thin layer of organic material

Fischer-Tropsch synthesis

Long hydrocarbon chains from CO + H₂ in presence of metal catalysts and high pressure, fatty acids and alcohols are minor by-products



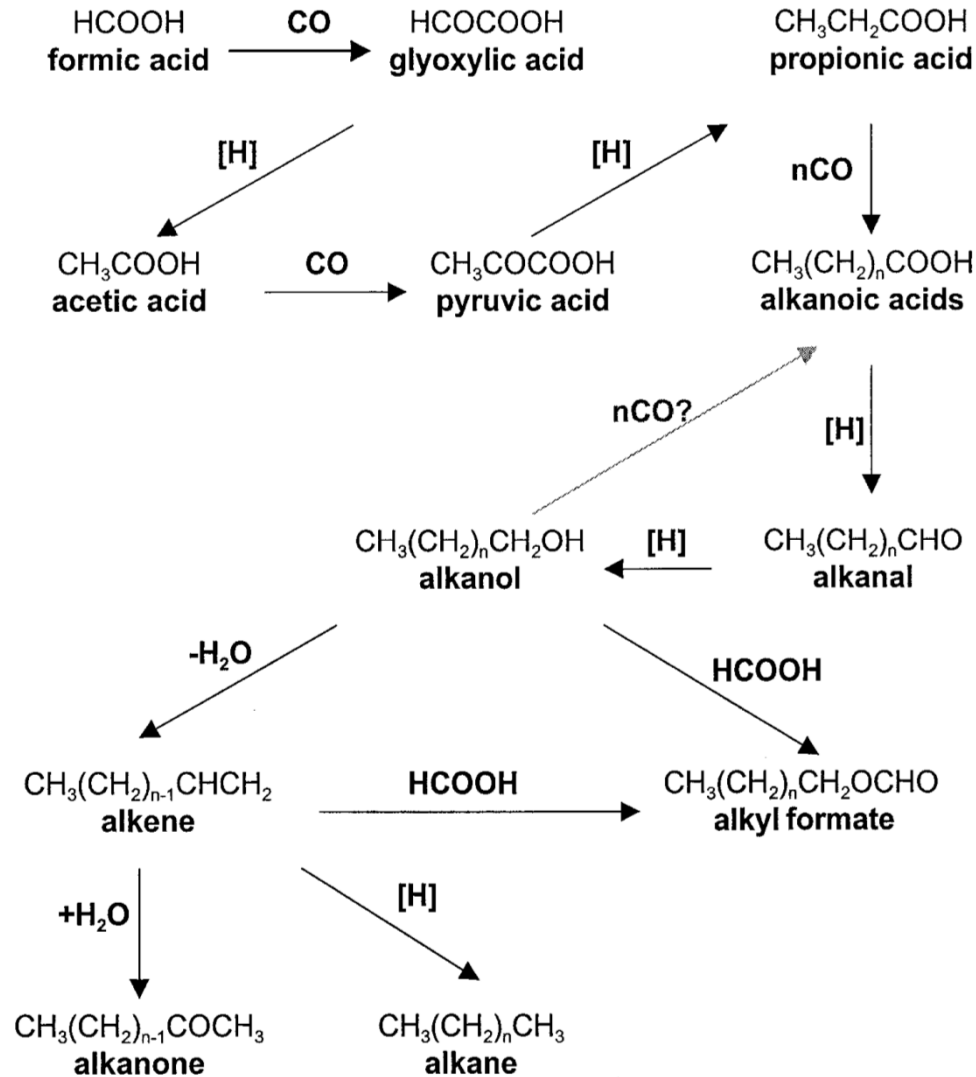
The mixture of D₂ and CO over meteoritic iron or iron ore produced alkanes and n-fatty acids

Oro, J. et al. Geochim. Cosmochim. Acta 1976, 40, 915-924.

Fischer-Tropsch synthesis

Main reactions	
1. Paraffins	$(2n+1)H_2+nCO \rightarrow C_nH_{2n+2} +nH_2O$
2. Olefins	$2nH_2+nCO \rightarrow C_nH_{2n} +nH_2O$
Side reactions	
3. Water-Gas-Shift (WGS)	$CO+H_2O \leftrightarrow CO_2+H_2$
4. Carbide formation	$yC + xM \leftrightarrow M_xC_y$
5. Alcohols	$2nH_2+nCO \rightarrow C_nH_{2n}+2O +(n-1)H_2O$
6. Boudouard reaction	$2CO \rightarrow C +CO_2$
7. Catalyst reduction and oxidation	$M_xO_y + yH_2 \leftrightarrow xM + yH_2O$
	$M_xO_y + yCO \leftrightarrow xM + yCO_2$
8. Coking	$H_2 + CO \rightarrow C + H_2O$

Hydrothermal Fischer-Tropsch synthesis



Formic or oxalic acid heated in water at 150-250⁰C (stainless steel reactor) yielded a mixture of C₁₂-C₃₃ lipids

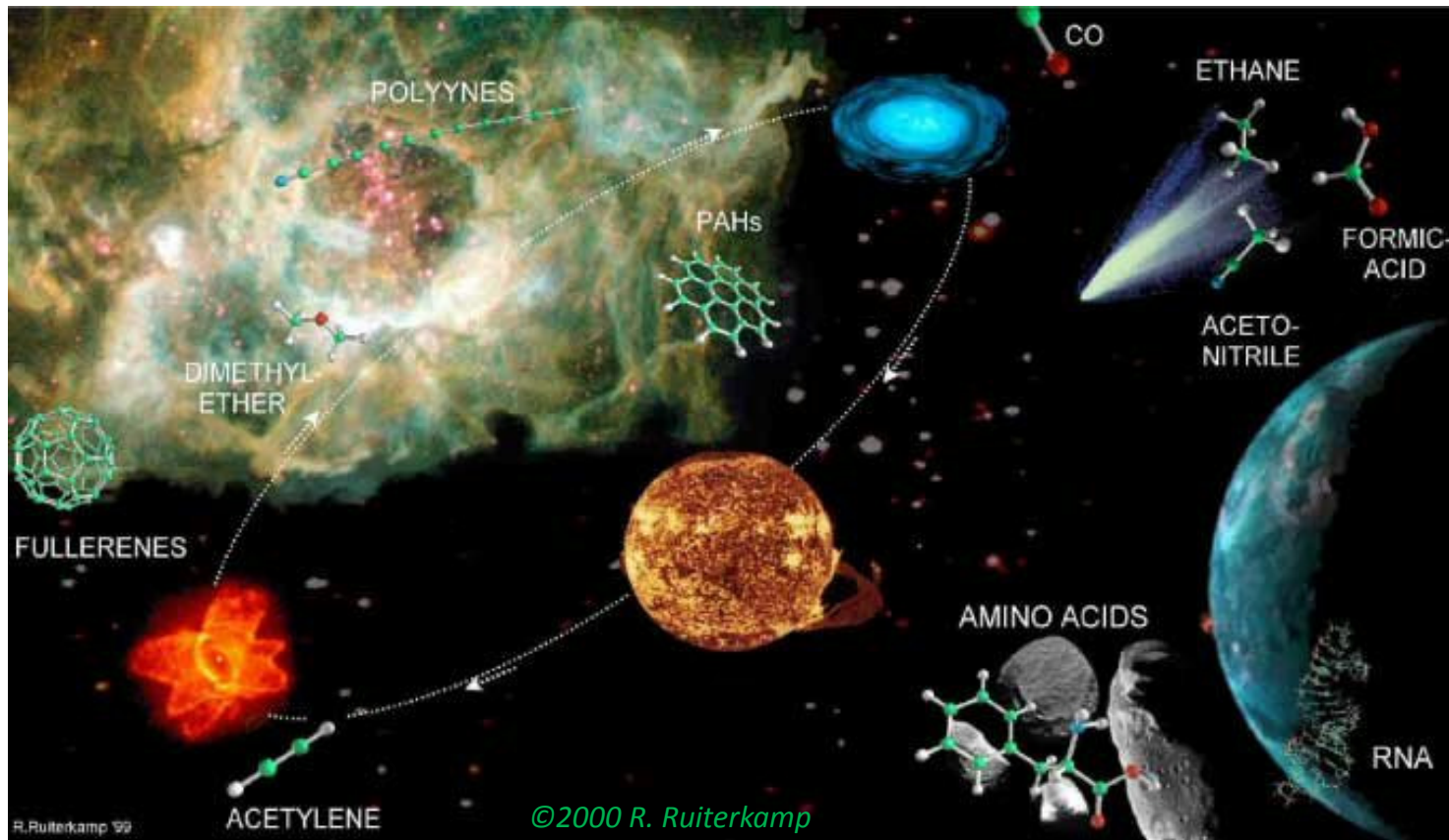
Rushdi, A., Simoneit B. Origins Life Evol. Biospheres **2001**, 31, 103-118

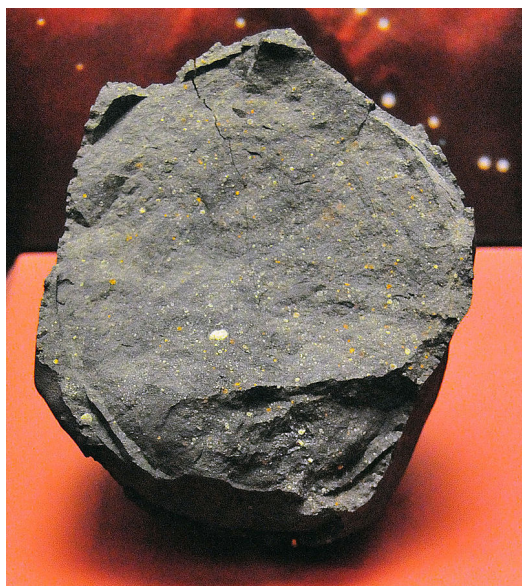
When CO, H₂ and NH₃ are allowed to react at 200-700⁰C in presence of Ni, Al, or clay catalysts, aminoacids are detected:

glycine, alanine, sarcosine, aspartic acid, glutamic acid, arginine, histidine, lysine and ornithine

Yoshino, D.; Hayatsu, R.; Anders, E. Geochim. Cosmochim. Acta **1971**, 35, 927-938

Extraterrestrial origin of biomolecules





Murchison meteorite
chondrite

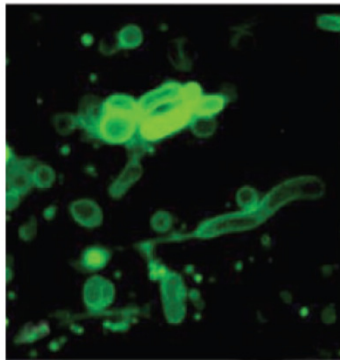
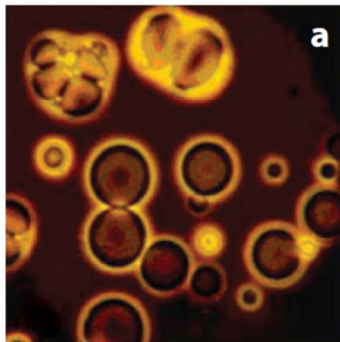
Table 1. Soluble Organic Compounds in the Murchison Meteorite^a

class of compounds	parts per million	<i>n</i> ^b
aliphatic hydrocarbons	>35	140
aromatic hydrocarbons	15–28	87
polar hydrocarbons	<120	10 ^d
carboxylic acids	>300	48 ^d
amino acids	60	75 ^d
imino acids	nd ^c	10
hydroxy acids	15	7
dicarboxylic acids	>30	17 ^d
dicarboximides	>50	2
pyridinecarboxylic acids	>7	7
sulfonic acids	67	4
phosphonic acids	2	4
<i>N</i> -heterocycles	7	31
amines	13	20 ^d
amides	nd ^c	27
polyols	30	19

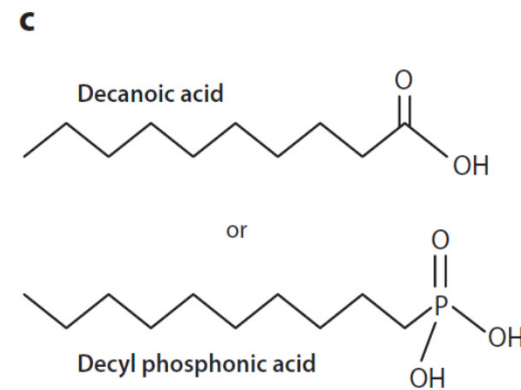
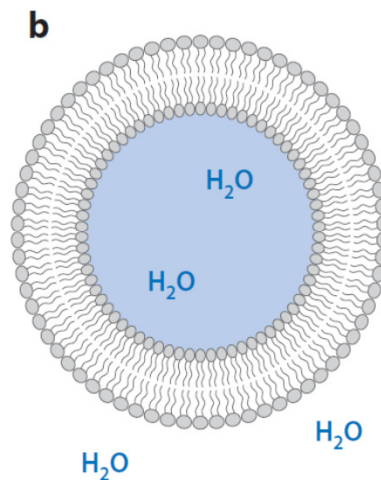
Encapsulation – essential for life

Fatty acids have been found in meteorites – plausible prebiotic synthesis pathways existed in the early Solar System

Meteorite extracts



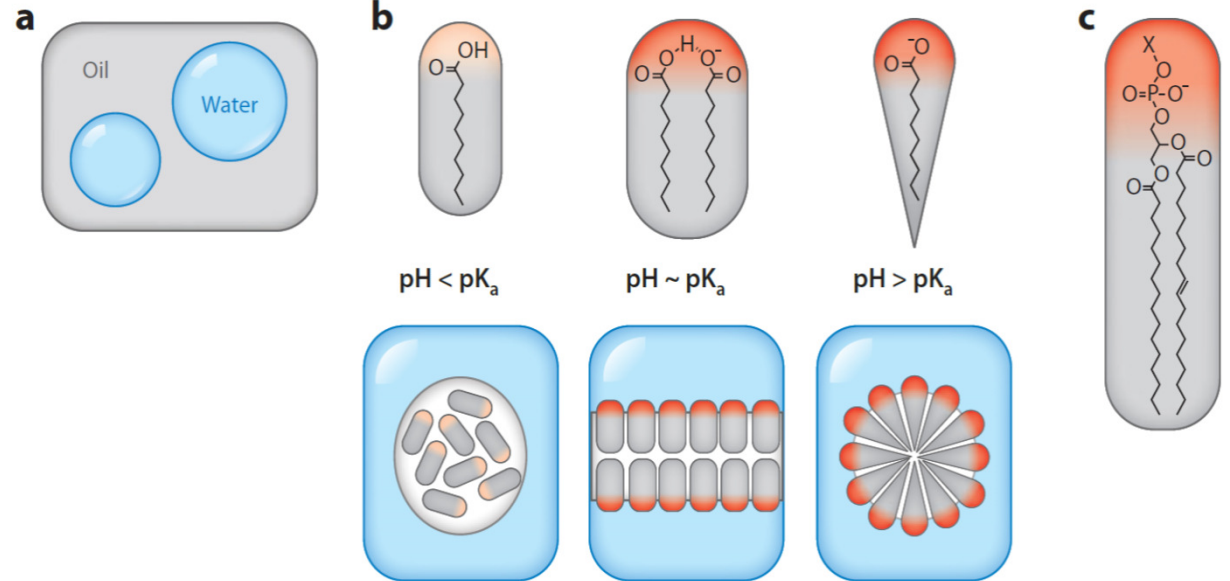
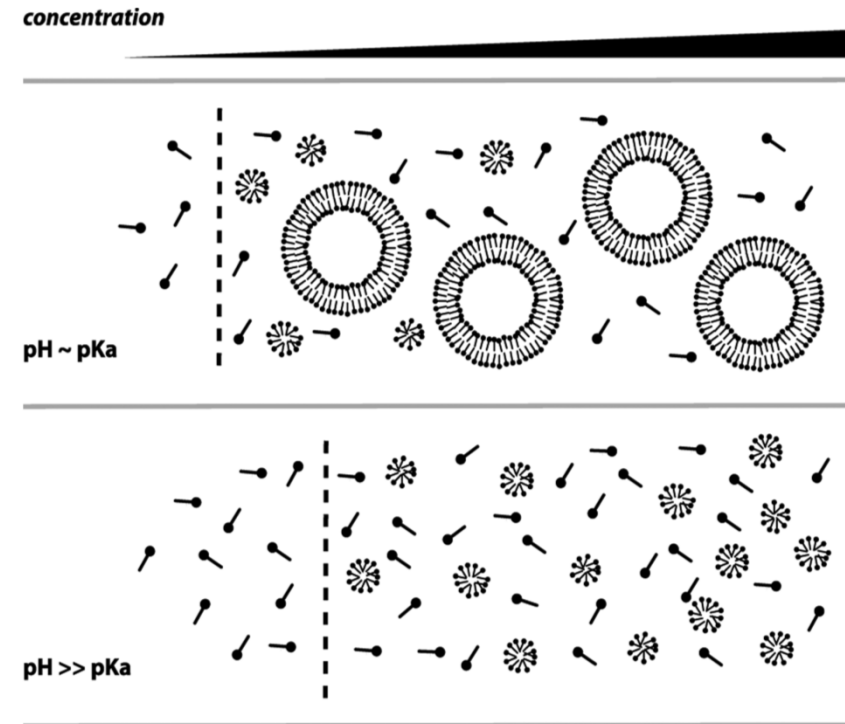
Decanoic acid



Extracts of meteorites containing these compounds spontaneously form vesicles when hydrated

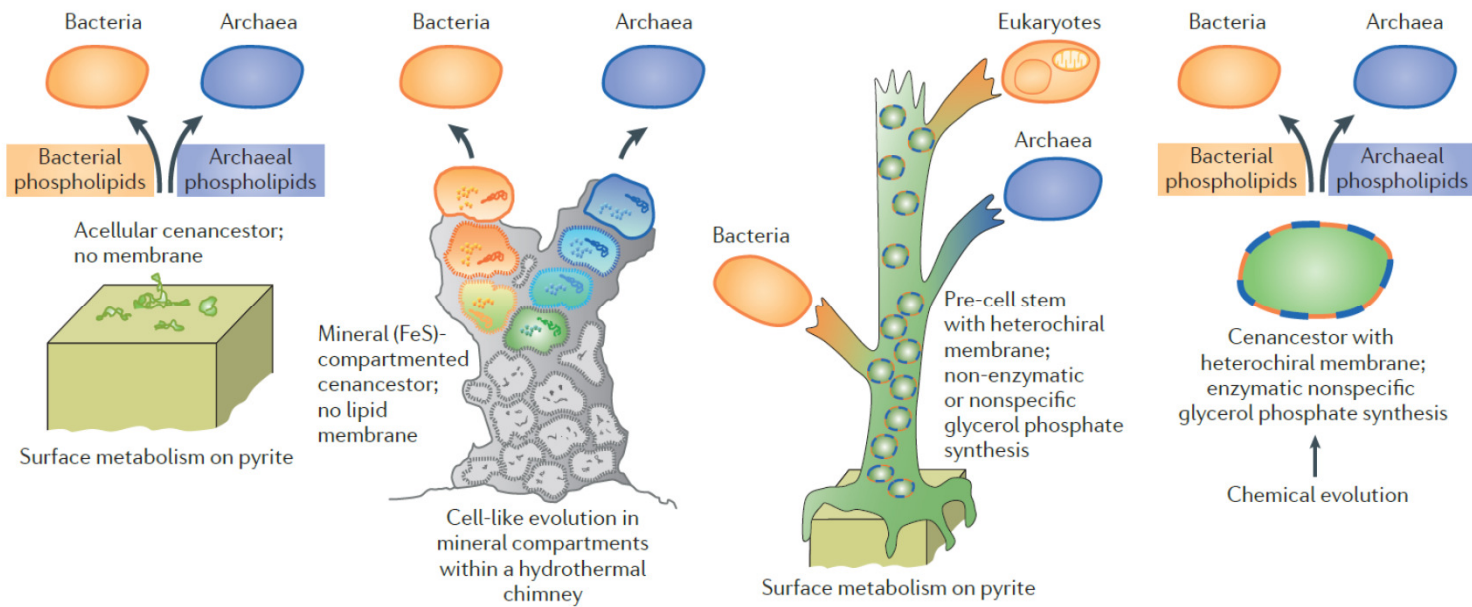
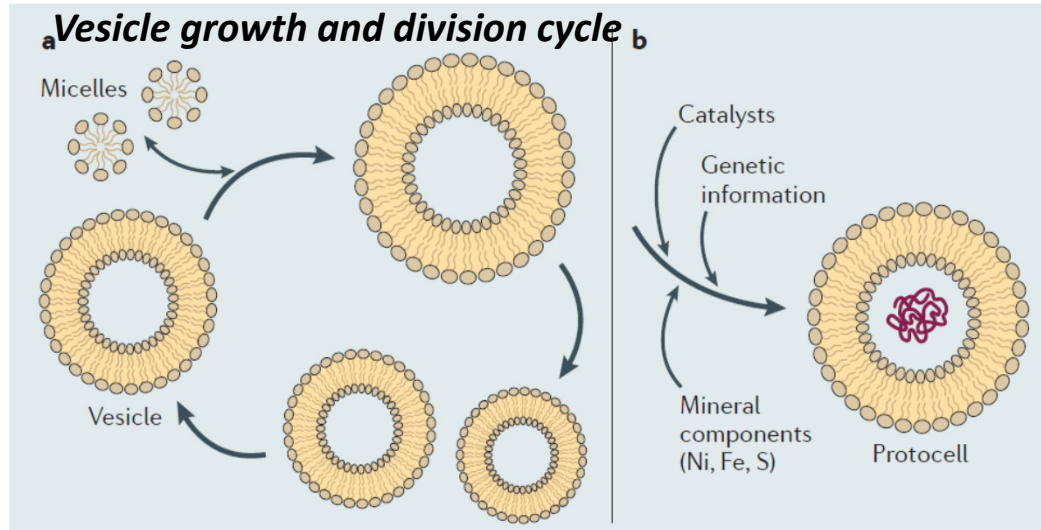
Spontaneous generation of lipid vesicles

The first protocell membranes may have assembled from fatty acids and related single-chain lipids available in the prebiotic environment.



At different concentrations, fatty acids can partition between several different phases, including soluble monomers, micelles, and lamellar vesicles, with higher concentrations favoring larger vesicle aggregates.

Transition: Micelles-Vesicles-Protocells





Jack Szostak

(* November 9, 1952) - Canadian American biologist of Polish British descent,

Nobel Prize laureate 2009 for Physiology and Medicine, for the discovery of how chromosomes are protected by telomeres; Professor of Genetics at Harvard Medical School.

Szostak has made significant contributions to the field of genetics. His achievement helped scientists to map the location of genes in mammals and to develop techniques for manipulating genes.

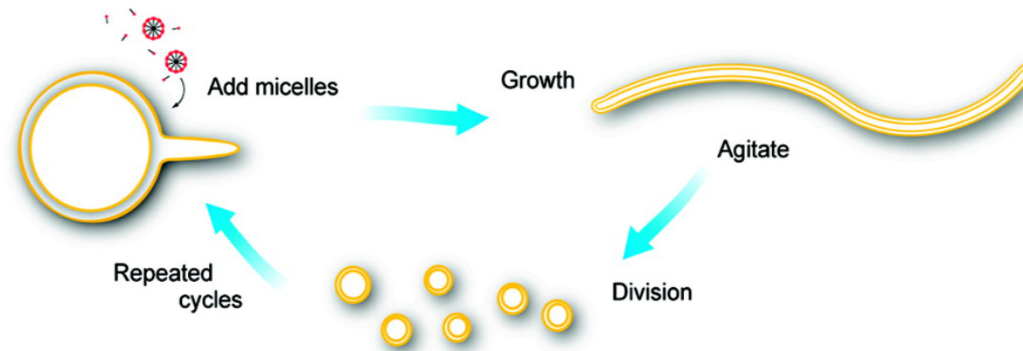
His research findings in this area are also instrumental to the Human Genome Project.

By Markus Pössel (Mapos)

In the early 90s his laboratory shifted its research direction and focused on studying **RNA enzymes**, which had been recently discovered by Cech and Altman. He developed the technique of **in vitro evolution of RNA** (also developed independently by Gerald Joyce) which enables the discovery of RNAs with desired functions through successive cycles of selection, amplification and mutation. He isolated the first **aptamer** (term he used for the first time). He isolated **RNA enzymes with RNA ligase activity** directly from random sequence (project of David Bartel).

Currently his lab focuses on the challenges of understanding the **origin of life** on Earth, and the construction of **artificial cellular life** in the laboratory

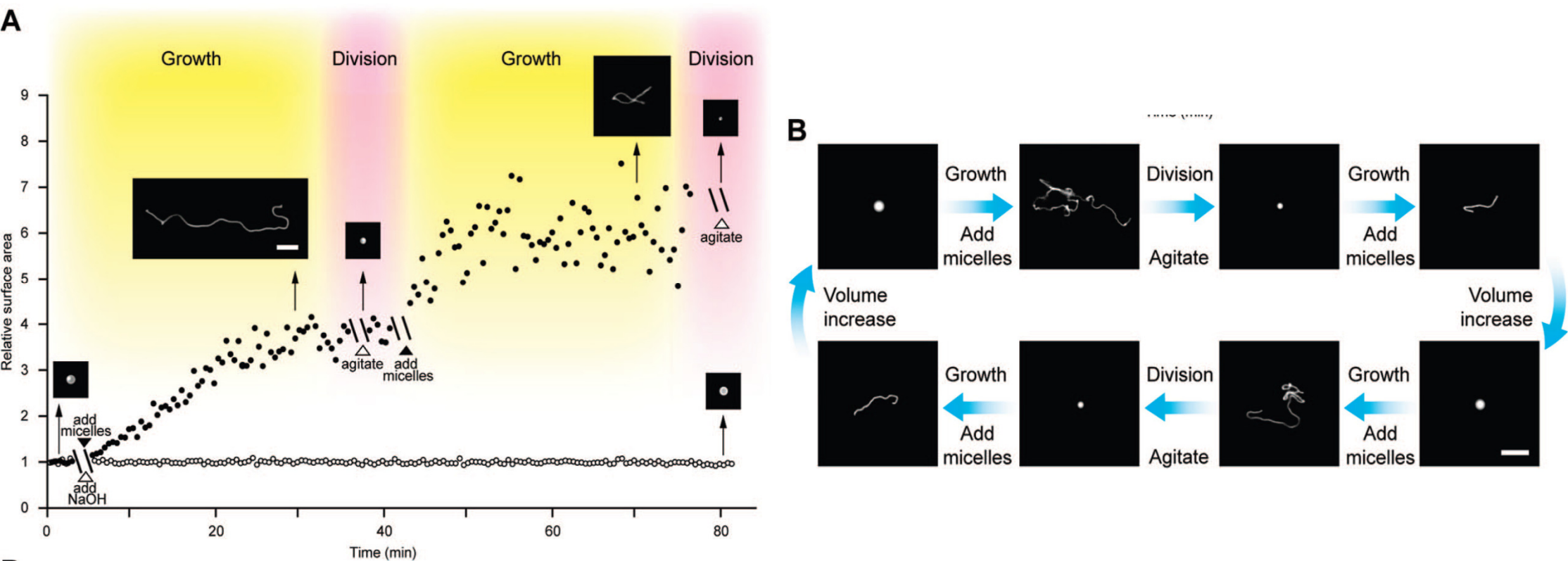
Coupled growth and division of model protocell membranes



The growth of large multilamellar fatty acid vesicles fed with fatty acid micelles, in a solution where solute permeation across the membranes is slow, results in the transformation of initially spherical vesicles into long thread-like vesicles, a process driven by the transient imbalance between surface area and volume growth. Modest shear forces are then sufficient to cause the thread-like vesicles to divide into multiple daughter vesicles without loss of internal contents.

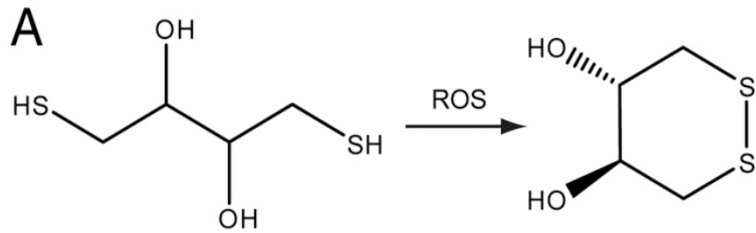


Coupled growth and division of model protocell membranes



Cycles of vesicle growth and division. (A) Relative surface area after two cycles of addition of 5 equiv of oleate micelles (solid circles) or 5 equiv of NaOH (open circles) to oleate vesicles, each followed by agitation. Inset micrographs show vesicle shapes at indicated times. Scale bar, 10 μm . (B) Vesicle shapes during cycles of growth and division in a model prebiotic buffer (0.2 M Na-glycine, pH 8.5, ~ 1 mM initial oleic acid, vesicles contain 10 mM HPTS for fluorescence imaging). Scale bar, 20 μm .

Ting F. Zhu, and Jack W. Szostak *J. Am. Chem. Soc.*, **2009**, 131 (15), 5705-5713



Photochemically driven protocell division

The illumination of filamentous fatty acid vesicles rapidly induces pearling and subsequent division in the presence of thiols.

Photochemically generated reactive oxygen species oxidize thiols to disulfide-containing compounds that associate with fatty acid membranes, inducing a change in surface tension and causing pearling and subsequent division.

Alternative route for the emergence of early self-replicating cell-like structures, particularly in thiol-rich surface environments.

The subsequent evolution of cellular metabolic processes controlling the thiol:disulfide redox state would have enabled autonomous cellular control of the timing of cell division, a major step in the origin of cellular life.

Oleate vesicle pearling and division.

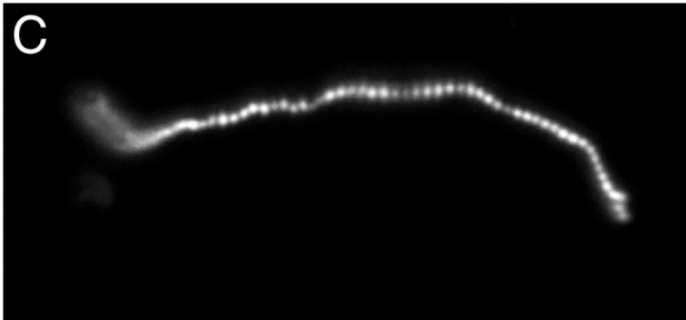
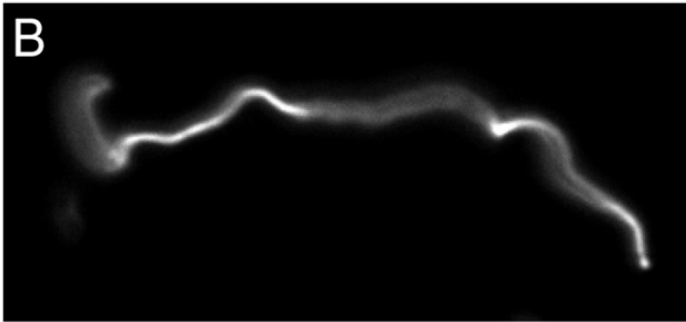
A. Radical-mediated oxidation of DTT.

B. An oleate vesicle (containing 2 mM HPTS, in 0.2 M Na-glycinamide, pH 8.5, 10 mM DTT) 30 min after the addition of five equivalents of oleate micelles.

C. and D. Under intense illumination (for 2 s and 12 s, respectively), the long thread-like vesicle went through pearling and division

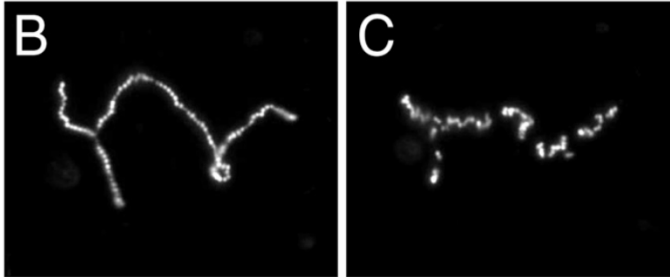
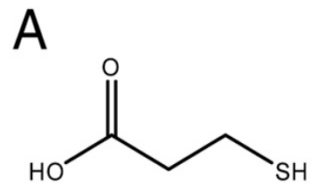
Scale bar, 10 μ m.

T. F. Zhu, K. Adamala, N. Zhang, J. W. Szostak *PNAS*, 2012, doi:10.1073/pnas.1203212109



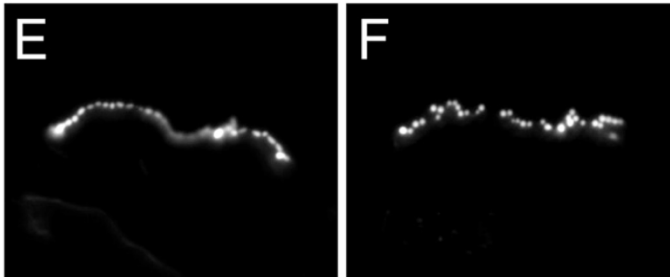
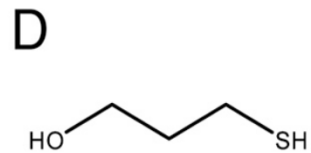
Photochemically driven protocell division

Oleate vesicle pearling and division with various thiols in the solution.



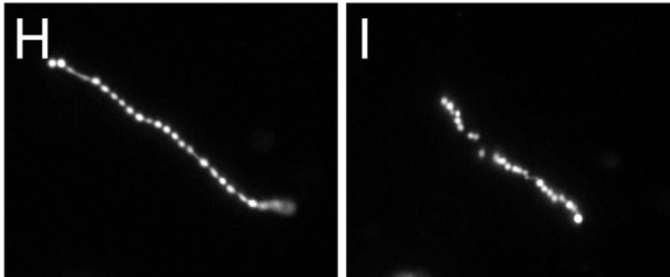
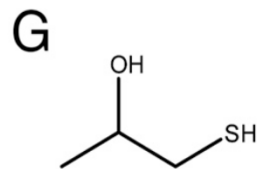
(A) 3-mercaptopropionic acid.

(B and C) An oleate vesicle (containing 2 mM HPTS, in 0.2 M Na-bicine, pH 8.5, 10 mM 3-mercaptopropionic acid, 30 min after the addition of five equivalents of oleatemicelles) went through pearling and division under intense illumination (for 3 s and 15 s, respectively).



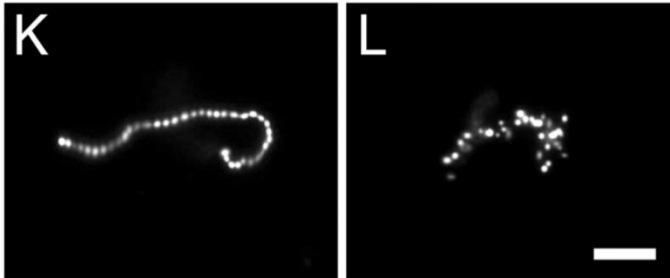
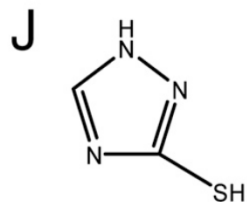
(D) 3-mercaptopropanol.

(E and F) An oleate vesicle as above but in 50 mM 3-mercaptopropanol, went through pearling and division under intense illumination (for 2 s and 10 s, respectively).



(G) 1-mercaptopropan-2-ol.

(H and I) An oleate vesicle as above but in 50 mM 1-mercaptopropan-2-ol went through pearling and division under intense illumination (for 2 s and 9 s, respectively).

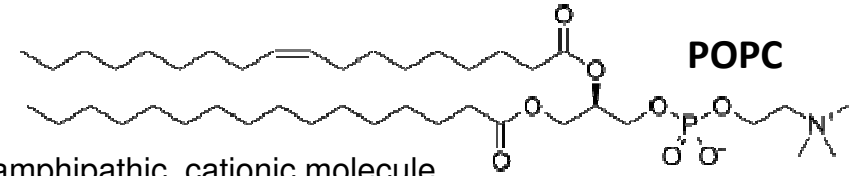
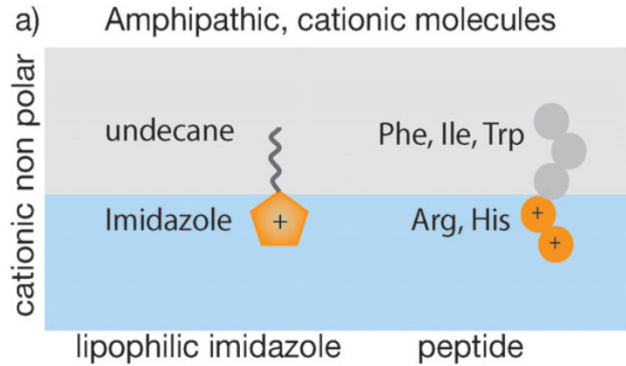


(J) 3-mercaptopropan-1,2,4-triazole.

(K and L) An oleate vesicle as above but in 50 mM 3-mercaptopropan-1,2,4-triazole went through pearling and division under intense illumination (for 3 s and 13 s, respectively).

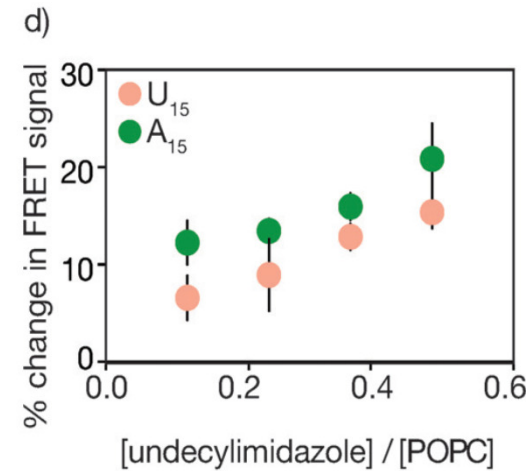
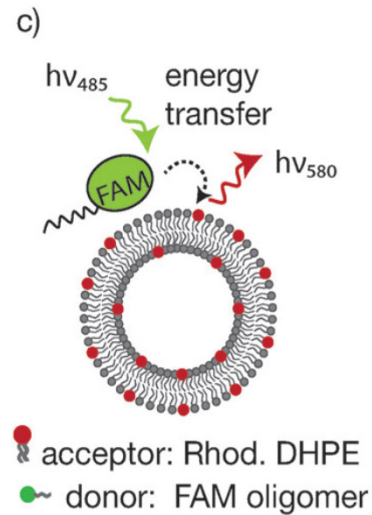
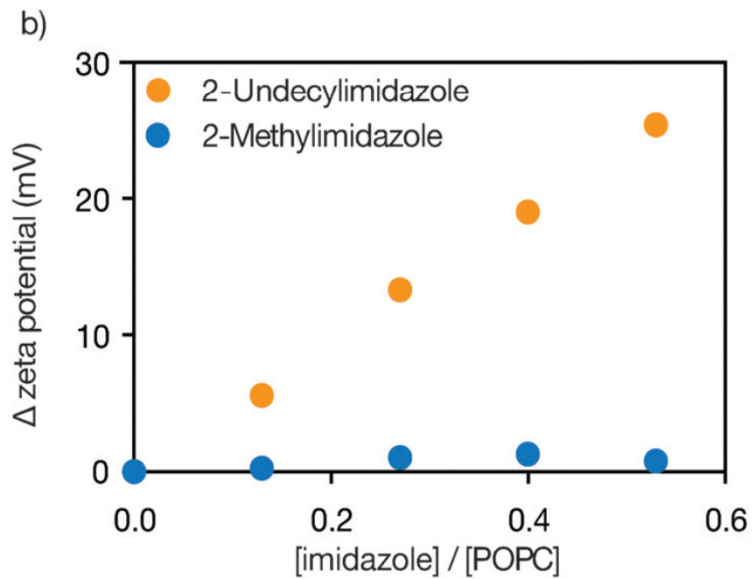
Scale bar, 20 μ m.

Noncovalent nucleotide association with membranes

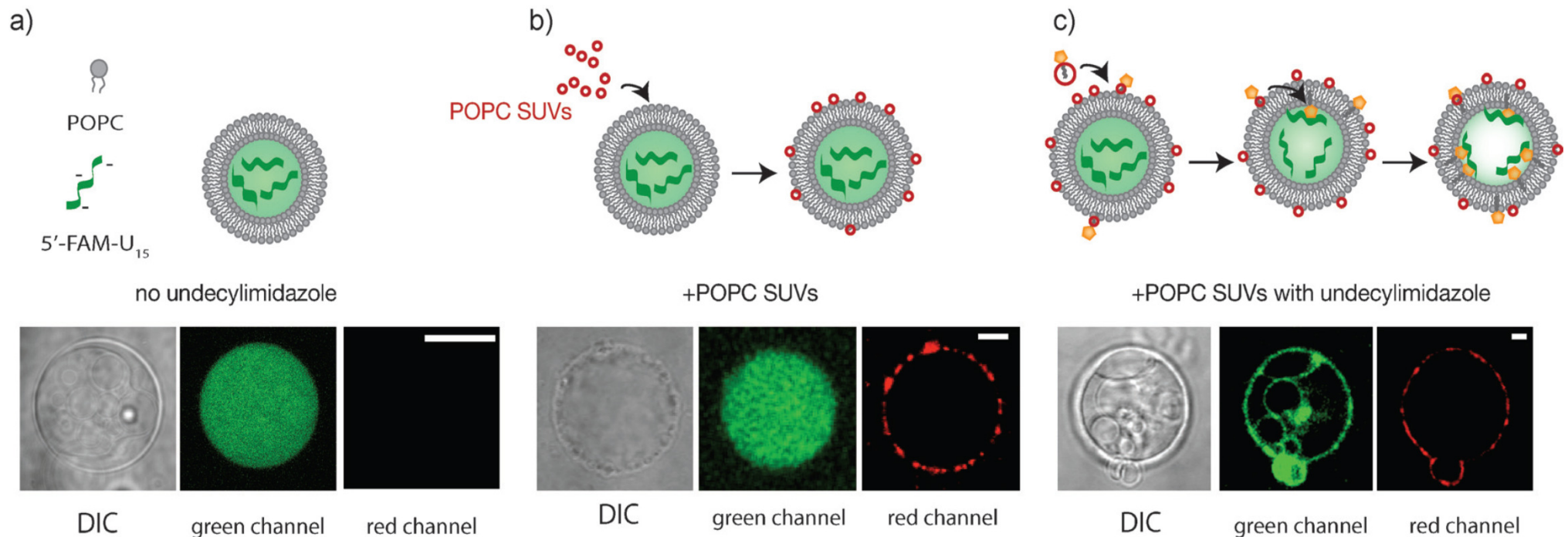


RNA localization with a model amphipathic, cationic molecule

- Design of RNA-localizing molecules that include both nonpolar and cationic regions.
- The change in zeta potential
- Schematic of the FRET assay used to assess RNA localization to vesicle membranes
- RNA (5'-FAM-U₁₅ and 5'-FAM-A₁₅) shows increasing localization to POPC membranes that contain increased amounts of undecylimidazole.



Noncovalent nucleotide association with membranes



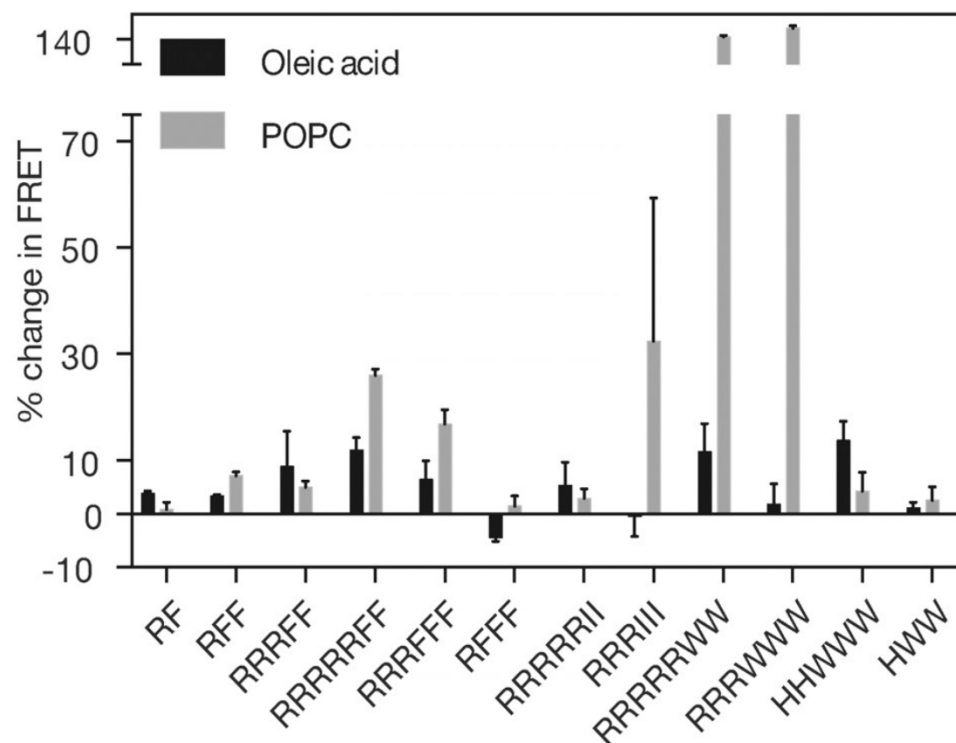
Microscopy of encapsulated RNA localization to POPC membranes with 2-undecylimidazole. Confocal images of 5'-FAM-U₁₅ RNA (green) association with giant POPC vesicles membranes in the presence of 2-undecylimidazole. Differential interference contrast (DIC) microscopy images are shown for each vesicle.

- RNA appears uniformly distributed in the interior of POPC GUVs.
- The addition of SUVs containing a rhodamine-labeled lipid (red) leads to SUV aggregation and association with the giant vesicle membranes, but RNA (green) remains uniformly encapsulated in the vesicle interior.
- The addition of SUVs containing a rhodamine-labeled lipid (red) and 40 mol% 2-undecylimidazole leads to SUV association with vesicle membranes and RNA (green) localizes to the vesicle surface. The scale bar is 20 nm.

SUV – small unilamellar vesicle **GUV – giant unilamellar vesicle (5-25 μm)**

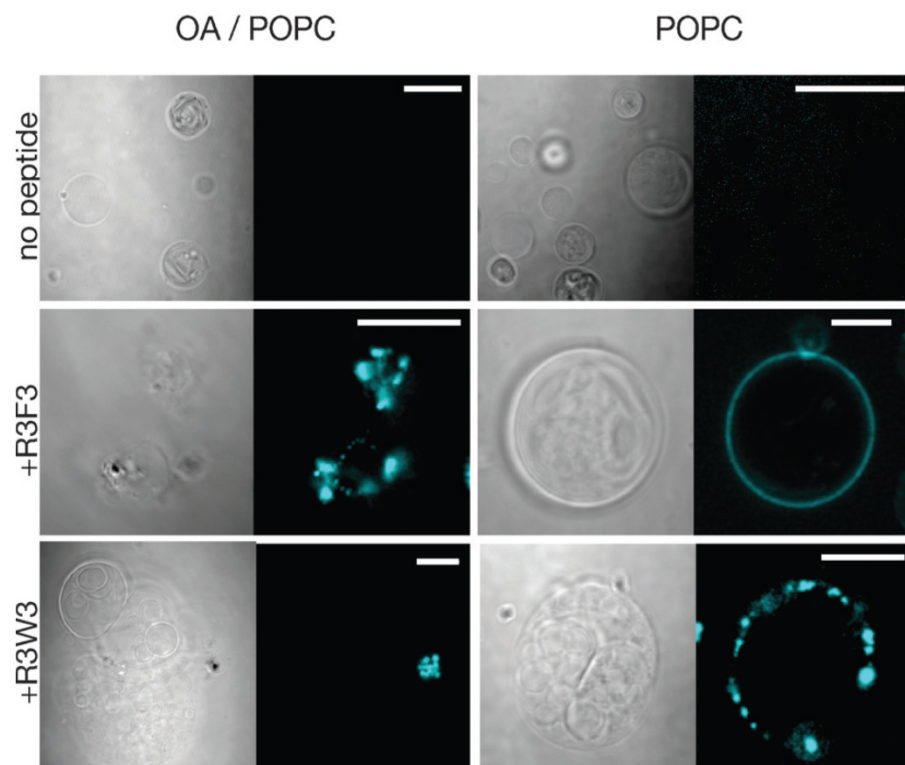
Neha P. Kamat, Sylvia Tobe, Ian T. Hill, and Jack W. Szostak *Angew. Chem. Int. Ed.* **2015**, *54*, 11735–11739

Noncovalent nucleotide association with membranes

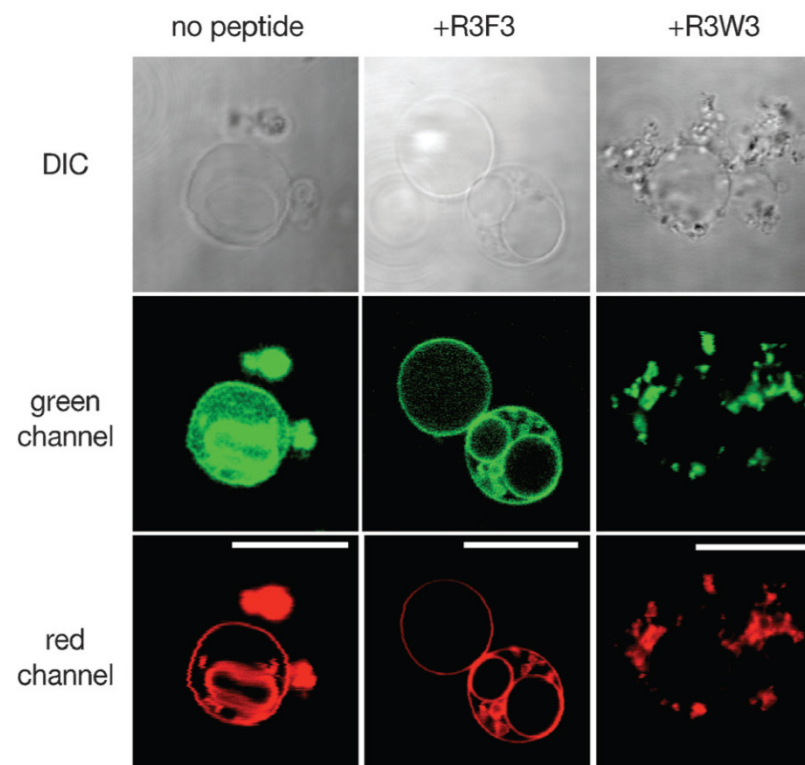


Peptide-induced RNA–membrane association. A FRET assay reports RNA localization (5'-FAM-U₁₅) to POPC and oleic acid membranes (7.5 μ m) 10 h after the addition of 1 μ M of various peptides to the vesicle solution at pH 8. Data is reported as a percentage change from control samples that lack peptide. n=4, error bars represent the standard error of the mean.

Noncovalent nucleotide association with membranes



Microscopy of peptide-induced RNA–membrane association. Confocal images show RNA localization (5'-AlexaFluor647-labeled 15-mer, cyan) to the outside of oleic acid/POPC (90%/10%) and pure POPC membranes in the presence of R3F3 and R3W3 peptides. Control samples had no peptide added. For each image, the left panel shows the DIC image and the right panel shows AlexaFluor647 fluorescence. The scale bar is 20 nm.



Microscopy of encapsulated RNA localization to POPC membranes with peptides. Confocal images show that RNA (5'-FAMU₁₅, green) encapsulated in POPC vesicles (containing a rhodamine-labeled lipid, red) becomes localized to the membrane of certain vesicles after an overnight incubation with R3F3 and R3W3 peptides. The scale bar is 20 nm.

Neha P. Kamat, Sylvia Tobe, Ian T. Hill, and Jack W. Szostak *Angew. Chem. Int. Ed.* **2015**, *54*, 11735–11739

Phosphates



Source: Google Images

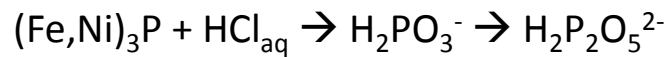


Wikimedia , Butcherbird

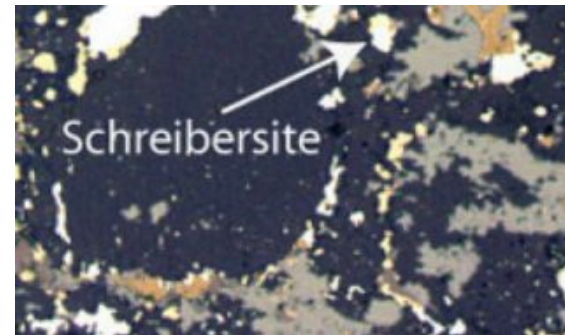
slice of the Gebel Kamil Meteorite with schreibersite rimmed by kamacite

Schreibersite is generally a rare iron-nickel phosphide mineral, $(\text{Fe,Ni})_3\text{P}$, though common in iron-nickel meteorites

Acidic schreibersite corrosion under anaerobic conditions (10% aq. HCl/N_2) \rightarrow soluble forms of phosphorus



T. P. Kee *et al.* *Geochimica et Cosmochimica Acta*. **2013** 109, 90-112



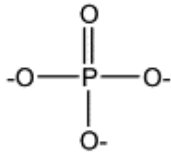
Virginia Smith, UA Lunar & Planetary Laboratory



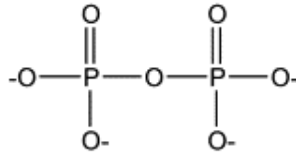
Image of schreibersite grain present in a thin-section of the enstatite meteorite, KLE 98300.

Phosphates

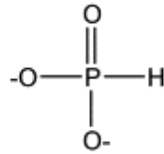
I. Orthophosphate



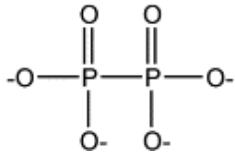
II. Pyrophosphate



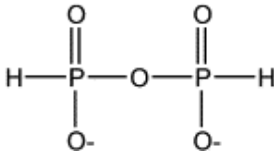
III. Phosphite



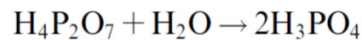
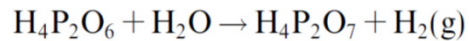
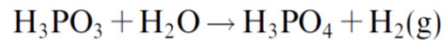
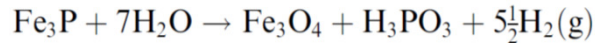
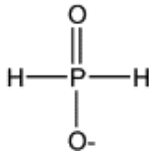
IV. Hypophosphate



V. Diphosphate

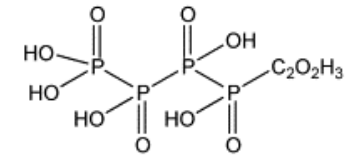
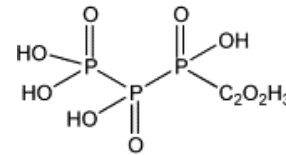
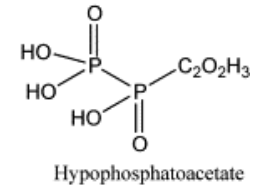
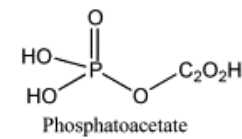
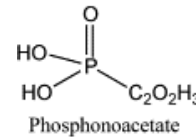
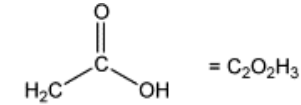


VI. Hypophosphite



Radical pathway of the corrosion is suggested.
In presence of simple organic molecules (e.g. acetic acid)
organophosphorous compounds are detected

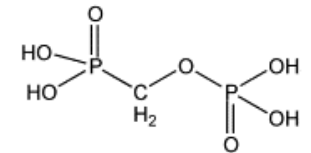
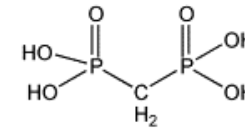
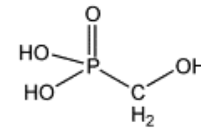
I. Acetyl-P compounds



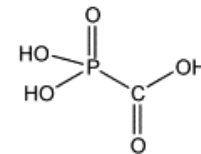
Etc.

Penta-P-Acetate

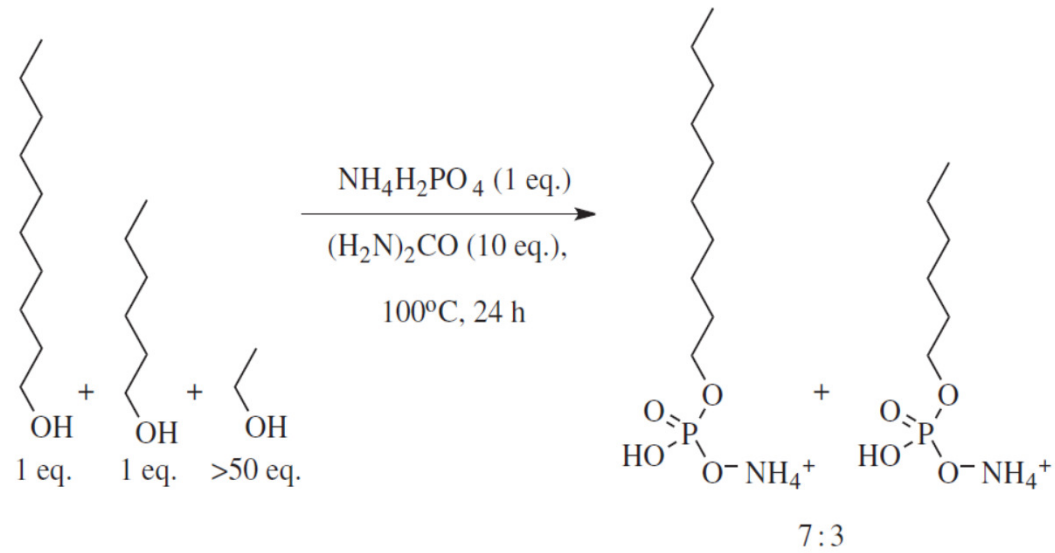
II. Methyl-P Compounds



III. Phosphonoformate



Phospholipids



Lipids - summary

Many amphiphilic organic compounds spontaneously form vesicles in water at sufficiently high concentrations

Current phospholipid membranes likely evolved late. Protocells probably encapsulated by fatty acids, fatty alcohols, prenyl oligomers, or phosphorylated alcohols

Nucleolipids are proposed as intermediates in templated oligonucleotide replication

Phosphorus was accessible upon corrosion of meteorite materials and could be incorporated into lipids

The origin of small reactive intermediates



Schreibersite (Fe,Ni)₃P, from iron-nickel meteorites: source of phosphorus, iron and nickel

Under more neutral conditions phosphates recombine with iron → Fe₃(PO₄)₂ (**vivianite**)

It should be re-solubilized to become accessible for following chemical transformations

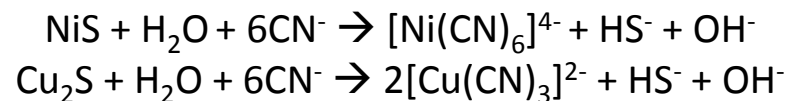
Wikimedia, Carles Millan

HCN – the crucial reactive intermediate – burning of carbon-rich chondrite meteorites into redox-neutral atmosphere containing N₂ and water



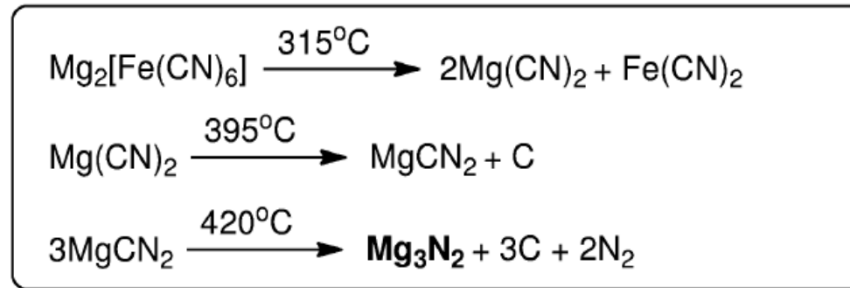
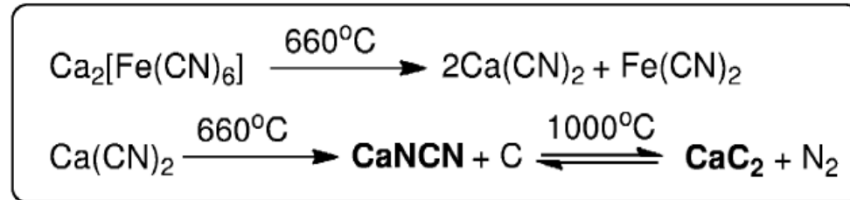
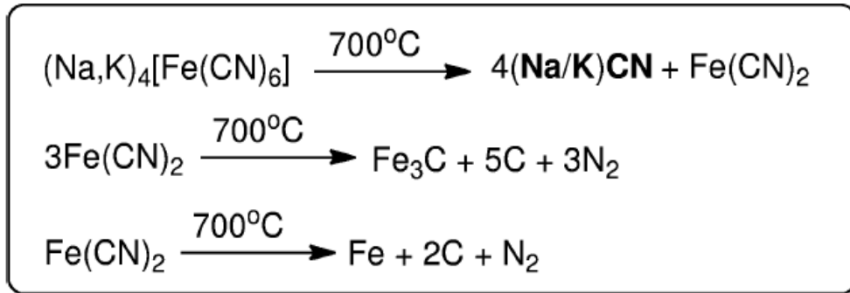
Two important functions: solubilization of phosphates and concentration of atmospheric HCN deposited as salts of mono- and divalent cations (Na, K, Mg, Ca)

Similar reactions take place with insoluble copper and nickel sulfides deposited by iron-nickel meteorite impacts (same occurrence as schreibersite, rich mining sources of these metals until today)



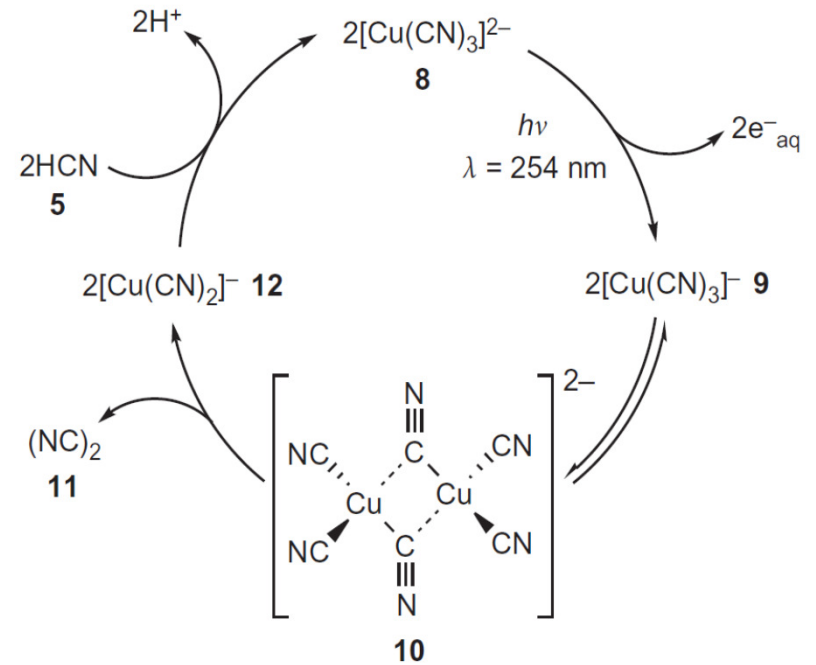
The origin of small reactive intermediates

Thermal decomposition of cyanoferrates (volcanic):

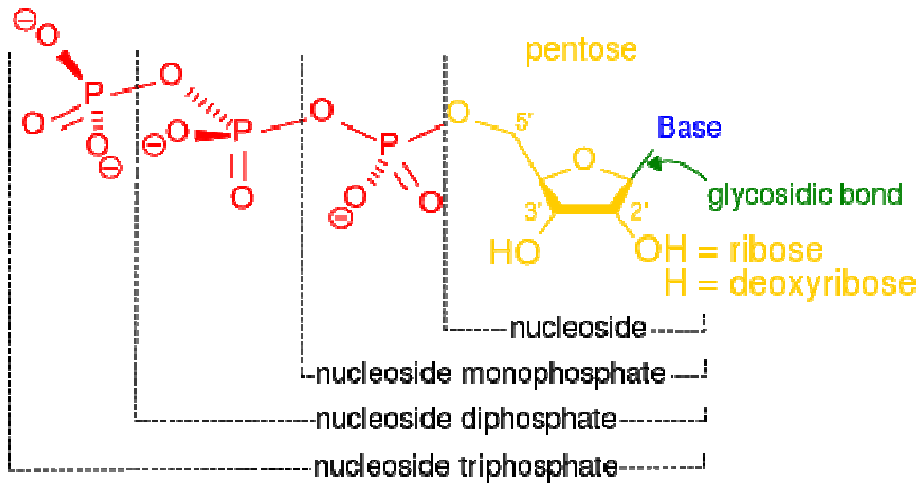
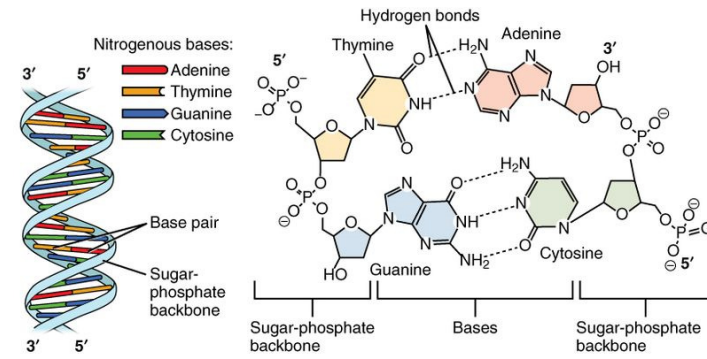
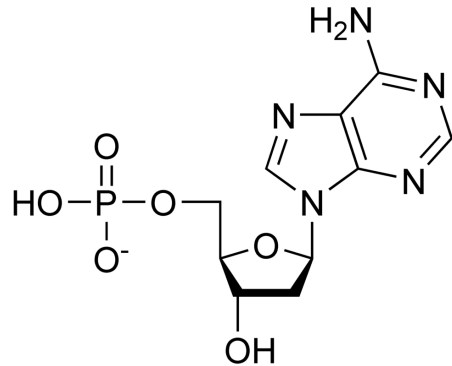


Action of water (buffered to neutral or slightly acidic) on that mixture produced concentrated HCN solution + cyanamide (from CaNCN) + acetylene (from CaC₂) + ammonia (from Mg₃N₂)

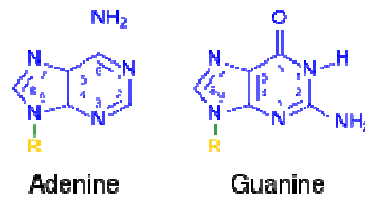
$\text{Cu}_2\text{S} + \text{H}_2\text{O} + 6\text{CN}^- \rightarrow 2[\text{Cu}(\text{CN})_3]^{2-} + \text{HS}^- + \text{OH}^-$
 cyanocuprates and HS⁻ are delivered by this process
 Photoredox cycle based on cyanocuprates may convert HCN into cyanogen



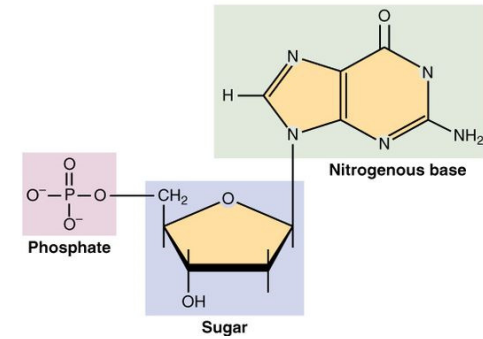
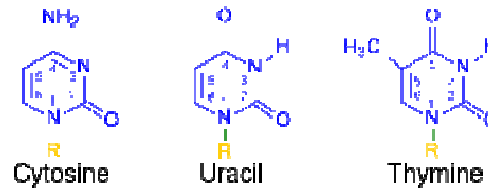
Nucleotides - components



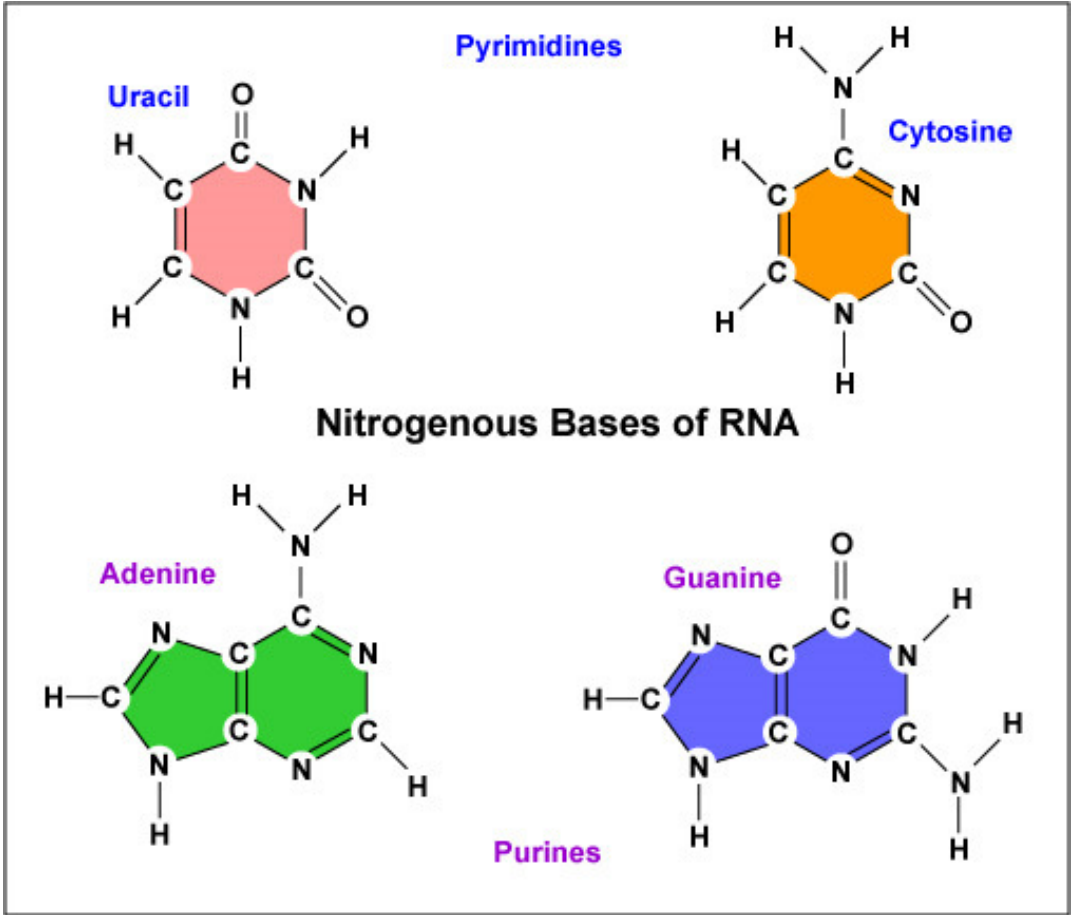
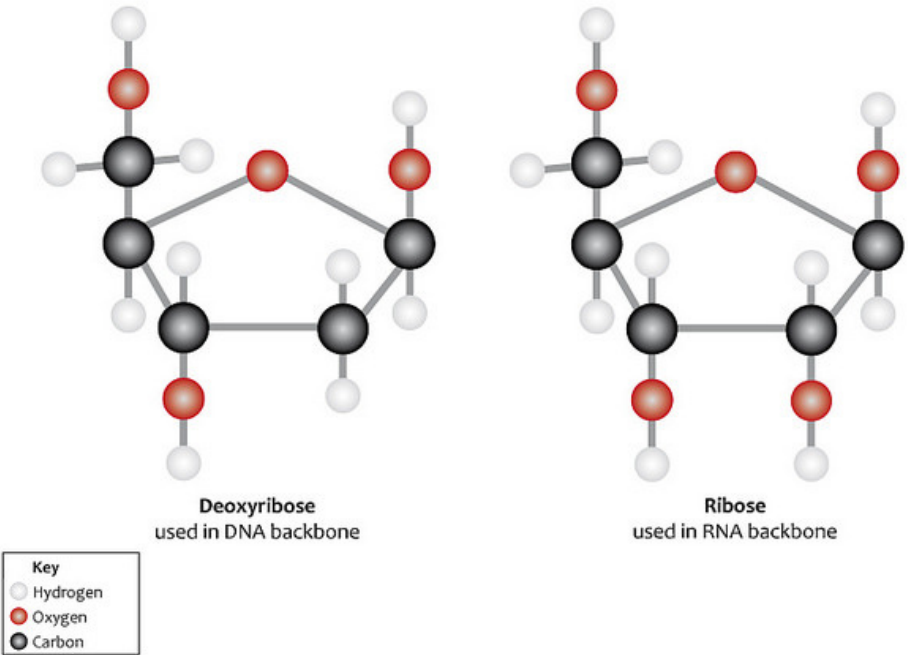
Purines



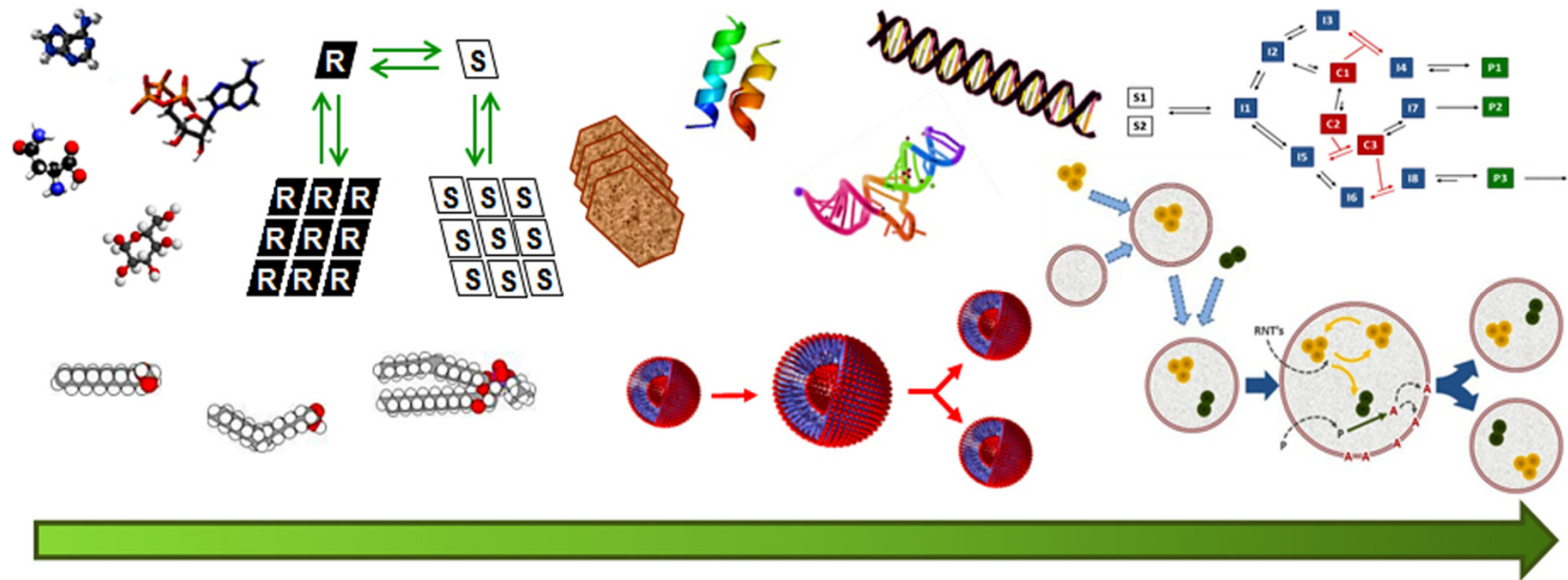
Pyrimidines



Nucleotides - nucleobases + sugars



Summary



Increasing complexity from molecules to systems

Summary

